Functional characterization of B- and T lymphocytes after aCD20 treatment in two different EAE models

Doctoral Thesis

In partial fulfillment of the requirements for the degree
"Doctor rerum naturalium (Dr. rer. nat.)"

in the Molecular Medicine Study Program
at the Georg-August University Göttingen

submitted by

Linda Feldmann
born in Achim

Göttingen, April 2017

MEMBERS OF THE THESIS COMMITTEE:

First member of the thesis committee and supervision:
Prof. Dr. Marin S. Weber
Department of Neuropathology
University Medical Center, Georg-August-University Göttingen

Second member of the thesis committee
Prof. Dr. Jürgen Wienands
Department of Cellular and Molecular Immunology
University Medical Center, Georg-August-University Göttingen

Third member of the thesis committee
Prof. Dr. Dieter Kube
Department of Hematology and Oncology
University Medical Center, Georg-August-University Göttingen

Date of disputation: _____

AFFIDAVIT

Here I declare that my doctoral thesis entitled “Functional characterization of B- and T lymphocytes after aCD20 treatment in two different EAE models” has been written independently with no other sources and aids than quoted.

_____

Göttingen, April 2017

In Erinnerung an
meinen geliebten geliebten Vater

List of Publications

Original acticles

Kinzel, S., Lehmann-Horn, K., Torke, S., Häusler, D., Winkler, A., Stadelmann, C., Payne, N**.,** **Feldmann, L.**, Saiz, A., Reindl, M., et al. (2016). *Myelin-reactive antibodies initiate T cell-mediated CNS autoimmune disease by opsonization of endogenous antigen*. Acta Neuropathol. (Berl.) *132*, 43–58

Lehmann-Horn K., Kinzel S., **Feldmann L**., Radelfahr F., Hemmer B., Traffehn S**.**, Bernard CC., Stadelmann C., Brück W., Weber MS. (2014). *Intrathecal anti-CD20 efficiently depletes meningeal B cells in CNS autoimmunity.* AnnClin Tranl Neurol. 1(7) 490-96

Winterberg T, Vieten G, **Feldmann L**, Yu Y, Hansen G, Hennig C, Ure BM, Kuebler JF.(2014*). Neonatal murine macrophages show enhanced chemotactic capacity upon toll-like receptor stimulation*. Pediatr Surg Int. 2014 Feb;30(2):159-64.

Abstracts

Feldmann L., Zamvil S., Brück W., Weber MS.
Enrichment of B cells with pro-inflammatory properties following anti-CD20 mediated B cell depletion in an EAE model actively involving B cells
13th Congress of the International Society of Neuroimmunology, September 26th-29th 2016, Jerusalem, Israel, Poster session

Feldmann L., Zamvil S., Brück W., Weber MS.
Enrichment of B cells with pro-inflammatory properties following anti-CD20 mediated B cell depletion in an EAE model actively involving B cells
12th European Committee for Treatment and Research In Multiple Sclerosis, October 7th-10th 2015, Barcelona, Spain, Poster session

Feldmann L., Weber MS.
Following anti-CD20 treatment, compartment-specific repletion with immune-competent B cells depends on activation of reappearing B cells
13th Congress of the International Society of Neuroimmunology, September 26th-29th 2014, Mainz, Germany, Oral presentation

Table of contents

Danksagung

Ein großer Dank geht an **Prof. Dr. Martin S. Weber**, dem ich auch dafür danke dass er mich mit diesem Projekt betraut hat. Die Arbeit mit dir hat mich sowohl in professioneller als auch in persönlicher Hinsicht sehr vorangebracht. Ich hatte eine sehr schöne Zeit in deiner Arbeitsgruppe.

Ich bedanke mich sehr bei **Prof. Dr. Wolfgang Brück** für die Gelegenheit meine Doktorarbeit in dem Institut für Neuropathologie anzufertigen

Des Weiteren bedanke ich mich auch bei **Prof. Dr. Jürgen Wienands** und **Prof. Dr. Dieter Kube** für Ihr Interesse und kritischen Anmerkungen während der Thesis committee Treffen.

Ich bedanke mich auch sehr bei **Cynthia** und **Heidi** für ihre Hilfe sowie den Mitarbeitern des Promotionsprogrammes Molekulare Medizin, vor allem **Dr. Erik Meskauskas**.

Ein riesiger Dank geht an **Caroline Jaß, Jan Einar Albin, Julian Koch, Mareike Gloth** und **Katja Grondey**, ohne deren großartige Unterstützung und übermäßiges Engagement einige Experimente nicht durchführbar gewesen wären. Zudem danke ich euch für viele lustige Stunden im Labor die mir den Alltag versüßt haben.
Ein großer Dank geht an **Darius** dafür dass du mir mit deinem professionellen Rat immer geholfen hast.
Ich bedanke mich sehr bei meinen Kolleginnen **Lena** und **Anne** die von Anfang an dafür sorgten, dass ich mich herzlich aufgenommen gefühlt habe und mir mit ihrer professionellen Meinung zur Seite standen.

Außerdem möchte ich mich wirklich sehr bei Sarah, Basti und Kim bedanken. Ihr seid in den letzten Jahren viel mehr als nur Kollegen für mich geworden!
Kim, nicht nur das du immer ein offenes Ohr und gute Ratschläge als Freundin für mich hattest sondern du bist sogar Teil meiner Familie geworden! Vielen Dank für deine Unterstüzung in allen Lebenslagen!
Basti, ich bedanke mich für sehr viele lustige Stunden im Büro! Du hast den Alltag sehr viel erträglicher gemacht und standest mit Rat und Tat immer zur Seite!
Sarah, meine Nummer 1! Du bist in den letzten Jahren einer der wichtigsten Personen geworden und warst immer für mich da und hast mich privat als auch professionell immer unterstützt ohne Wenn und Aber! Ich danke dir dafür aus ganzen Herzen!

Ich bedanke mich bei meinen Freunden **Helene** und **Maleen.** Ihr wart immer für mich da sowohl mit aufbauenden Worten als auch guten Ratschlägen!
Ein sehr großer Dank geht an **Matzie**! Seit 10 Jahren bist du immer an meiner Seite und gibst mir Halt!

Ein großer Dank geht an meine Familie.
Ich danke meinen verstorbenen **Eltern, Uwe, Marvin, David** und **Jenny** für eure Unterstützung ohne euch wäre das nicht möglich gewesen.

Zu Letzt möchte ich mich bei **Henning** dafür bedanken, dass du mich jeden Tag glücklich machst!

Abstract

Multiple sclerosis (MS) is one of the most common causes of persisting disability in young adults. Its clinical course can be heterogeneous with a varying extent of inflammatory central nervous system (CNS) lesions, demyelination and axonal loss accumulating over time. Earlier concepts assumed that MS is primarily a T cell driven disease. Current evidence suggests that B cells may play an equally important role in MS pathogenesis. This notion was boosted by the extensive and rapid benefit of B cell depletion via anti-CD20 antibodies in recent clinical trials in patients with relapsing, remitting MS. Notwithstanding these results, it is currently not clear whether patients with MS and related disorders need to be permanently depleted of B cells to maintain clinical stabilisation. As the related mechanistic question, it is thus far unknown when B cells reappear in compartments other than the blood and in particular, in what functional status B cells return upon cessation of anti-CD20 treatment. To address these questions, we utilized two murine MS models of experimental autoimmune encephalomyelitis (EAE), one in which B cells remain naïve, and one on which B cells get actively involved in a pathogenic manner. Using these opposing models, we monitored reappearance of B cells as well as their functional phenotype in bone marrow, spleen, lymph node, blood as well as the CNS. First, and independent of the model used, we observed that B cells reappeared in bone marrow and spleen substantially prior to the blood, which indicates that monitoring B cells in the blood of patients may not be a suitable strategy to assess B cell reappearance. Second, we observed that despite extensive anti-CD20 treatment, a population of CD20+ B cells remained un-depletable in the spleen of mice with EAE. These B cells were found to be differentiated and antigen-experienced germinal center B cells, while naïve B cells were rarely detected. Of note, this finding was pronounced in the EAE model in which B cells are activated. Upon recovery from anti-CD20 treatment, this population strongly expanded in vivo in parallel to de novo generation of naïve B cells in the bone marrow. I consequence, we observed that upon return of B cells, mice which had received the B cell-involving EAE induction regimen contained a higher ratio of antigen-activated / naïve B cells when compared to the EAE model in which B cells remain naïve. Functionally, this translated into an enhanced antigen-presenting function of reappearing B cells in the B cell-EAE model. These findings indicate that in a B cell activating milieu, remaining antigen-experienced B cells can expand in secondary organs after anti-CD20 treatment, which may result in a relative shift towards pro-inflammatory B cell function when compared to the status of B cells prior to depletion.

Recent findings suggest that besides B cells, a small population of differentiated human T cells express CD20. To date it is not clear whether these T cells play a pathogenic role in MS. Following this observation mechanistically, we could detect that mice with EAE indeed contain a population of CD20+ T cells, which is rapidly depleted upon anti-CD20 treatment. Paralleling the compartment-specific repletion of B cells, CD20+ T cells sequentially reoccurred in spleen, lymph nodes and blood after anti CD20 treatment. Further studies aim to dissect to what extent depletion of these T cells may possibly contribute to the clinical benefit of anti-CD20 treatment independent of B cells.

List of Figures:

List of Tables

Abbreviations

APC	Antigen-presenting cell
APP	Amyloid precursor protein
Ag	Antigen
BAFF	B cell activation factor
BBB	Blood brain barrier
BCR	B cell receptor
BV	Brilliant violet
CD	Cluster of differentiation
CFSE	Carboxyfluorescein succinimidyl ester
CIS	Clinical isolated syndrome
CNS	Central nervous system
CSF	Cerebrospinal fluid
ctrl	control
dH_2O	Distilled water
ddH_2O	Bidistilled water
DMD	Disease-modifying drug
DMF	Dimethyl fumarate
DNA	Deoxyribonucleic acid
EAE	Experimental autoimmune encephalomyelitis
EC	Endothelial cell
EDSS	Expanded disability status scale
e.g.	Exempli gratia
FACS	Fluorescence activated cell sorting
FCS	Fetal calf serum
FITC	Fluorescein isothiocyanate
GA	Glatiramer acetate
h	Hour(s)
H2O2	Hydrogen peroxide
HCl	Hydrochloric acid
IFN	Interferon
Ig	Immunglobulin
i.p.	intrapertoneal
mAb	Monoclonal antibody
MBP	Myelin basic protein
mg	Milligram
MHC	Major histocompatibility complex
min	Minute(s)
µl	Microliter
ml	Milliliter
µm	Micrometer
µM	Micromolar
MOG	Myelin oligodendrocyte glycoprotein
MRI	Magnetic resonance imaging
MS	Multiple Sclerosis
OPC	Oligoclonal Band
PBMC	Peripheral blood mononuclear cell

PBS	Phosphate buffered saline
PE	Phycoerithrin
PFA	Paraformaldehyde
PPMS	Primary progressive multiple sclerosis
PML	Progressive multifocal leukoencephalopathy
PLP	Proteolipid protein
PTX	Pertussis Toxin
rMOG	Recombinant Myelin oligodendrocyte glycoprotein
RRMS	Relapsing-remitting multiple sclerosis
RT	Room temperature
s	Second(s)
s.c.	Subcutaneous
SPMS	Secondary progressive multiple sclerosis
Th1	T helper cells 1
Th17	T helper cells 17
TNF	Tumor necrosis factor

1. Introduction

1.1.Multiple sclerosis

Multiple sclerosis (MS) is one of the most common inflammatory diseases of the central nervous system (CNS) in young adults in the western world, affecting about 2.5 million patients[1]. MS is characterized by inflammation of the CNS, demyelination and axonal loss resulting in neurodegeneration. MS is a heterogeneous disease and its trigger is still unknown. The extent of heterogeneity became clear by characterizing neuro myelitis optica (NMO) as a sub type of MS for years, which is now known to be triggered by aquaporin-4 antibodies.

1.1.2. History and Epidemiology

MS was first described by Robert Carswell in 1838. A more detailed description of MS was published by Jean Cruveillier in his manuscript "Anatomie pathologique du corps human" (1829-1842)[2]. However, the first correlation between the clinical symptoms and pathological features, such as inflammation, demyelination and axonal loss was made by Jean Martin Charcot in 1868[3].

The risk to develop MS increases with the distance to the equator. Areas with an elevated prevalence of MS are Europe, Russia, Israel, Northern US, Canada and New Zealand[4]. The prevalence of MS in Germany is around 127 out of 100000 citizen[5]. The average age at disease onset is 29 years and females are affected twice as often as males[6].

Until today, the exact cause of MS is unknown but many risk factors were described. There is evidence for environmental, genetic, hormonal and/or infectious factors which are linked with MS. A genetic factor of MS is the HLAII gene which is known to be associated with the risk to develop MS since the 1970s[7]. Investigating environmental factors, low vitamin D levels were identified as a possible risk factor for MS, while higher serum levels of vitamin D seem to reduce the relapse rate[8–11]. Additionally, the infection with Epstein-Barr virus (EBV) is controversially discussed as a risk factor but due to a low number of uninfected patients, it is challenging to investigate[12]. Furthermore, smoking is known to elevate the risk to develop MS and to fasten the transition from relapsing remitting MS to secondary progressive MS[13–15].

1.1.3. Clinical course

MS is a heterogeneous disease. For a better communication and to avoid ambiguities, the MS society advisory committee distinguished four different subtypes of clinical courses in 1996 and revised these in 2014[16,17]. The classical four subtypes are described as followed:

The relapsing remitting (RRMS) form is the most common disease course, affecting around 85% of all patients at the onset of disease. It is defined by clinical relapses from which patients can

fully or partially recover (remission) (figure 1)[16]. A relapse is defined as an episode of neurological symptoms typical for an inflammatory demyelinating event in the CNS that lasts for at least 24 hours in the absence of fever or infection.

Most of the patients with RRMS transit over time into secondary progressive MS (SPMS) which is characterized by continuous worsening of disease and relapses with minor recovery phases [18]. A further type of MS is the primary progressive MS (PPMS) which is characterized by continuous progression of the disease from the onset without any phases of recovery. Only about 10% of MS patients are affected by this subtype[19]. The last type of MS is the primary relapsing MS (PRMS). It is the rarest type of MS and is defined by progression from disease onset combined with relapses which are followed by incomplete recovery.

The revised classification is focused on RR disease or progressive disease. The precursor state of RRMS is the clinically isolated syndrome (CIS). CIS shows inflammatory demyelination that can develop to MS, but has not yet fulfilled the criteria of dissemination. In case CIS additionally shows activation, which is determined by clinical relapses and/or MRI activity, it can progress to RRMS whether such activity fulfils the criteria of dissemination.

Progression of disease is characterized by clinical evaluation with continuous disease progression. Whether multiple assessments are not possible, activity and progression are "indeterminate". If PPMS patients show further activity but no progression, they are described as PPMS-without progression. SPMS patients that show progression but no activity or show neither progression nor activity are defined as stable[17].

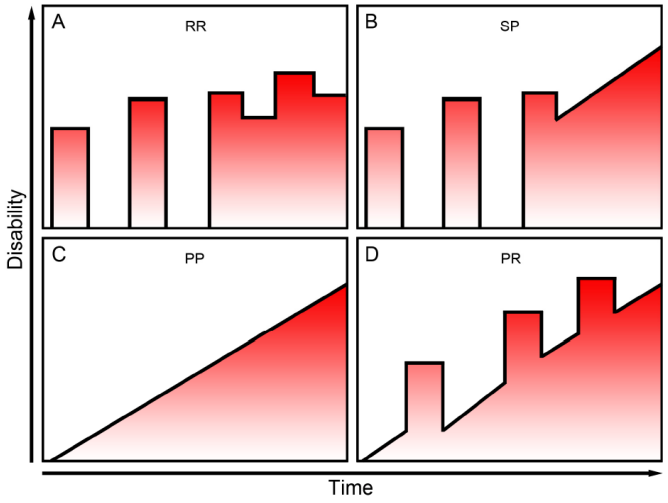

Figure 1: Classical MS subtypes
A) relapsing remitting MS B) secondary progressive MS C) primary progressive MS D) progressive remitting MS (modified from Lublin et al., 1996[16], and adapted from Häusler[20])

1.1.4. Pathogenesis of MS

The exact factors which trigger MS are still unknown. Researchers try to investigate the disease using different animal models. Many of the mechanisms of MS are investigated in the inflammatory animal model experimental autoimmune encephalomyelitis (EAE). Reviewing experimental data of EAE, we have to keep in mind the differences between EAE and MS as well as the complexity of MS.

Findings in EAE model show that immune cells infiltrate in the CNS and cause a pro-inflammatory immune response[21]. T cells are reported to be the first activated cells which infiltrate the CNS. These autoimmune T cells release pro-inflammatory cytokines such as tumor necrosis factor-α (TNF-α) and interferon β (IFNβ)[22]. This pro-inflammatory milieu leads to an activation of endothelial cells of the blood brain barrier (BBB) which lead to upregulation of cell adhesion molecules (CAM)[23]. This upregulation of CAM attracts more immune cells of the periphery such as monocytes, B and T cells, plasma cells and dendritic cells (DC) which invade into the CNS. This invasion of immune cells causes inflammation which interferes with the astroglial and oligodendroglial homeostasis. Autoimmune antibodies, released by infiltrating plasma cells, might lead to the damage of glial cells and the myelin sheath[21]. Further axonal damage and injury of the myelin sheath can be caused by release of reactive oxygen of microglia and macrophages[24].

The initiation of the disease by T cells, however, is just one of the hypothesized mechanisms but there is evidence that different T cell subtypes influence the pathogenesis of MS. It is known that pro-inflammatory T helper 1 (Th1) and T helper 17 (Th17) cells can induce EAE by adoptive transfer of these cells. Th17 are able to release IL-17A, IL-17F, IL-21, IL-9, IL-22 and TNF-α and can be found in lesions of MS patients[25,26]. In contrast, T helper 2 (Th2) cells show an anti-inflammatory function by released anti-inflammatory cytokines such as IL-4 and IL-13, for example after being activated by type II monocytes[27].

Regulatory T cells also appear to be implicit in the pathogenesis of MS. The suppressive function of regulatory T cells is profoundly compromised in MS patients, which possibly might contribute to the pathogenic activation of Th1 and Th17 cells [28,29].

1.1.4.1. Role of B cells in MS

For decades, MS was thought to be a mainly T cell driven disease. Therefore B cells were believed to play only a secondary role by releasing autoimmune antibodies. However, more recent studies suggest an important function of B cells in MS. The success of B cell depleting therapies

in patients with RRMS particularly brought B cells into the focus of MS research for their possible importance in MS pathogenesis.

The earliest indication that B cells contribute to MS pathology dates back to the detection of intrathecal IgGs with moving boundary electrophoresis by Elvin Kabat in 1942[30]. These oligoclonal bands (OBCs) in the cerebrospinal fluid (CSF), caused by expansion of B cells and plasma cells, can be detected in more than 95% of MS patients[31].
Furthermore, accumulations of B cells were found in the meninges of patients with SPMS. They are located in follicular like structures together with follicular dendritic cells and T cells[32,33].

However, the strongest evidence for the role of B cell in the pathogenesis of MS is the rapid clinical benefit of B cell depletion by aCD20 antibodies as shown in 2008 by Hauser et al.[34]. After aCD20 Ab treatment, a relative reduction in gadolinium-enhancing lesions by 91 % could be observed in patients with RRMS. Accordingly, the number of new lesions was reduced in this study[34].
A closer look at the mechanism of aCD20 depletion reveals that the release of autoimmune antibodies is not altered substantially because CD20 is not expressed on plasma cells which produce and release autoimmune antibodies[35,36].
The fact that plasma cells are not affected by aCD20 therapy suggest an additional B cell function that influences the pathogenesis of MS. One important function of B cells is their ability to present antigens to T cells which influence the pathogenesis of MS. For antigen presentation and subsequent T cell priming, major histocompatibility complex II and the costimulatory molecules of CD80, CD86 and CD40 are necessary. In MS patients, these co-stimulatory molecules are known to be upregulated[37]. Furthermore, the cytokine profile of MS patients is dysregulated. Barr et al.[38] show that B cells release more pro-inflammatory IL-6 and tumour necrosis factor alpha[3736]. These cytokines are reported to induce pathogenic Th1 and Th17 cell differentiation which can cause demyelination and axonal loss[39]. After B cell depleting therapies, the levels of pro-inflammatory cytokines in patients are decreased[40].
This shows that B cells might play a role in the pathogenesis of MS. But current studies report the presence of CD20+ T cell population which depletable by aCD20 treatment[41]. Holley et al.[42] show the presence of these CD20+ T cells in the brain as well as in the blood of RRMS patients. The influence and depletability of this CD20+ T cells might also explain the benefit of aCD20 depleting therapy or a combination of B cell and CD20+ T cell depletion causes successful treatment. However, the extract mechanism of aCD20 treatment is still not fully understood

1.1.5. Histopathology of MS

The pathology of MS is characterized by typical multifocal lesions in the CNS. Typical hallmarks are infiltration of immune cells, white matter demyelination, reactive gliosis and relative axonal preservation. Traditionally, MS lesions are classified according to their density and location. Active lesions are characterized by pronounced macrophages infiltration whereas chronic active lesions show a hypocellular centre and an inflammatory rim of microglia and/or macrophages. The chronic inactive lesions are solely defined by a hypocellular centre.

A more recent classification distinguishes between early active, late active and inactive lesions. Early active lesions are characterized by the presence of macrophages, expressing myeloid related protein 14 and containing myelin degradation products such as myelin-associated glycoprotein, myelin oligodendrocyte protein (MOG), myelin basis protein (MBP), myelin proteolipid protein (PLP) and cyclic nucleotide phosphodiesterase. Late active lesions are only positive for MOG and PLP. In contrast, no degradations products are present in inactive lesions [43]. T cell infiltrations are mostly located perivascularly and parenchymally.

Four different patterns of active lesions are described in MS patients:

MS Pattern I demyelination is characterized by massive T cell and macrophage infiltration.

Pattern II shows additional immunoglobulin and complement deposition.

Pattern III is also characterized by immune cell infiltrates and the absence of immunoglobulin and complement deposition. In contrast to Pattern I, oligodendrocyte apoptosis is observed in MS pattern III.

The MS Pattern IV is very rare, but known to show a T cell and macrophage infiltration without immunoglobulin or complement deposition except for the non-apoptotic degeneration of oligodendrocytes[35].

1.1.6. Current MS therapies

Current treatment strategies for patients with RRMS can be divided in disease modulatory treatment (DMT) and treatment during acute relapses. The choice of the DMT depends on the disease activity and the risk-benefit profile of the drug.

As first line therapies for RRMS patients with mild disease activity, glatiramer acetate (GA), IFNβ, teriflunomide and dimethyl fumarate (DMF) are most widely used.
IFNβ and GA are injectable therapeutics whereas teriflunomide and DMF are oral medications. These four first line therapies are moderate immune modulators and show a good benefit-risk profile. Reduction of the relapse rate and a decreased development of new MRI lesions are reported[44–49].
In order to switch from a first line DMT to a second line treatment, RRMS patients must be diagnosed with at least two disabling relapses within the last year. As a second line therapy, monoclonal antibodies such as natalizumab and alemtuzumab or oral treatments such as fingolimod are used. These medications show a significantly higher therapeutic efficacy compared to first line DMT. MRI activity, relapse rate and disability scores were highly decreased after these medications[50–52]. Although natalizumab is beneficial in MS, it also elevates the risk of patients to develop progressive multifocal leukoencephalopathy (PML)[53,54]. If these treatment options are not successful in controlling disease activity, further therapeutic options are available such as daclizumab, mitoxantrone and rituximab[55–57]. Daclizumab and rituximab are monoclonal antibodies and are known to reduce relapse rate in RRMS patients. Mitoxantrone is an immunosuppressive drug and shows a reduction of relapse rate and disease symptoms in RRMS patients [57].

During acute relapses, the standard medication is a daily, high dosage, intravenous application of corticosteroids for 3-5 days[58]. Secondary treatment options are immunoadsorption or plasma exchange for patients which show an incomplete recovery after steroid treatment[59,60].

In progressive disease forms of MS (PMS), most of the immunomodulatory drugs failed to control disease activity[61]. Mitoxantrone treatment is known to reduce relapse in SPMS but does not affect the continuous progressive process[62,63]. Due to the limited success of immunomodulatory drugs, other therapeutic approaches may be more successful. However, the incomplete understanding of the pathogenesis of PMS complicates the development of new drugs. At the moment, a broad number of new therapeutics are under investigations. In the MS SMART trial three neuroprotective-drugs (amiloride, riluzole, fluoxetine) are investigated for their efficacy in SPMS[64].

1.1.7. B cell depleting therapy

In the last decades, B cell therapies came into the focus of MS research, which was initiated by the finding that B cell depletion causes rapid clinical benefit in MS patients[34].

Rituximab is a chimeric mouse-human monoclonal IgG1 antibody directed against CD20, a lineage marker of B cells. CD20 expression starts at the late pre B cell development and it is present on pre, immature, mature and memory B cells, but not on CD138+ plasma cells (figure 2)[65]. Therefore, an antibody directed against CD20 affects all B cell stages except very early B cells and plasma cells. It is used since 1994 to treat non-Hodgkin's lymphoma (NHL), chronic lymphocytic leukemia (CLL), rheumatoid arthritis (RA) and lupus nephritis[66–69].

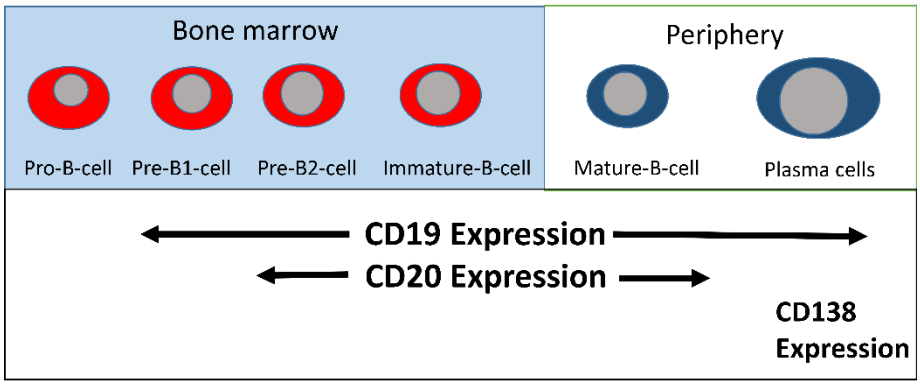

Figure 2 Development of surface lineage marker on B cells.
Expression of CD19, CD20 and CD138 in different stages of B cell development.

The efficiency of rituximab has been shown in various clinical trials. In 2008, a small study with RRMS patients was published which shows a significant reduction of gadolinium enhanced lesions after 2 courses of rituximab treatment. Lesion load was significantly reduced. This effect was observed until 48 weeks after the first dosage of rituximab[34]. In a phase II clinical trial with PPMS patients, rituximab could not reduce the EDSS score. Hence, rituximab may not affect progressive forms of MS[70].

Described side effects are related to a reaction after the first injection, which are rashes, itchiness, lowered blood pressure and a shortness of breath. However, the following infusion is usually much better tolerated[71].

Another therapeutic antibody targeting CD20 is the humanized monoclonal antibody ocrelizumab that binds to a different but overlapping epitope such as rituximab. Due to the more humanized form of ocrelizumab, it is thought to induce less of an immune response to foreign antigens and shows a higher binding ability to the CD20 molecule. The depleting mechanism in contrast to rituximab is mediated mainly over the antibody-dependent cell- mediated

cytotoxicity (two to fivefold higher compared to rituximab) than over complement induced cytotoxicity (three to fivefold lower compared to rituximab)[55,72].
In a phase III trial of ocrelizumab vs Interferon beta, ocrelizumab showed a reduction of relapse rate (46-47%), gadolinium enhanced T1 lesions (94-95%) compared to trial beginning and disability rate (40% compared to IFN-beta) in RRMS patients[73].

Ofatumumab is a completely humanized monoclonal aCD20 antibody which is approved for chronic lymphocytic leukemia. Ofamutumab, which binds to a different epitope than ocrelizumab and rituximab, mediates B cell depletion over antibody-depend cytotoxicity and complement activation. The first Phase II trial in RRMS patients showed a relative reduction of gadolinium enhanced T1 and T2 lesions up to 99% after infusion[74]. No side effects were described in the Phase II trial. Currently, further studies are planned.

1.1.7.1. Mechanism of aCD20 antibody mediated depletion

The effective depletion of B cells by rituximab is mediated by two different pathways after binding of the antibody to CD20: complement induced cytotoxicity (CDC), antibody-dependent cell-mediated cytotoxicity (ADCC).

The main route of B cell depletion by rituximab is via the activation of the complement system. It consists of different ≥30kDA plasma proteins which become activated after antibody binding, resulting in the formation of the membrane attack complex (MAC) leading to the lysis of the cell membrane. The complement cascade can be triggered by different pathways. Rituximab is known to trigger the classical pathway. In this pathway, the C1b complement protein binds to the Fcγ region of the antibody and the cascade is activated, leading to the insertion of the MAC into the cell membrane of the CD20+ B cells resulting in cytolysis[75].

The second pathway, by which rituximab mediates B cell depletion is via antibody-dependent cell-mediated cytotoxicity (ADCC). Monocytes/macrophages, granulocytes and natural killer cells can bind the Fc region of ocrelizumab, three- to fivefold higher than rituximab, via their Fc-receptor. This leads to the cross-linking of Fc receptors, triggering degranulation of cytotoxic substances into a lytic synapse and subsequent apoptosis of the bound B cell[76].

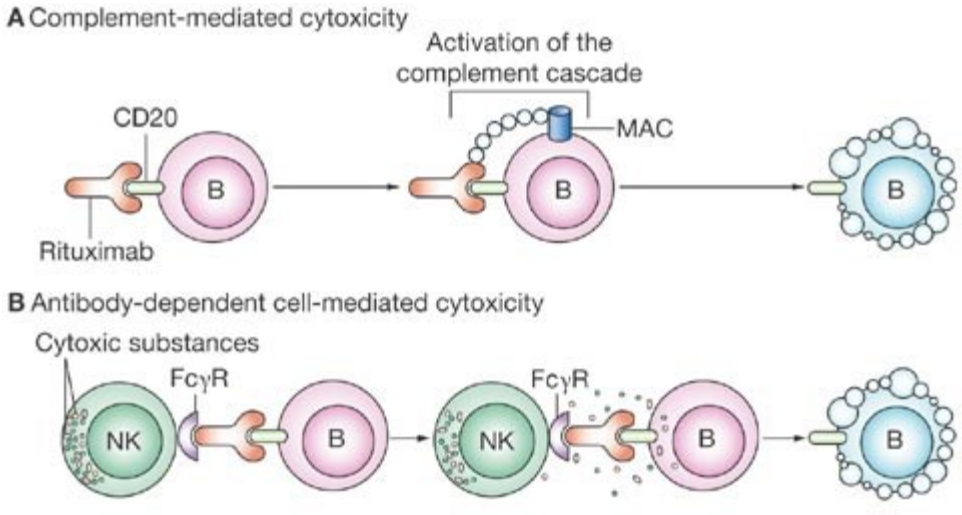

Figure 3: Mechanism of rituximab.
a) complement mediated cytotoxicity b) antibody-dependent cell-mediated cytotoxicity (adapted and modified from Jagadesh et al[77]).

1.2. Experimental autoimmune disease (EAE)

1.2.1. Pathogenesis of EAE

EAE was first described in 1933 and is one of the most common and best described animal models for MS reflecting the inflammatory side of MS[78].

EAE can be induced by "active immunization" in different animals, primary in rodents and primates. "Active immunization" is conducted with a myelin sheath protein or peptide, e.g. MBP, PLP or MOG. The clinical outcome and progression based on the choice of species and used protein for EAE induction.

In mice, the most common immunization protein is MOG. Here, the peptide with the amino acid sequence p35-55 (MOG p35-55) emulsified in CFA (Complete Freund's adjuvants) is most widely used[79,80].

In the MOG p35-55, induced EAE Th1 and Th17 are thought to be the effector cells. First pathogenic effect of IFNβ releasing Th1 cells were described[81]. Adaptive transfer of these Th1 cells induced EAE[82]. IL-12 is a central cytokine for the differentiation of Th1 cells, but interestingly, IL-12-deficient mice are still susceptible to EAE induction[83]. Furthermore, transfer of pathogenic Th17 cells cause EAE induction[82,84]. However, none of the single cell types is essential for EAE induction.

Another important effector cell type are the anti-inflammatory regulatory T cells. Regulatory T cells are reported to inhibit the differentiation of autoimmune T cells. Adoptive transfer of these IL-10 producing T cells can also inhibit EAE induction[85–87]. During the course of EAE, regulatory T cells are essential for the recovery phase[88].

MOG p35-55 immunization leads to the introduction of antigen on B cells or macrophages on their surface via the MHCII molecule to activated T cells[89–91]. After migration into the CNS, the autoreactive T cells are reactivated by local or infiltrating APCs which present myelin fragments and can then mediate a breakdown of the BBB[92,93]. This reactivation induces further inflammatory processes which lead to demyelination and axonal damage[90,94]. Interestingly, Weber et al.[95] described in 2010 a clinical worsening after B cell depletion in MOG p35-55 immunized mice which led to the hypothesis that MOG p35-55 induced EAE is T cell mediated and most of the B cells seems to have a regulatory function.

It is also possible to induce EAE by injecting the complete recombinant murine MOG protein (rMOG 1-117), emulsified with CFA in mice. In contrast to MOG p35-55 EAE, the rMOG protein needs to be internalized, processed and presented by APC, especially B cells, to activate T cells[91]. This induces the generation of antigen specific B cells. These antigen-activated B cells produce

MOG-specific antibodies[96]. Here, the EAE , in contrast to "T cell mediated" MOG p35-55 induced EAE, is B cell and T cell mediated and B cell depletion causes clinical worsening[95]. A third opportunity to induce EAE by MOG protein is to use human MOG protein (hMOG), which induces a B cells dependent EAE. Lyons et al.[97] show that B cell deficient mice are not able to develop hMOG induced EAE but MOG p35-55 induced EAE.

1.2.2. B cell function EAE

Several studies show the contradictory role of B cells. On the one hand, B cell deficient mice developed a more serve EAE without remission[98–100]. On the other hand, the release of autoimmune MOG specific antibodies enhanced demyelination and inflammation[97,101]. In addition, B cells may have an essential role in EAE as antigen presenting cells (APC)[80,102]. This dichotomy of B cell functions is due to a variety of B cell functions in different B cell subsets.

1.2.2.1. B cells differentiate into plasma cells and release autoimmune antibodies

After antigen recognition, B cells can differentiate into memory B cells and CD138+ plasma cells which are able to generate antibodies against specific antigens. When these specific antibodies target their antigen, the complement system is activated.

Similar to MS lesions where myelin sheath specific antibodies are found in areas with massive myelin breakdown, in rMOG protein EAE MOG specific antibodies are present in these CNS regions[103].

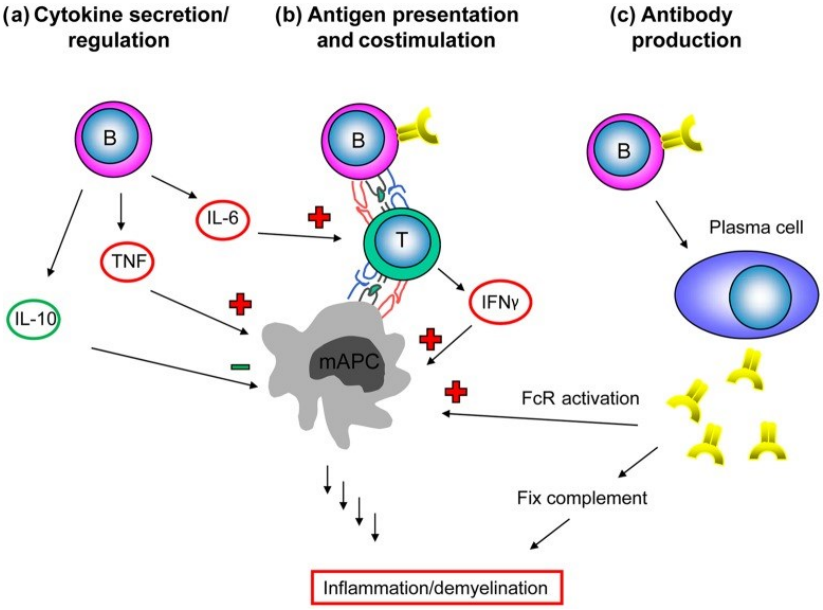

Figure 4: Schematic overview of B cell function.

Figure 1.2.1: Schematic overview of B cell function. a) cytokine secretion/regulation b) APC function and co-stimulation and c) antibody production (adapted from Lehmann-Horn et al., 2013[104]).

1.2.2.2. B cells act as antigen presenting cells

In the periphery, many different professional APCs are well studied, including dendritic cells (DC), monocytes/macrophages and B cells. Furthermore, in the CNS antigen presentation plays a major role for reactivating infiltrating T cells. Two different types of APCs are known, the resident APCs, including astrocytes and microglia and the non-resident APCs such as B cells, macrophages/monocytes and dendritic cells, which play an important role in EAE[105,106].

Different APCs are known to be essential for EAE induction. This was shown by Greter et al.[107] in 2005 for DCs. MHCII restricted antigen presentation by DC was shown to be sufficient to induce EAE. For B cells, it is reported that in complete protein EAE they are necessary as professional APCs. After internalization of complete MOG protein B cells act as superior APCs. The antigen presentation to CD4+ T cells via the B cell receptor (BCR) is 10.000 times better compared to the unspecific antigen uptake of T cells[108]. In comparison to DCs, which are more specialized to present peptides, antigen specific B cells are more efficient in processing and presenting protein antigens which they have recognized with their BCR[108–110].

The BCR recognizes complete proteins and after internalization and processing, the resulting peptides are presented on MHCII molecules and the B cell up regulates costimulatory molecules such as CD40, CD80 and CD86[37].

In 2013, Molnarfi et al.[111] reported that B-cell$^{MHC\ II-/-}$mice were resistant to EAE induced by recombinant human MOG protein. They conclude that MHCII-dependent antigen presentation by B cells is necessary for EAE induction.

1.2.2.3. B cells secrete pro- and anti-inflammatory cytokines

The dichotomy of B cell function becomes clear by facing the distinct cytokine profile of B cells. B cells are able to produce pro- as well as anti-inflammatory cytokines. One of the most important pro-inflammatory cytokines in EAE is IL-6 which induces generation of encephalitogenic Th17 cells[39]. IL-6 deficient mice are reported to be completely resistant to EAE[112]. This becomes more clearer in another study where IL-6 deficiency is restricted to B cells. Mice in this which IL-6 deficiency is restricted to B cells develop a milder EAE progression while this effect is no longer observed after transfer of wild type B cell which were able to produce IL-6[112].

Lymphotoxin-alpha (LT-α) and tumor necrosis factor alpha (TNFα) are also pro-inflammatory cytokines secreted by B cells in MS[40].

In contrast, B cells can secrete anti-inflammatory cytokines such as IL-10 and IL-35. IL-10 deficient mice are not able to recover from EAE. Even after a transfer of IL-10-competent B cells, mice do not fully recover from relapses[99].

Inhibition of the secretion of IL-10 or IL-35 in B cells increases the disease severity and prevents physiological recovery from an acute disease relapse[113].

2. Material and Methods

2.1. Material

2.1.1 Reagents

Table 1: Reagents

Reagents	SOURCES OF SUPPLY
Acetic Acid	Merck Millipore, Germany
Agarose	Starlab GmbH, Germany
BD FACS Clean™	BD Biosciences, USA
BD FACS Flow™	BD Biosciences, USA
BD FACS Rinse™	BD Biosciences, USA
BD FACS™ Lysing Solution, 10x	BD Biosciences, USA
BD Pharm Lyse™, 10x	BD Biosciences, , USA
Boric Acid	Merck Millipore, Germany
Crystal Violet	Sigma Aldrich, USA
Cytofix/Cytoperm™	BD Biosciences, , USA
Cytofix™	BD Biosciences, USA
Chloral Hydrate	Merck Millipore, Germany
Citric Acid	Merck Millipore, Germany
DAB (3,3'-Diaminobenzidine)	Sigma-Aldrich Chemie GmbH, Germany
DDSA (2-Dodecenylsuccinic Acid Anhydride)	Serva Electrophoresis GmbH, Germany
DEPEX	VWR International, Germany
DMSO (Dimethyl Sulfoxide)	Sigma Aldrich, USA
EDTA (Ethylenediamine Tetraacetic Acid Disodiumsalt Dihydrate)	Carl Roth, Germany
Ethanol, 100%	Merck Millipore, Germany

Ethidium Bromide	Sigma Aldrich, USA
Eosin G	Merck Millipore, Germany
FCS (Fetal Calf Serum)	Sigma Aldrich, USA
Generuler™, 100 Base Pairs (bp) DNA Ladder Plus	ThermoFisher Scientific, USA
Go-Taq® DNA Polymerase Buffer, 5x	Promega, USA
HCl (Hydrochloric Acid)	Merck Millipore, Germany
H2O2 (Hydroxic Peroxide), 30%	Merck Millipore, Germany
Isopropyl Alcohol	Merck Millipore, Germany
L-Glutamine, 200 Mm	Sigma Aldrich, USA
LPS (Lipopolysaccharide)	Sigma Aldrich, USA
Mayer's Hemalum	Merck Millipore, Germany
NaCO3 (sodium carbonate)	Merck Millipore, Germany
NaHCO3 (sodium hydrogen carbonat)	Merck Millipore, Germany
NaF (sodium fluoride)	Merck Millipore, Germany
PBS (Phosphate Buffered Saline), 10x	Biochrom AG, Germany
PBS (Phosphate Buffered Salt Solution), Sterile	Sigma Aldrich, USA
Penicillin, 10,000 Units	Sigma Aldrich, USA
Perm/Wash™ Buffer, 10x	BD Biosciences, USA
PFA (Paraformaldehyde), Powder	Merck Millipore, Germany
PMA (Phorbol 12-Myristate 13-Acetate)	Sigma Aldrich, USA
RPMI-1640 (Roswell Park Memorial Institute-1640)	Sigma Aldrich, USA
Sodium Pyruvate, 100 mM	Sigma Aldrich, USA
TMB (3,3',5,5'-Tetramethylbenzidine) Substrate Solution	Ebioscience, USA

Tris (Tris(Hydroxymethyl)Aminomethane)	Carl Roth, Germany
Trypan Blue	Sigma Aldrich, USA
Tween	Merck Millipore, Germany
β-Mercaptoethanol	Sigma Aldrich, USA

2.1.2. Solution

Table 2:Solutions, buffers and cell culture media

Solutions, buffers and cell culture media	COMPOSITION
Blocking Buffer for Immunohistochemistry	PBS
	10% FCS
CFA (Complete Freund's Adjuvant)	Paraffin oil
	15% mannide monooleate
	6.7 mg/ml *Mycobacterium tuberculosis* H37RA
Citric Acid Buffer, 10 Mm	2.1 g citric acid
	1 l distilled water
	NaOH, adjust to pH 6
Coating buffer	8.4 g NaHCO3
	3.5 g NaCO3
	1 l distilled water
	Stir filter, adjust to pH 9.5
3,3'-Diaminobenzidine Tetrachloride (Dab) Working Solution	PBS
	0.5 mg/ml DAB
	add 20 µl 30% hydrogen peroxidase per 50 ml DAB solution before use
ELISA wash buffer	200 ml 10x PBS

	1 ml Tween
	1.8 l distilled water
ELISA stop solution	1 N H2 SO4 solution
1% Eosin	70% isopropyl alcohol
	1% eosin G
	stir filter, before use add 0,5% acetic acid
(Fluorescence-Activated Cell Sorting) Buffer	PBS, sterile
	2% FCS
1% HCl	1% HCl absolute
	70% ethanol
MACS (Magnetic-Activated Cell Sorting) Buffer	PBS, sterile
	0.5% FCS
	2 mM EDTA
	pH 7.2
Neutralization buffer	40 mM Tris
	250 ml distilled water
10x PBS	95.5 g PBS
	1 l distilled water
RD1 buffer (ELISA block buffer)	200 ml 10x PBS
	20 g BSA
	1.8 l distilled water
RPMIcomplete	RPMI-1640
	10% FCS
	1 mM sodium pyruvate

	50 µM β-Mercaptoethanol
	100 units penicillin
	2 mM L-glutamine
TAE (Tris, acetic acid, EDTA) buffer	40 mM Tris
	20 mM acetic acid
	1 mM EDTA
	1 l distilled water (adjusted to pH 8)
Tail lysis buffer	25 mM NaOH
	2 mM EDTA
	250 ml distilled water

2.1.3. Protein enzymes and inhibitors

Table 3:Proteins, enzymes and inhibitors

Proteins, enzymes and inhibitors	
BSA (bovine serum albumin)	SERVA Electrophoresis GmbH, Germany
Recombinant mouse MOG-protein1-117	Monash University, Australia
PTX (pertussis toxin)	List biological laboratories, USA
DNase I	Roche, Basel, Switzerland
Dreamtaq green PCR master mix (2x)	Thermo Fisher Scientific, USA
MOG p35-55 peptid	Auspep, Austria
Proteinase K	Sigma Aldrich, USA
Trypsin, 0.05%	Gibco/Invitrogen, USA

2.1.4. Monoclonal antibodies for flowcytometry

Table 4: Monoclonal antibodies for flow cytometry

Monoclonal antibodies for flow cytometry	**FLUOROCHROME**	**CLONE**	**DILUTION**	**SOURCE OF SUPPLY**
B220	FITC	RA3-6B2	1:100	BioLegend
B220	PE-Cy7	RA3-6B2	1:100	BD Biosciences
CD1D	Pacific Blue	1B1	1:100	BioLegend
CD4	BV510	GK1.5	1:100	BioLegend

CD4	PE	RM4-5	1:100	BioLegend
CD5	PerCP-Cy5.5	53-7.3	1:100	BioLegend
CD8a	FITC	53-6.7	1:100	BioLegend
CD19	APC-Cy7	6D5	1:100	BioLegend
CD20	AlexaFlour 488	SA275A11	1:200	BioLegend
CD23	APC	B3B4	1:100	BioLegend
CD27	FITC	LG.3A10	1:100	BioLegend
CD37	PE	Duno85	1:100	BioLegend
CD38	Pacific Blue	90	1:100	BioLegend
CD69	PerCP-Cy5.5	H1.2F3	1:100	BD Biosciences
CD80	APC	16-10A1	1:100	BD Biosciences
CD86	PE	GL1	1:100	BD Biosciences
CD95 (FAs)	PE	Jo2	1:100	BD Biosciences
CD138	PE	281-2	1:100	BioLegend
GL-7	FITC	GL7	1:100	BioLegend
IFNΓ	APC	XMG1.2	1:100	BioLegend
IgM	FITC	RMM-1	1:100	BioLegend
IgD	PE	11-26c.2a	1:100	BD Biosciences
MHC-II	Pacific Blue	AF6-120.1	1:200	BioLegend

2.1.5. Monoclonal antibodies for antigen independent activation in vitro

Table 5: Monoclonal antibodies for antigen-independent activation of T cells in vitro

Monoclonal antibodies for antigen-independent activation of T cells in vitro	CLONE	SOURCE OF SUPPLY
LEAF™ purified anti-mouse CD3	145-2C11	BioLegend
LEAF™ purified anti-mouse CD28	37.51	BioLegend

2.1.6. Primary antibodies for immunohistochemical staining

Table 6: Primary antibodies for immunhistochemical staining specificity

Primary antibodies for immunhistochemical staining specificity	SPECIES/CLONE	ANTIGEN RETRIEVAL/FIXATION	DILUTION	SOURCE OF SUPPLY
B220	rat	microwave, citric acid buffer	1:200	BD Pharmingen
CD3	rat/ CD3-12	microwave, citric acid buffer	1:200	Biorad
MAC3	Rat/ M3/84	microwave, citric acid buffer	1:200	BD Pharmingen

2.1.7. Secodary antibodies for immunohistochemical staining

Table 7: Secondary antibodies for immunohistochemical staining

Secondary antibodies for immunohistochemical staining	DILUTION	MANUFACTURER
Anti-mouse IgG, biotinylated	1:200	GE Healthcare Europe GmbH, Germany
Anti-rabbit IgG, biotinylated	1:200	GE Healthcare Europe GmbH, Germany
Anti-rat IgG, biotinylated	1:200	GE Healthcare Europe GmbH, Germany

2.1.8. Applied Kits

Table 8: Applied Kits

Applied Kits	SOURCE OF SUPPLY
CD4+ T cell isolation kit II, mouse	Miltenyi Biotec, Germany
Cell lineage panel kit, mouse	Miltenyi Biotec, Germany
Dylight 405 Antibody labeling Kit	Thermo Fisher Scientific, USA
BD Pharmingen™ BrdU Flow Kits, FITC	BD Biosciences

2.1.9. Primers

Table 9: Primers

Primers	SEQUENCE	SOURCE OF SUPPLY
Ja18-2D2	5’-CCC GGG CAA GGC TCA GCC ATG CTC CTG-3’	Eurofins Scientific, Germany
Va3-2-2D2-M	5’-GCG GCC GCA ATT CCC AGA GAC ATC CCT CC-3’	Eurofins Scientific, Germany

2.1.10. Consumables

Table 10: Consumables

Consumables	SOURCE OF SUPPLY
Bottle Top Filter, 0.2 µm	Sarstedt, Germany
Cell Culture Plates, Flat Bottom (6 Well, 24 Well, 96 Well)	Greiner bio-one, Austria
Cell Strainer (70 µm)	Greiner bio-one, Austria
FACS Tube, 5 ml	Sarstedt, Germany
LS Columns	Miltenyi Biotec, Germany
Needles	BD Biosciences, USA
Nunc™ Maxisorp® 96 Well ELISA Plate	Thermo Scientific, USA
96 Well Plate Round	Sarstedt, Germany
Pre-Separation Filters, 30 µm	Miltenyi Biotec, Germany
Syringes	BD Biosciences, USA
Tubes (50 ml, 15 ml, 10 ml, 2 ml, 1,5 ml,	Sarstedt, Germany
0.2 ml)	

2.1.11. Technical devices

Table 11:Technical devices

Technical devices	SOURCE OF SUPPLY
Bx51 Olympus light microscope equipped with DP71 digital and XM10 monochrome camera	Olympus, Germany
Centrifuge 5415 R	Eppendorf, Germany
Centrifuge 5810 R	Eppendorf, Germany
FACS LSR II	BD Biosciences, USA
Cell Incubator BBD6220	Thermo Scientific, USA

IMARK™ Microplate Reader	Bio-Rad, Germany
Microscope	Olympus
Microtome	Leica, Germany
Microwave	Bosch, Germany
Neubauer Chamber	Superior Marienfeld , Germany
QuadroMACS™ Separator	Miltenyi Biotec, Germany
T3 Thermocycler	Biometra, Germany

2.1.12. Software

Table 12: Software

Software	APPLICATION	SOURCE OF SUPPLY
BD biosciences FACSDiva software 6.1.2	Data acquisition flow cytometry	BD Biosciences, USA
FlowJo 10.1	Data analysis flow cytometry	Tree Star Inc., USA
GraphpadPrism 6	Statistical analysis and Graphs	GraphPad software Inc., USA
ImageJ 1.47d	Data analysis histology	National Institutes of Health, USA
PSremote 1.6.5	Gel documentation	Breeze systems limited, UK

2.1.13. Mice

C57BL/6 mice were purchased from Charles River (Sulzfeld, Germany). Animals were used at 6-8 weeks of age.

2D2 mice express the MOG35-55-specific T cell receptor Vα3.2/ Vβ11 on CD4+ T cells. In 2003, Bettelli et al. generated and characterized 2D2 animals[114]. 2D2 CD4+ T cells were used in co-culture experiments. Mice breeding was performed in the animal facility in university medical center Göttingen.

2.2. Methods

2.2.1. Genotyping of genetically modified mice of 2D2

For the genotyping of 2D2 mice, tissue was obtained via a tail biopsy. Afterwards DNA was extracted and amplified with specific primers and PCR products were separated by agarose gel electrophoresis as described below.

DNA extraction

DNA was isolated from the tissue gained by the tail biopsies of 2D2 mice. The tissue was digested in 100 µl of lysis buffer at 99°C for 30 min. Afterwards, 100 µl of neutralization buffer was added.

PCR reaction

Each reaction sample contained 1 µl of genomic DNA, 10 µl of Dream Taq® PCR Mix 2x, 1 µl of each primer and 7 µl of water (nuclease free).

Primer 1: 5'-CCC GGG CAA GGC TCA GCC ATG CTC CTG-3'

Primer 2: 5'-GCG GCC GCA ATT CCC AGA GAC ATC CCT CC-3'

PCR conditions

- Initial denaturation: 94°C, 2 min
- 35 cycles: Denaturation: 94°C, 1 min

Annealing: 58°C, 1 min

Extension: 72°C, 1 min

- Final extension: 72°C, 10 min

Agarose gel electrophoresis

5 µl of PCR product was loaded on an agarose gel (2% (w/v) in TAE buffer) containing 3 µl of ethidium bromide/GelRed. Electrophoresis was performed in a Sub-Cell GT Agarose Gel

Electrophoresis System at 120V for 45 min. Gel-documentation by UV-light was used for evaluation of PCR products.

2.2.2. B cell depletion by aCD20 treatment

Preventive B cell depletion in C57Bl6/j mice was achieved by three intraperitoneal (i.p.) injections once a week of 200 µg of murine aCD20 IgG monoclonal antibody (provided by Roche) solved in 200 µl of PBS. As a control group, C57Bl6/j mice were treated with an RAG weed isotype control antibody which has the same IgG isotype as the aCD20 antibody. B cell depletion or control treatment were performed preventively 3 weeks before analyzing in naive mice or 3 weeks before immunization in both EAE models described below.

2.2.3. Experimental autoimmune encephalomyelitis

After treatment with aCD20 or control Ab, T cell mediated EAE was induced by 100 µg of MOG p35-55 injected subcutaneously (s.c.) and 300ng Pertussis toxin (PTX). PTX injection was repeated after 48h. The B cell mediated EAE was induced by using 75µg recombinant MOG protein 1-117 (kindly provided by C.A. Bernard and synthesized, purified and refolded as previously reported) subcutaneously and two injections of 300ng PTX.

2.2.4. Clinical EAE score

To assess EAE severity, body weight and disease scores were evaluated daily in each animal from day ten after immunization until the end of the experiment. The criteria defining the clinical EAE score used in this study are summarized in *Table 13*. Animals reaching a disease score of 4 had to be sacrificed, due to ethical reasons.

Table 13: EAE Score

EAE Score	Clinical signs
0	no clinical disease
1	tail weakness
2	hind limb weakness
3	one paralyzed hind limb
4	two paralyzed hind limbs
5	moribund or dead animals

2.2.5. Preparation of a single cell suspension for characterization of remaining and reappearing B- and T cells

For characterizing of remaining and reappearing B cells after aCD20 depletion, mice were treated with aCD20 or control antibodies described in part 2.2.1.2.. For experiments

characterizing remaining and reappearing B and T cells mice were scarified at different time points after preventive depletion or control treatment. Single cell suspension of peripheral organs were prepared described in the following parts. Each experiment was repeated at least two times with n=2-4 animals per group and time points.

2.2.5.1. Preparation of lymphocytes suspension from spleen, lymph node and bone marrow

Single cell suspensions were prepared from spleen, lymph node and blood for further analysis. All centrifugation steps were performed for 10 min at 300 x*g* and 4°C and cells were washed in 10 ml of PBS, if not stated otherwise.

Tibia and femur of one hind leg were flushed with ice cold PBS to isolate bone marrow. Single cell-suspension of bone marrow was prepared by flushing the suspension through a 70µm cell strainer. Spleen and lymph node were disrupted over a 70µm cell strainer to prepare single cell suspension. Single cell suspensions of all investigated compartments were washed two times for 10 min at 300xg at 4°C.

2.2.5.2. Preparation of blood cells

50µl blood was collected in 300µl 0.1mM EDTA buffer to avoid aggregation. Blood was centrifuged at 1400rpm for 5min. Pellet was solved in 500µl Pharm Lyse™ solution (1:10) for lysis of erythrocytes in the blood for 3min. Lysis was stopped with 1ml FACS buffer (PBS, 2% FCS). Cell suspension was washed two times.

2.2.5.3. FACS staining procedures

Single cell suspension was washed and centrifuged in FACS buffer. Afterwards 200µl of single cell suspension were added per well in a 96-well plate. Cells were centrifuged and washed with FACS buffer. Cells were resuspended in 30 µl blocking buffer, consisting of anti-CD16/CD32 antibody diluted 1:100 in FACS buffer, then incubated for 5 min at 4°C. Fluorochrome-labelled antibodies were diluted 1:50 in FACS buffer. 50 µl of this antibody mix were added to each well which lead to a final concentration of 1:100. A 96-well plate was incubated for 15 min on ice in the dark. After incubation, single wells were filled with 140 µl of FACS buffer and the plate was centrifuged. Cells were washed and resuspended then washed again with 200 µl of FACS. Cells were resuspended in 100µl of FACS buffer and 100µl of 4% PFA solution was added at each well (final concentration: 2% PFA) to fixate cells. After 20 min, incubation cells were centrifuged and washed with 200µl of FACS buffer. Finally, cells were stored in 200µl of FACS buffer. Fixed cells were analysed by flow cytometry with BD Fortessa LSR.

2.2.5.3. Cell counting

The Neubauer chamber was used for the determination of cell numbers. The cell suspension was diluted 1:10 in trypan blue (diluted 1:10 in PBS) to exclude dead cells prior to counting. After counting four squares, the concentration of cells in the original sample was calculated by the following formula:

Cells counted/4 * 10 * 10^4 = cells/ml

The total cell number was extrapolated to the sample volume.

2.2.6. Characterization of B cells and T cells after aCD20 treatment

For the characterization of C57Bl6/j mice after treatment with aCD20 antibody or control antibody in EAE models or naïve mice, mice were sacrificed weekly after 0-14 weeks after the last aCD20 treatment. Single cell suspensions of spleen, lymph node, bone marrow and blood were prepared as described above.

2.2.6.1. Phenotyping of reappearing B cells in EAE

B cell depleted or control antibody treated immunized mice were sacrificed after 8 and 12 weeks after the last treatment. Here, single cell suspensions of splenocytes were stained by following antibody panels by FACS.

Table 14: B cell phenotyping

B cell phenotype	Surface marker
Naive B cells	CD23-, IgM+, IgD- P
Mature B cells	CD23+, CD38+, IgM-, IgD+
Memory B cells	$B220^{high}$, CD38+, IgD-
Regulatory B cells	$CD1d^{high}$, CD5+
Germinal center cells	CD37+, GL7+
Activated B cells	CD27+, CD69+, CD80+,
Antigen-activated B cells	CD27+, CD69+, CD80+, $MHCII^{high}$
Plasma cells	CD138+, MHCII-
Plasma blasts	CD138+, MHCII+

2.2.7. Co-culture experiments

2.2.7.1. Isolation of B cells and MOG-specific T cells

Splenocytes were isolated as described above in 2.2.5.1.. B cells and T cells were isolated by magnetic associated cell sorting (MACS). Single cell suspension of the spleen was washed two times with MACS buffer and treated according to the manufacturer's instructions. B cells were sorted negatively by using Lineage panel (mouse, BD). T cells were purified using the CD4+ T cell isolation kit II (mouse, BD). Afterwards, the LS columns and the QuadroMACS™ separator were used to isolate the specific cell population according to manufacturer's instructions. Isolated B cells and T cells were used for co-culture or further experiments.

2.2.7.2. CFSE staining of isolated T cells

For analyzing T cell proliferation, T cells were stained with carboxyfluorescein succinimidyl ester (CFSE). CFSE can penetrate the intact cell membrane and binds irreversibly to intracellular proteins. At each cell division CFSE stained cytoplasma is halved. Due to this fact CFSE staining makes it possible to distinguish proliferation and their division status. Isolated T cells were counted and resuspended in 1ml PBS. 800µl of this cell suspension were incubated with 200µl CFSE solution (1:100, 5mM CFSE stock solution) for 10 min. Afterwards cell suspension was washed two times with RMPI complete.

2.2.7.3. LPS/CpG stimulation of reappearing B cells *ex vivo*

B cells of aCD20 or control antibody treated immunized mice were isolated 8 and 12 weeks after last aCD20 or control treatment as described in 2.2.3.1.. 200.00 B cells per well were plated in 200µl RPMI complete. These isolated B cells were stimulated with 5 µg/m, 10µg/ml LPS or 1µg/ml, 10µg/ml CpG overnight (18h). Supernatant was analyzed for released IL-6 and IL-10 by ELISA.

2.2.7.4. MOG-Binding assay

For analysing antigen-binding capacity, isolated reappearing B cells were incubated with fluorescence labelled rMOG protein for 2h at 37°C and 5% CO_2. Labelling of rMOG protein was performed according to manufacturer's instructions. After the incubation, B cells were washed with 200 µl FACS buffer, then resuspended in 200 µl FACS buffer and immediately analysed by flow cytometry.

2.2.7.5. Co-culture of reappearing B cells and MOG specific T cells

To investigate the APC function of reappearing B cells after aCD20 treatment, co-culture assays were performed. Preventively aCD20 or control treated mice of rMOG and MOG p35-55 EAE were sacrificed at week 7, 8, 12, 14 and 18 after last treatment. Single cell suspension of splenocytes was prepared as described in 2.2.5.1. and B cells were isolated by MACS separation (2.2.7.1). Further MOG specific T cells of 2D2 mice were isolated and stained with CFSE (2.2.7.2.).

500.000 isolated B cells were co-cultured with 20.000 MOG specific, CFSE stained T cells and plated in 96-well plate in 200µl of RPMI complete. Different concentrations of rMOG protein (0, 5, 25, 50µg/ml) and MOG p-35-55 (0, 5, 25, 100 µg/ml) were used to re-stimulate the B cells according to their immunization. Cells were co-cultured for 72h at 37°C, 5%CO_2, 95% humidity. Afterwards, supernatant was analyzed for IL-17, IL-2, IFN and IL-6 by ELISA. T cells were analyzed for proliferation rate by FACS.

2.2.7.6. Stimulation of T cells during B cell repletion

For investigating influence of aCD20 treatment on T cells during B cell repletion, T cells were isolated by MACS (s. 2.2.3.1.) and antigen independent stimulation with aCD3/aCD28 antibodies was performed. 96-U-buttom well plate was coated with different concentrations of aCD3 antibody (0, 0.125, 0.25, 0.5, 1 µg/ml) and aCD28 antibody (10µg/ml) for 6-8h at room temperature. A 96-well plate was washed two times with 200µl PBS and 200µl of isolated CFSE stained T cells ($1x10^6$ cell/ml in RPMI complete) were added immediately. Cytokines in supernatant were measured by ELISA. Proliferation rate was analyzed by FACS.

2.2.8. *In vivo* proliferation experiments

2.2.8.1. *In vivo* proliferation of remaining B cells after aCD20 treatment

Ten days after immunization of the preventively depleted or control treated Ab C57Bl6/j mice were injected intraperitoneally with 150µl of Bromodeoxyuridine (BrdU). BrdU is a synthetic nucleotide analog to thymidine and allows to investigate the proliferation of cells *in vivo*. BrdU was built into the DNA after cell division and proliferation can be determined. After 48h mice were sacrificed and spleen and lymph node were investigated for proliferating cells. Therefore, single cell suspension was prepared according to manufacturer's instructions. Single cell suspension was stained for BrdU+ cells with an antibody against BrdU according to the manufacturer's instructions.

2.2.8.2. *In vivo* proliferation of reappearing B cells 8 weeks after aCD20 treatment

For investigating the proliferation of B and T cells in spleen, lymph node and bone marrow of reappearing B cells 8 weeks after the last depletion, the same experimental setting as described in 2.2.8.1. was used. Instead of day 10 after immunization, BrdU was injected at day 52 (end week 7) and the proliferation was analyzed at week 8 (day 56).

2.2.9. ELISA

Cytokines of co- or single culture experiments and *ex vivo* stimulation were measured in supernatant by ELISA. The Mouse IFNγ or GM-CSF ELISA MAX™ standard set was used. 96-well plates were coated with 100µl of capture antibody solution (1:200 diluted in coating buffer). The next day, three washing steps were performed and then plates were blocked for 1h with RD1 buffer at RT. Standard solutions were prepared according to the manufacturer's instructions.

After three washing steps, 30µl of the sample were added and incubated over night at 4°C. Again three washing steps and antibody detection were performed (1:200 in RD1 buffer) and then incubated for 2h. Afterwards, three times of washing was performed and 100µl Avidin-HRP was added for 30 min. Subsequently, four washing steps were performed and 100µl of TMB was added until the colour changed into blue. After that, the colour change reaction was stopped by ELISA stop buffer. OD were determined by iMaik™ microplate reader at 450 nm with 540 nm wavelength correction.

2.2.10. Histology

2.2.10.1. Perfusion, tissue collection and sample preparation

Mice were analyzed 14 weeks after the last aCD20/control treatment. Mice were sacrificed and perfusion was performed by punctuation of the left heart ventricle and flushing first by ice-cold PBS followed by 4%PFA for fixation. Brain, spinal cord, liver and spleen were collected in 4% PFA. After 2 days, PFA was replaced by PBS and stored for at least 24h. Brain was sliced in four transverse sections and spinal cord in 10-12 sections.

Organ sections were watered and then gradually dehydrated overnight before paraffin embedding. This was done by an automated tissue processor which is performing a graded alcohol/xylene/paraffin series. Afterwards, paraffin blocks were sliced into 1µm thick slices by microtome and then laid on glass slides.

Prior to any staining procedure, deparaffination and rehydration were performed in the following steps:

4x 10 min xylol

1x 5 min isoxylol

2x 5 min 100% isopropyl alcohol (IPA)

1x 5 min 90% isopropyl alcohol (IPA)

1x 5 min 70% isopropyl alcohol (IPA)

1x 5 min 50% isopropyl alcohol (IPA)

Distilled water

After finishing the staining procedure, the slices were dehydrated in reverse order.

2.2.10.2. Luxol Fast Blue/Periodic Acid Schiff (LFB/PAS staining)

LFB/PAS staining was performed to access demyelination in the CNS. Myelin was stained by LFB in blue by binding to lipoproteins, while PAS staining demyelinated areas in pink. After deparaffination and rehydration, slices were incubated overnight in LFB solution. The next day,

after washing the slices in 90% IPA, they were differentiated by dipping them into 0.05% lithium carbonate solution followed by a short dip into 70% IPA and a rinsing in dH2O. Then, slices were incubated with 1% periodic acid. Subsequently, slices were washed under tap water and dH_2O. Slices were incubated in Schiffs's solution for 20min and washed with tap water. 5 min of incubation with Mayer's hemalaun were followed by differentiation in 1%HCl-alcohol (1%HCl-alcohol in 90% isopropyl). The last step was washing the slices under tap water. Finally, the tissue was dehydrated and mounted in DePex medium.

2.2.10.3. Immunohistochemical staining

Visualization of signals was done by binding of avidin couples peroxidase (POX) and oxidation of DAB by POX in presence of H_2O_2. Different pre-treatments allowed enhancement of the signals. This included heating by microwave at 800W for 5x3min, acid (1mM citric acid or 1mM Tris-EDTA) or proteinase treatment (10min, 37°C). After deparaffination, rehydration and pre-treatment slices were washed 3x with dH_2O. One further washing step with PBS was performed and slices were blocked with endogenous peroxidase to avoid unspecific signals. After rinsing 3x with hH_2O pre-incubation with 10% FCS for 20 min, unspecific antigen-binding was reduced. Again slices were washed 3x times and then incubated with the primary antibody (diluted 10% FCS/PBS) overnight in a humidified chamber. Afterwards washing steps were performed followed by incubation with biotin conjugated secondary antibody (diluted in 10% FCS/PBS) for 1h. The slides were rinsed with hH_2O and then incubated in 0.1% POX for 1h. Signal development was performed by putting slices into DAB for several minutes and then rinsed immediately in PBS. Nuclei counterstaining was performed with Meyer's hemalaun for 30sec followed by short washing with PBS. The differentiation was performed with 1% HCl-alcohol (1% HCl in 90% isopropyl alcohol). Rinsing slices with tap water was done for blueing of the tissue. The slices were dehydrated and mounted in DePex medium.

2.2.11. Statistical analysis and data analyzation

Flow cytometric data were evaluated with BDDiva™ and FlowJo 10.1 software. Statistics were calculated using the software GraphPad Prism 6. Unpaired t-test or Mann-Whitney-U test were used for all statistical comparison. A value of $p<0.05$ was considered as significant. Data are presented as mean ± SEM.

3. Results

3.1. Analysing depletion and repletion of B cells after aCD20 treatment

3.1.1. Characterization of remaining B cells after aCD20 treatment

Previous research has shown that B cell depletion is not completed by using aCD20 treatment[95]. Small remaining B cell populations are still present in all immune relevant compartments. The goal of this study was to investigate the status of these remaining B cells and to understand the effect of B cell depletion by analysing B cell frequency in different immune relevant compartments.

To investigate the efficiency of the aCD20 treatment, C57Bl6/j mice were treated with 0.2mg aCD20 monoclonal antibody or isotype control antibody (from now on referred to as control treated) three times. To analyse the number of B cells, a FACS staining with antibodies against B220, CD19, CD20 and CD27 was performed (figure 5).

The results show that B220+ CD19+ B cell frequency was significantly reduced from 59.53±1.58 % to 9.24±3.98 % upon aCD20 treatment in spleen ($p<0.05$). A similar reduction was measured in the lymph node from 33.52%± 1.32 B cells in the control treated group and 7.22± 0.58 %in the aCD20 treated group ($p<0.05$).

The most effective reduction of B cells was found in the blood. Here, the control group showed 41.25% to 50.40% B cells. After depletion with aCD20 Ab these B cell populations were significantly abolished (2.74±1.6%, $p<0.005$). In the bone marrow, a less effective, but still significant depletion of B220+CD19+ B cells was detectable. Here, aCD20 treatment reduced the B cells frequency from 28.2± 1.84% in the control group to 18.3± 1.84% in aCD20 treated group ($p<0.05$).

Due to this uncomplete depletion in the investigated compartments (figure 5), CD20 expression of the remaining B cells after aCD20 treatment was analysed. In spleen, lymph and even in blood the remaining B cells show a CD20 expression from 97.3-99.8%, while in the bone marrow a non depletable CD20-population was detected (figure 5 b). This CD20- B cell population was also measured in the control group and 32.45±3.57% of the B cells in bone marrow are CD20- and not affected by CD20 antibody treatment. In bone marrow B cell development take place and CD20- precursor B cells are usually present.

Further characterisation of the remaining B cell population showed an enrichment of CD27+ B cells which are defined as activated B cells upon aCD20 treatment in the spleen (figure 5 c). Especially in the spleen (remaining B cells 31.28±5.45% vs 13.14±2.19% ctrl treated B cells,

$p<0.05$) and in the lymph node (remaining B cells 21.57±3.03% vs 11.6±1.72% ctrl treated B cells, $p<0.05$) this enrichment was measured with a significantly higher amount of CD27+ activated B cells compared with in the control group ($p<0.05$).

To investigate the localization and abundance of B cells in the spleen after treatment with aCD20 or control Ab, a histology was conducted. This histology stained with an antibody against B220 (figure 5 d) confirmed a reduction of B cells and revealed that the remaining B cells are located in the germinal centre structure.

In summary, the remaining B cells in the spleen, the lymph node and the blood are CD20+, which means that they theoretically can be affected by the aCD20 Ab treatment. Here, the histology of aCD20 treated spleen revealed that the remaining B cells are possibly structurally protected against the aCD20 Ab. This hypothesis could also explain the high enrichment of CD27+ activated B cells which were mostly found in germinal centre structures.

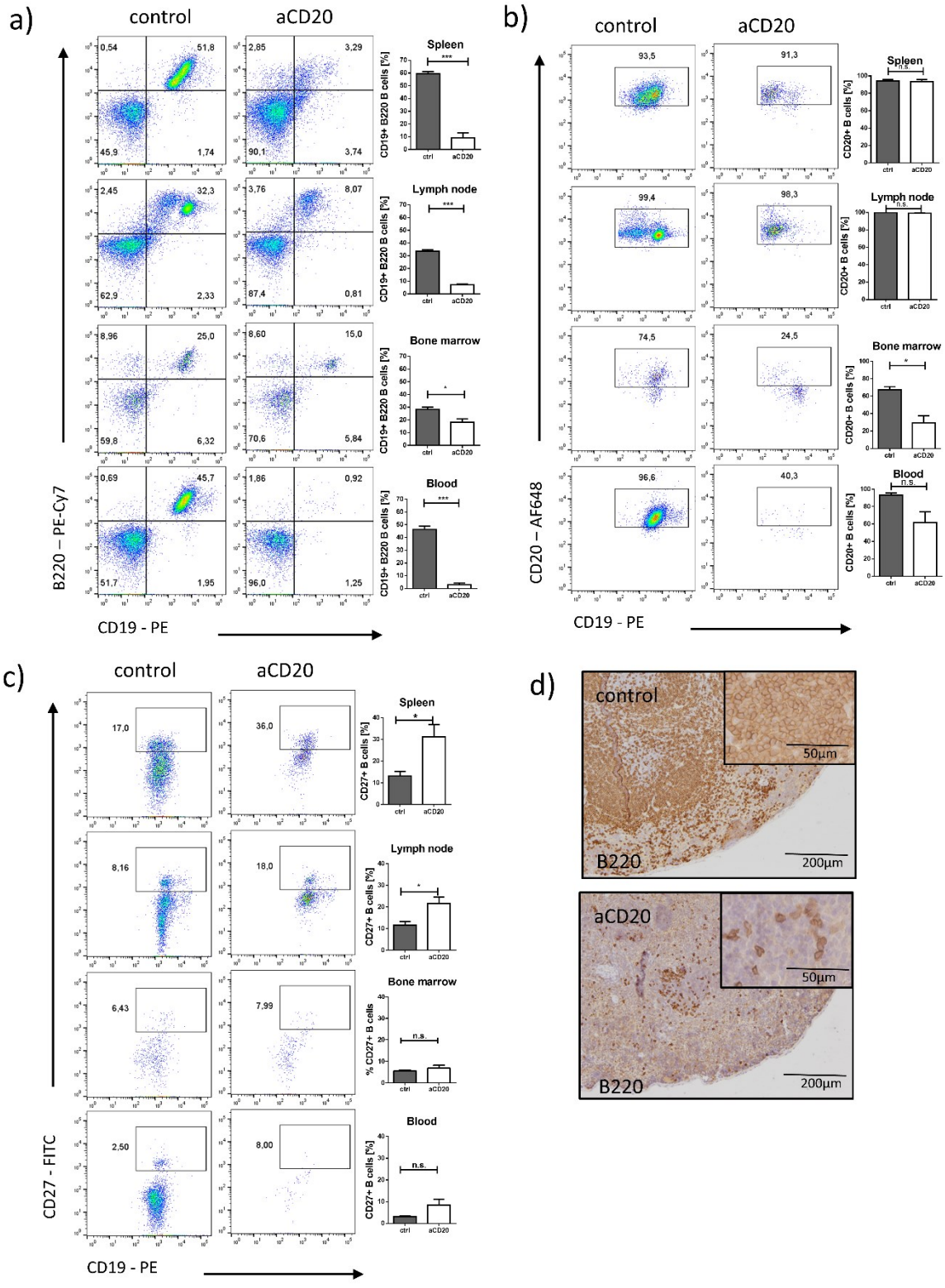

Figure 5: Characterization of B cells after aCD20 treatment.

C57bl6/j mice were treated three times with 0.2 mg of aCD20 or control Ab. a) shows representative FACS plots and frequencies of B220+ CD19+ B cells in spleen, lymph node, bone marrow and blood. b) shows the frequencies of remaining CD20+ B cells and c) the frequencies of CD27+B cells. d) representative sections of spleen from control or aCD20-treated mice are shown which were stained for B220+ cells. Means are shown of n=3 per group.

3.1.2. B cell repletion in naïve mice

MS patients treated with aCD20 Ab are monitored for the reappearance of B cells in the blood. To address the question whether the blood is the suitable monitoring compartment, we analysed the reappearance of B cells in naïve mice by FACS at several points of time in the spleen, the lymph node, the bone marrow and the blood.

To investigate the repletion kinetic at different points in time after aCD20 treatment the B cell frequency of aCD20 treated and control treated mice were measured in different compartments. For each investigated time point the B cell frequency of control treated mice was set at 100% and B cell frequency of aCD20 treated mice was normalized to this value.

The first evidence of reappearing B cells were observed in the spleen and the bone marrow after the last aCD20 treatment at week 7. This effect was not seen in the blood or in the lymph node at that time. In week 9 after the last treatment, B cells were also detected in the blood and the lymph node while reappearance of B cells was almost fully completed in the spleen and the bone marrow.

Directly after three times of depletion, the CD19+B220+ B cell population is clearly depleted in all investigated compartments as described previously in this study. Even in week 4 after the last aCD20 treatment, no increase of the B cell population in all investigated compartments was observed. The first increase of B cells took place at week 7 after the last depletion while no increase of the B cell population was observed in any of the other compartments. In the bone marrow, a small increase was measured compared to control group. In contrast, the B cells in the blood were still fully depleted and B cells did not reappear until week 9 (figure 6). However, in all investigated compartments, the repletion was completed 12 weeks after last injection of aCD20 Ab.

These results show that the B cell repletion in mice after aCD20 depletion is not equally distributed in all immune relevant compartments and B cell reappearance in blood and lymph node lacks behind compared to B cell reappearance in spleen and bone marrow.

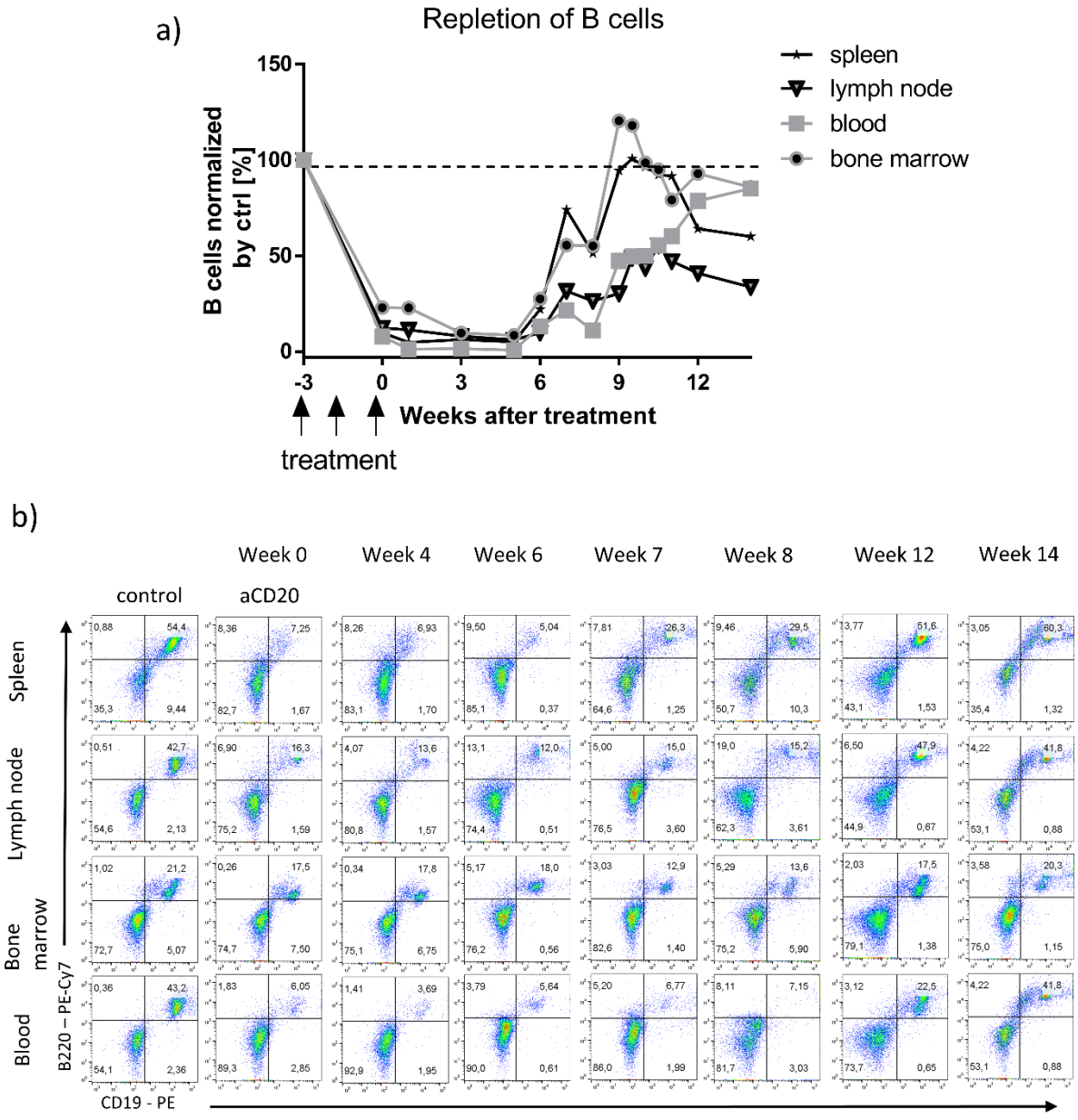

Figure 6: B cell repletion kinetic of naïve mice after aCD20 treatment.
a) shows frequencies of CD19+ B220+ B cells in spleen, lymph node, bone marrow and blood of mice treated three times with 0.2 mg aCD20 Ab or isotype. Data are normalized to mice at the identical point in time. b) shows representative FACS plots of CD19+ B220+ B cells of control-treated mice and reappearing B cells in spleen, lymph node, bone marrow and blood of aCD20-treated mice during B cell repletion. Repletion kinetic shows means of two independent experiments with n=2 per group and point in time.

3.1.3. B cell repletion in the EAE models

To assess whether blood is the optimal monitoring compartment for the reappearance of B cells and the consequence of reappearing B cells in patients with MS, two different EAE models were used. The first EAE model was induced by MOG p35-55, were EAE is T cell mediated. The second EAE model was induced by rMOG protein. In this model, B and T cells are actively involved in the disease progression.

C57Bl6/j mice were preventively treated with aCD20 or control Ab three times and then immunized with MOG p35-55 or rMOG, both were additionally treated with pertussis toxin.

During EAE course, the B cell frequency changes in the different compartments. Therefore, it is necessary to use control for each investigated time point after aCD20 treatment to investigate the repletion kinetic. For each investigated point in time, the B cell frequency of control treated mice was set at 100% and B cell frequency of aCD20 treated mice was normalized to this value.

In week 7, the reappearance of B cells was observed in the spleen and in the bone marrow. In contrast, in the blood and the lymph node no B cells were detectable at this time. Around week 9, upon the last aCD20 treatment, B cells reappeared in the blood and the lymph node. In week 12, B cells were fully repleted in all investigated compartments (figure 7).

The repletion kinetic of B cells after aCD20 treatment in rMOG EAE started in the spleen and the lymph node. B cells reappeared earlier in rMOG EAE compared to repletion MOG p35-55 and naïve mice around week 6. A further difference between the repletion kinetics was seen in rMOG immunized mice: the repletion started in the lymph nodes and the blood simultaneously. B cell reappearance was more distributed in all investigated compartments in comparison to mice with MOG p35-55 EAE. The B cell repletion in mice with rMOG EAE was fully completed after the last treatment.

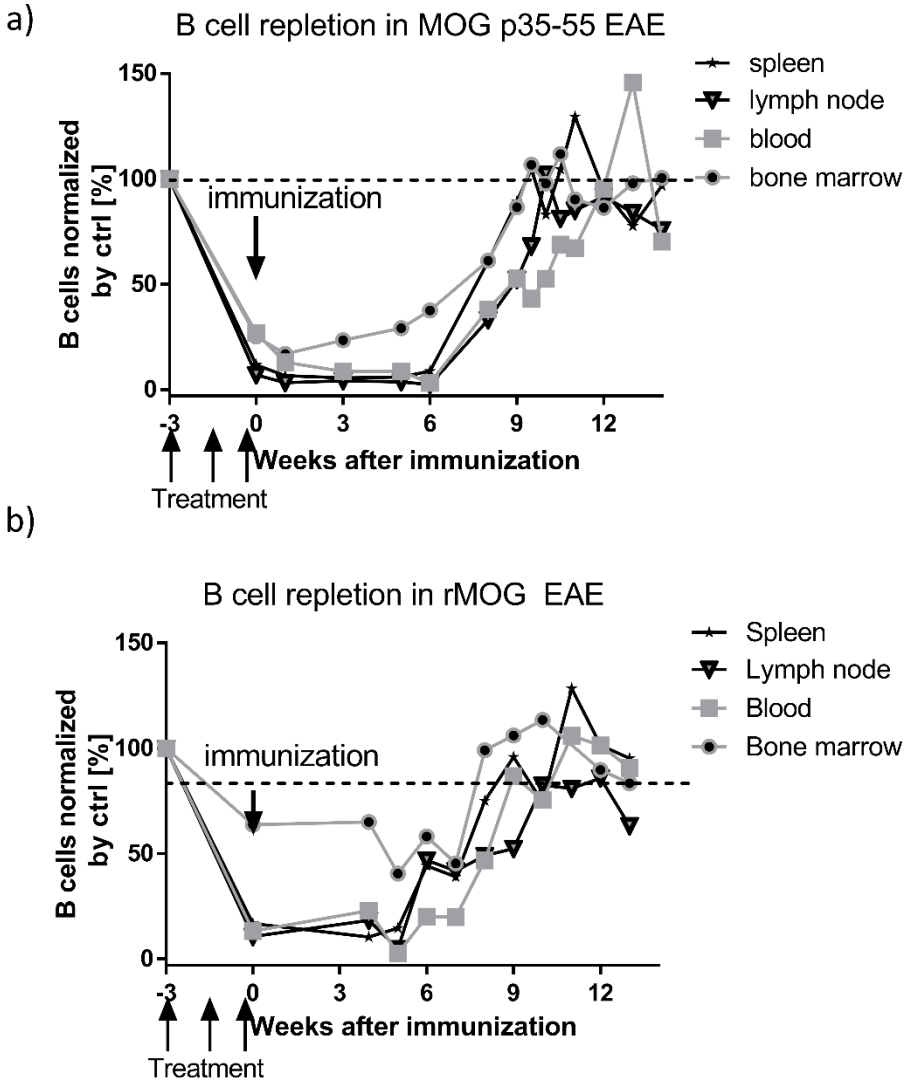

Figure 7: Repletion kinetic in EAE models.

Repletion kinetic of B cells in spleen, bone marrow, lymph node and blood after preventive aCD20 Ab treatment or control Ab in MOG p35-55 EAE (a) or rMOG EAE (b) after aCD20 treatment normalized to a time according control. Mean of two different experiments is shown with n=2 per group and point in time for each experiment was normalized to time according control.

3.1.4. Clinical score after aCD20 treatment in the EAE model

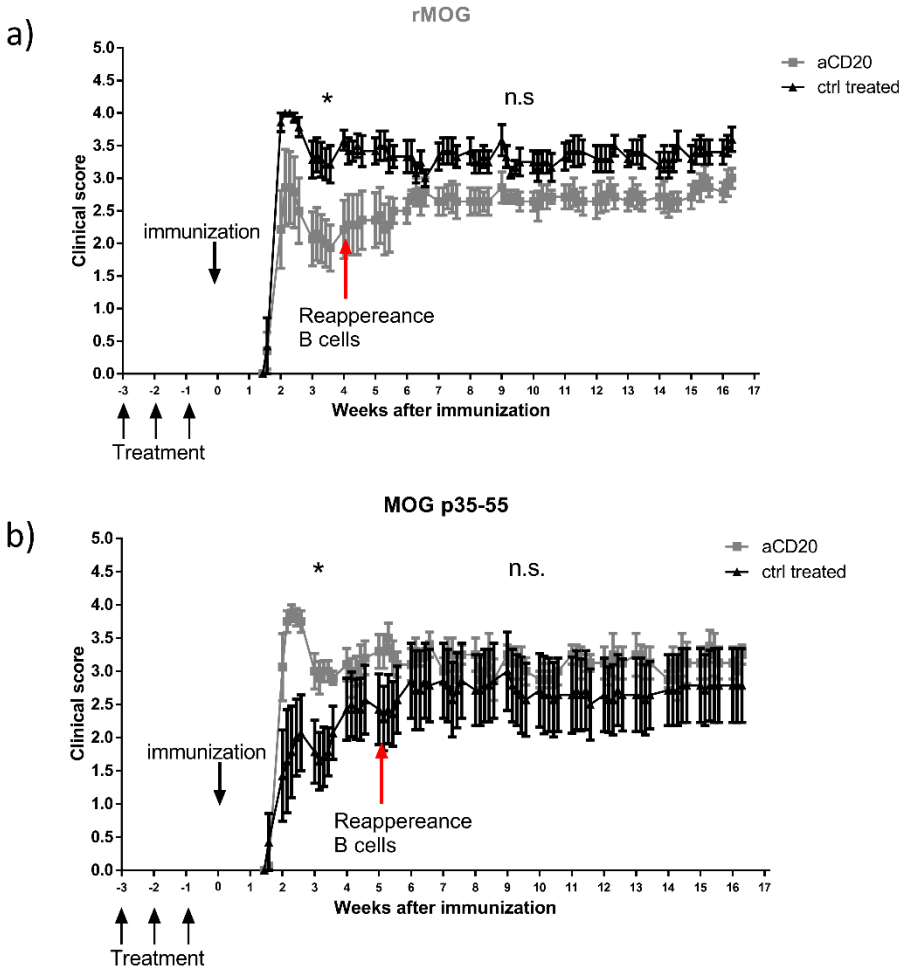

Figure 8: Reappearance of B cells causes different clinical outcome in rMOG and MOG p35-55 EAE.
C57Bl6/j mice were treated three times with aCD20 or control Ab and then immunized with rMOG or MOG peptide. The disease score was monitored daily (s. material and methods). Mean score of n= 4-7 mice per group is shown.

To address the question what the clinical effect of aCD20 treatment in mouse EAE is, the clinical score of the two models was evaluated. The MOG p35-55 EAE is a T cell induced EAE model where B cells are not activated. In contrast, rMOG EAE is a T cell and B cell mediated model in which B cells are actively involved.

In MOG p35-55 induced EAE, a clinical worsening can be observed after preventive treatment with aCD20 antibody (figure 8 b). The most significant difference between control group and aCD20 treated group was found at day 18, defined as the peak of the disease ($p<0.05$) or the inflammatory phase after immunization. This clinical worsening stagnates after the reappearance of B cells (day 60, $p>0.05$).

In contrast, in rMOG EAE (figure 8 a) where B cells are actively involved in EAE progression, the development of the clinical effect was the other way around; B cell depletion (aCD20 treated group mean score 1.5±0.42) caused a significant clinical benefit compared to the control treated group (mean score 3.35±0.26, $p>0.05$) at the peak of the disease. However,

this effect was abolished after reappearance of B cells. When B cells were fully repleted no the clinical difference between the groups were detected (day 60, $p>0.05$).

3.1.5. Characterization of reappearing B cells in EAE

3.1.5.1. Phenotyping of reappearing B cells in EAE

The previous experiments in this study revealed that remaining B cell population of CD27+ activated B cells is enriched after aCD20 treatment. Furthermore, we measured differences in the repletion kinetic between our two EAE models. This leads to the hypothesis that the reappearing B cells are more activated in mice with rMOG EAE than in the T cell mediated EAE model, induced by MOG p35-55.

In the following experiments the phenotype of reappearing B cells were characterized by FACS analysis after aCD20 or control treatment by using several markers.

By analysing CD23 expression, a marker for mature B cells, in reappearing B cells in rMOG EAE (1.22±0.15%) the expression was significantly reduced compared to CD23+ B cells (68.6±1.75%). The same tendency was found in MOG p35-55 EAE. Here, the CD23 expression of the reappearing B cells (22.4±6.2%) was higher in comparison to rMOG EAE. The CD23 expression of both controls, rMOG (66.8±1.75) and MOG p35-55 EAE (68.8±0.55), were at a comparable level (figure 9).

The upregulation of CD27 in the reappearing B cells was most substantial finding. The highest CD27 expression was measured in reappearing B cells of mice with rMOG EAE with 73.45±2.65% compared to the control with 19.35±0.07% CD27 expressing B cells. In MOG p35-55, CD27 expression was upregulated in reappearing B cells (43.00±2.65%) compared to the B cells of control treated mice (18.87±3.72%).

Additionally, the analysed frequency of plasma blasts (CD138+ MHII-) and plasma cells (CD138+ MCHII+) showed a gentle increase in reappearing B cells of mice with rMOG EAE (plasma blast: reappearing B cell 13.29±2.31 vs. 10.63±2.06% ctrl treated B cells; plasma cell: reappearing B cell 19.9±1.25% vs 5.45±0.25% ctrl treated B cells) but a reduction in mice with MOG p35-55 EAE (plasma blast: reappearing B cell 9.28±0.42 vs 14.88±0.98% ctrl treated B cells; plasma cell: reappearing B cells 11.79±0.67% vs 5.33±0.83% ctrl treated B cells). This could be due to the frequency shift caused by the missing depleted B cell population. Thus, the population of plasma blast and plasma cells might not be affected by the aCD20 treatment.

In addition, the phenotype of reappearing B cells in week 12 was analysed after the last aCD20 treatment when B cells are fully repleted in all immune relevant compartments. Reappearing B cells of mice with rMOG EAE consist of more CD27+ activated B cells than the corresponding control. However, the CD23 expression is still lower in repleted B cells than in

control treated mice, but higher compared to CD23 expression in reappearing B cells in week 8.

In contrast, the reappearing of B cells of mice with MOG p35-55 EAE model showed no difference in the composition of B cells compared to their respective controls. Only the frequency of CD27+ expressing B cells is still higher (~2.5%) while frequencies of CD23+ B cells, plasma blast and plasma cells are at a comparable level.

In summary, B cells which reappeared in mice of the rMOG EAE model showed a more activated phenotype than B cells in control treated mice. Additionally, B cells which reappeared in mice of the MOG p35-55 EAE-model also showed a more differentiated phenotype their control but less than reappearing B cells of mice in the rMOG EAE model. The difference between these two different EAE models is even pronounced after the full repletion of B cells.

Next Page

Figure 9: Phenotyping of reappearing B cells 8 and 12 weeks after last aCD20 Ab treatment.
a) Representative FACS plots show the frequencies of CD23+ B cells, CD27+ Memory B cells, plasma blast and plasma cells of all CD19+ B cells. b) shows the B cells subtypes in percentage of CD19+ B cells. c) shows the percentage of CD23+ B cells, CD27+ B cells, plasma blast and plasma cells. The sum of this whole B cell pool was set to 100%. Representative experiment of n=2 per group and time point is shown.

a)

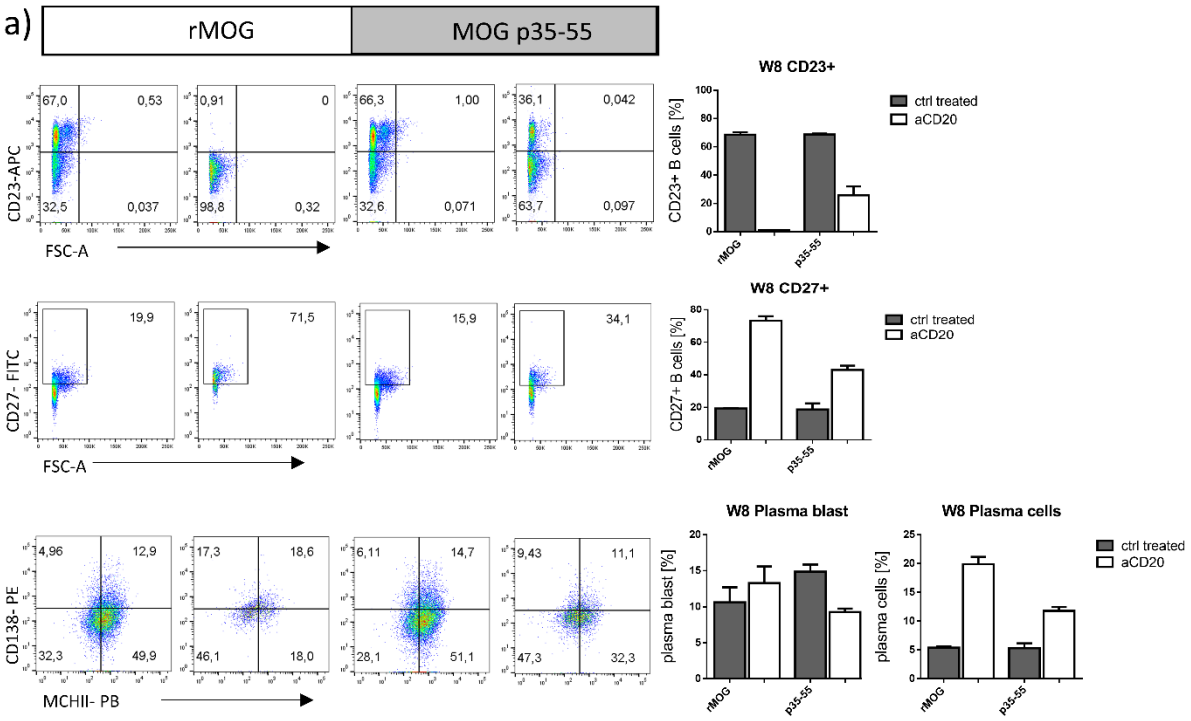

b)

	Week 8				Week 12			
	Ctrl	aCD20	Ctrl	CD20	Ctrl	aCD20	Ctrl	CD20
CD23+ B cells	68,6	1,22	68,8	25,8	69,47	49,87	65,52	59,77
CD27+ B cells	19,35	73,45	18,77	43	21,75	28,9	22,87	23,2
CD38+IgD- B cells	11,75	95,97	12,57	54	12,32	28,52	15,92	16,92
Germinal center cell	12,25	21,27	14,75	19,82	7,43	13,65	8,15	9,43
Regulatory B cells	4,37	8,76	3,45	9,78	2,97	4,66	3,09	3,97
Plasma cell	5,4	19,9	5,33	11,78	3,94	3,76	7,11	5,18
Plasma blast	10,63	13,29	14,87	9,28	11,57	14,95	13,97	13,6
Antigen activated B cells	6,74	24,1	4,99	14,02	1,85	3,15	2,37	2,48

c)

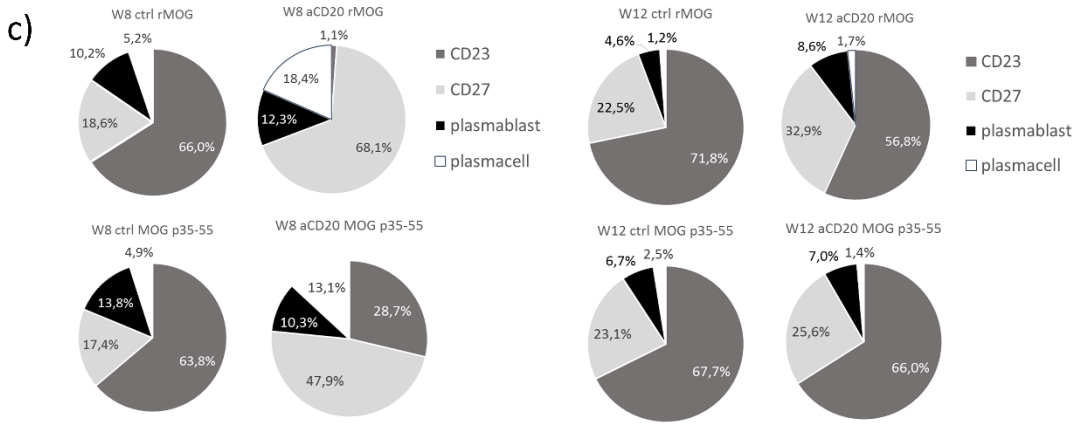

3.1.5.2. Cytokine release after LPS or CpG stimulation

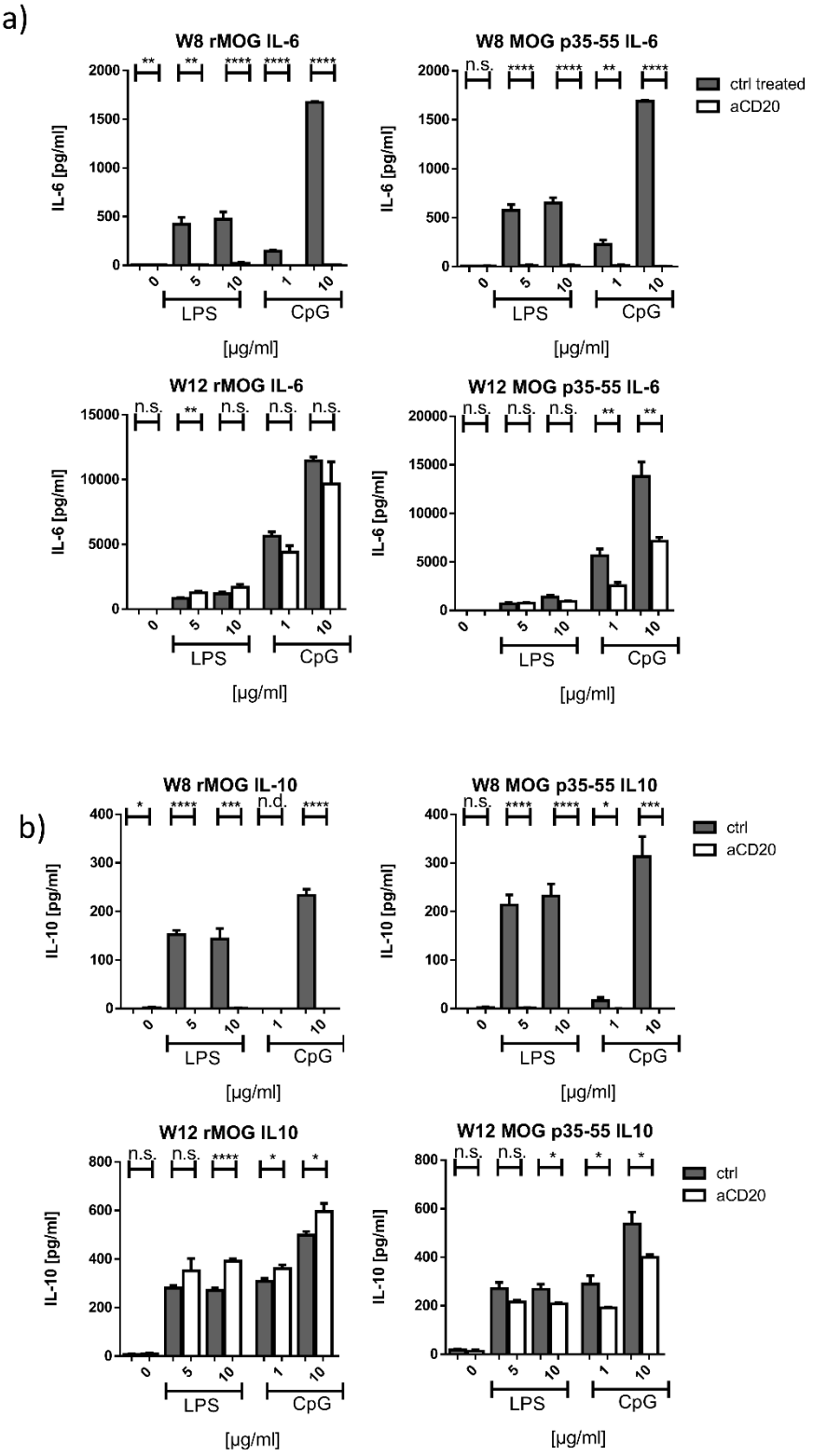

Figure 10: Cytokine release of reappearing B cells after LPS or CpG stimulation.
a) IL-10 and b) IL-6 release of isolated reappearing B cells (week 8 or 12 after last treatment) of aCD20 Ab treated or control treated B cells were stimulated with different concentrations of LPS or CpG. Cytokines were measured in the supernatant by ELISA. Mean of n=3 per group and time point is shown.

To identify the difference of reappearing B cells in rMOG EAE as well as in MOG p35-55 EAE, the release of IL-6, a pro-inflammatory cytokine, and IL-10, an anti-inflammatory cytokine, were investigated after LPS and CpG stimulation. Here the immune response of the two different B cell phenotypes was characterized.

The results show that the IL-10 release was significantly decreased in reappearing B cells of mice with rMOG EAE (5µg/ml LPS: reappearing B cells 0pg/ml vs 132.7±8.59pg/ml ctrl treated B cell, $p>0.0001$; 10µg/ml LPS: reappearing B cells 0.7±0.66pg/ml vs 143.1±21.9pg/ml ctrl treated B cell, $p>0.005$; 1µg/ml not detectable; 10µg/ml: reappearing B cells 0pg/ml vs 233.1±12.58pg/ml ctrl treated B cell $p>0.001$) and mice with MOG p35-55 EAE (5µg/ml LPS, $p>0.0001$; 10µg/ml LPS, $p>0.0005$; 1µg/ml CpG not detectable; 10µg/ml CpG, $p>0.0001$) after LPS as well as after CpG stimulation (1µg/ml not detectable; 10µg/ml $p>0.0001$) in week 8 after the last treatment with aCD20 Ab (figure 10 a). In week 12 after the last treatment, the IL-10 release was higher in reappearing B cells compared to their control (5µg/ml LPS $p<0.005$; 10µg/ml LPS $p>0.0005$; 1µg/ml CpG $p>0.005$; 10µg/ml CpG $p>0.005$), while repleted B cells of mice with MOG p35-55 EAE released a lower amount of IL-10 in comparison to B cells of control treated mice after LPS and CpG (5µg/ml LPS $p<0.005$; 10µg/ml LPS $p>0.005$; 1µg/ml CpG $p>0.005$; 10µg/ml CpG $p>0.005$).

The release of the cytokine IL-6 was significantly lower in reappearing B cells in comparison to B cells of control treated mice in the rMOG EAE in week 8 after aCD20 treatment (5µg/ml LPS $p>0.01$; 10µg/ml LPS $p>0.001$; 1µg/ml CpG $p>0.001$; 10µg/ml CpG $p>0.001$) (figure 10 b). At week 12 after last aCD20 treatment B cells are fully repleted and the released amount of IL-6 was significant higher after stimulation with 5µg/ml LPS ($p<0.05$). After 10µg/ml LPS stimulation, the released IL-6 showed no significant difference compared to the B cells of control treated mice. Also, no significant difference in the release of IL-6 was observed after CpG stimulation. In MOG p35-55 EAE, no significant difference was found in the released amount of IL-6 compared to reappearing B cells and B cells of control treated mice ($p>0.05$). In contrast, reappearing B cells of mice in MOG p35-55 EAE showed a lower amount of released IL-6 after CpG stimulation even after full repletion of the B cells (1µg/ml CpG $p<0.01$; 10µg/ml CpG $p<0.01$).

3.1.5.3 Higher rMOG binding ability of reappearing B cells in rMOG EAE

For analysing antigen-binding capacity, isolated reappearing B cells were incubated with fluorescence labelled rMOG protein.

Reappeared B cells, 8 weeks after the last aCD20 treatment, showed a 5.36±0.22 % binding of rMOG (figure 11), which was significantly higher than in the control group (4.59± 0.21%, $p<0.05$). In contrast, reappearing B cells in MOG p35-55 EAE (3.50±0.05%) displayed a similar binding ability compared to the control treated B cells (3.59±0.11%, $p>0.05$). Further observation revealed a generally lower, however not significant, rMOG binding of isolated B cells od MOG p35-55 EAE in comparison to the B cells of the rMOG EAE (figure 11).

Thus, reappearing B cells of mice with rMOG EAE is able to bind more rMOG protein, while B cells in MOG p35-55 EAE mice showed no difference in rMOG binding ability.

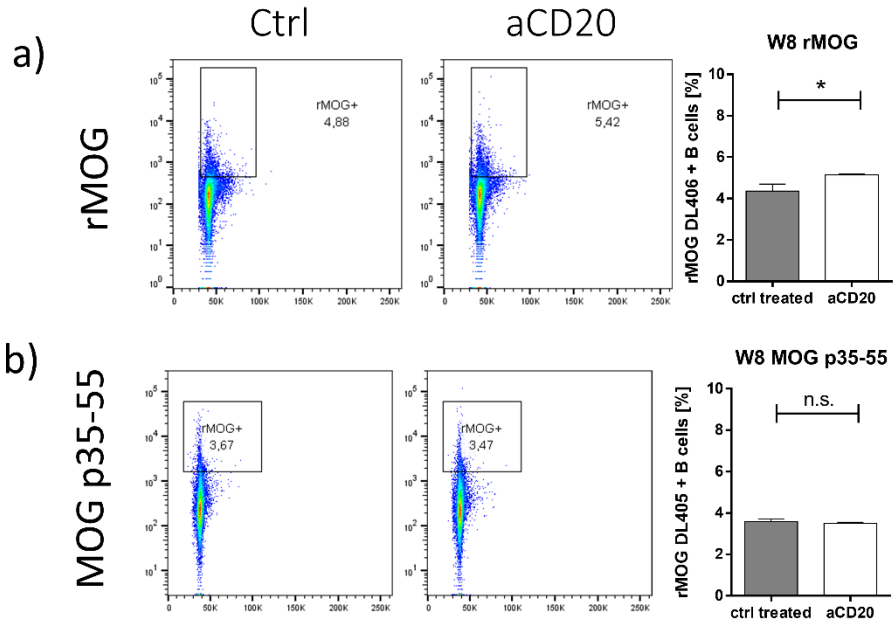

Figure 11: Increased rMOG binding to reappearing B cells in rMOG EAE.
B cells of aCD20 or control treated mice of a) rMOG EAE or b) MOG p35-55 EAE was incubated with fluorescence labelled rMOG for 2h. Shown is one representative experiment of 4 n=3 per group.

3.1.6. Functional characterization of reappearing B cells in two EAE models

3.1.6.1. Superior antigen presenting function of reappearing B cells in rMOG EAE

In the previous part, it was established that reappearing B cells in the rMOG EAE model showed a phenotype with signs of higher activation. Particularly, reappearing B cells showed differences in the cytokine release after LPS or CpG stimulation compared to B cells from control treated mice.

To analyse this phenomenon, further characterization of functional differences was needed and therefore reappearing B cells or B cells from control treated mice were isolated from mice in rMOG EAE or MOG p35-55 EAE model and incubated with MOG specific T cells from 2D2 mice. This co-culture of T and B cells was re-stimulated according to their immunization stimulus with rMOG protein or MOG p35-55. To measure T cell proliferation, the MOG specific T cells were stained with CFSE to investigate the different proliferation stages. After every cell division the fluorescent intensity is halved due to the divided amount of CFSE is between each cell (figure 12 a).

Reappearing B cells of mice with rMOG EAE induced a significantly higher T cell proliferation of MOG specific T cells (figure 12 b) in comparison to B cells of control treated mice. In contrast, reappearing B cells compared with B cells of control treated mice of MOG p35-55 EAE showed a lower T cell proliferation rate. In figure 12 c) the T cell proliferation, caused by reappearing B cells, was normalized to the T cell proliferation rate caused by the control treated B cell control after the last aCD20 treatment at different points in times. At every investigated point in time, the reappearing B cells induced a higher T cell proliferation in MOG specific T cells compared to the control treated B cells (grey points: week 7 mean 132.1±21.39%, week 8 mean 130.08±3.15%, week 12 mean 135.67±25,48%, week 14 mean 134.23±11.85%, week 18=144.30%). The T cell proliferation rate induced by the reappearing B cells from MOG p35-55 EAE mice was normalized to their control. Here, the T cell proliferation, caused by reappearing B cells, is lower or similar compared to the proliferation rate caused by the B cells of control treated mice (black points: week 7 mean 75.69±15.17%, week 8 mean 90.16±2.5%, week 12 mean 87.28±4.52%, week 14 mean 80.30±4.96%, week 18=77.37%).

In summary, reappearing B cells of rMOG EAE mice are superior antigen presenting cells compared to B cells of control treated mice after re-stimulation with the antigen used for immunization and to reappearing B cells of MOG p35-55 EAE mice.

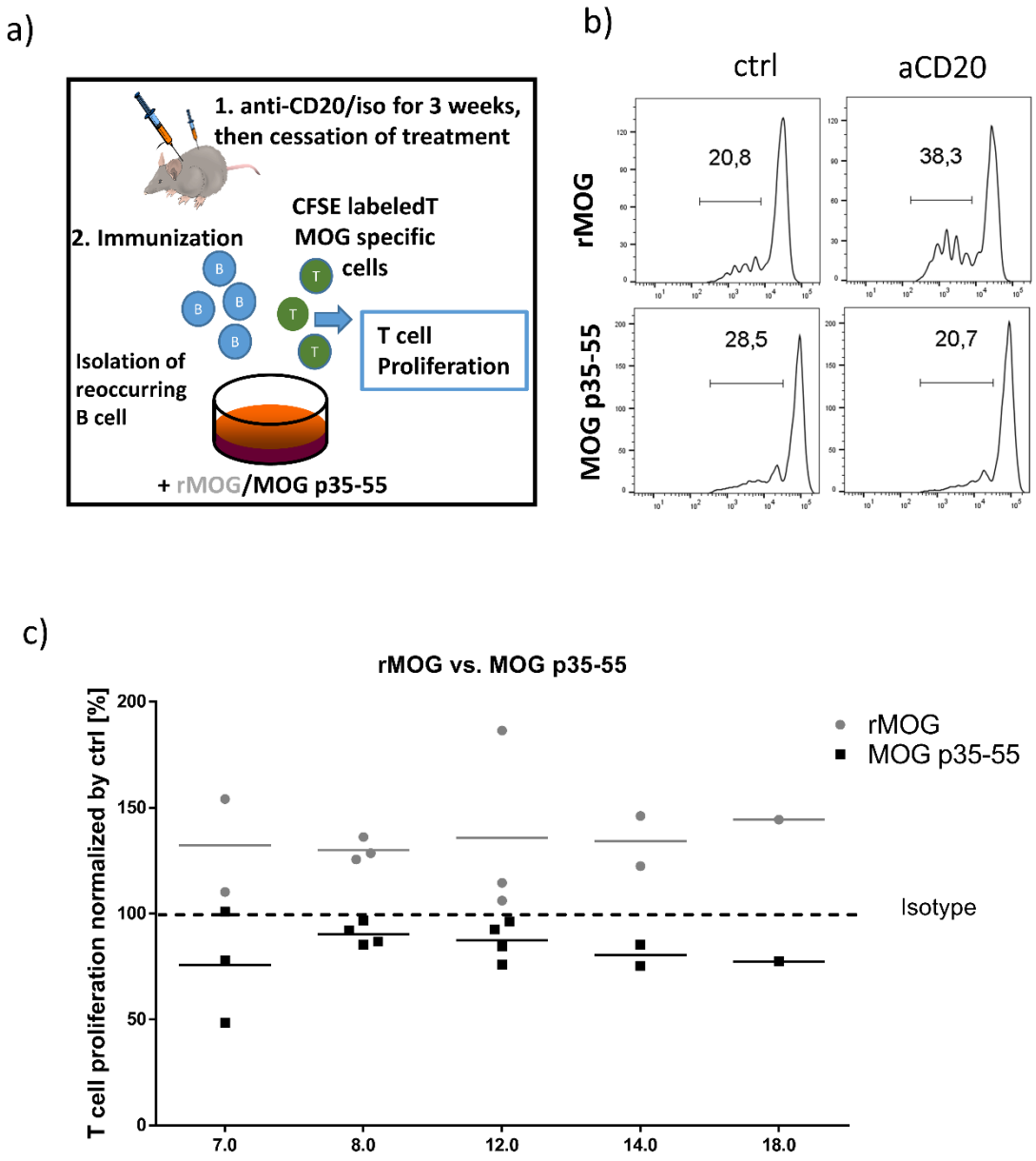

Figure 12: Increased T cell proliferation caused by reappearing B cells in rMOG EAE.
a) shows a schematic representation of the experimental setting. b) shows representative FACS plots of T cell proliferation caused by reappearing B cells or control-treated B cells of mice immunized with rMOG or MOG peptide. c) shows the T cell proliferation rate normalized to the respective control treated group at the identical points in time after the last aCD20 treatment. Single dots show mean of one experiment with n=2 per group and time point.

3.1.6.2. Cytokine release during antigen presentation

To understand how B cells influence T cells during antigen presentation, cytokine release was measured in the supernatants by ELISA. The supernatants were analysed for cytokines commonly released by T cells.

In week 8 after aCD20 treatment (figure 13 a), the co-cultured T cells and reappearing B cells (583.9±24.6pg/ml IFN y) released more IFN y compared to the co-culture with B cells of control treated mice (7.49±4,75pg/ml IFN y). IL-17 was not detected in the co-culture in any condition. Furthermore, the IL-6 release of co-cultured reappearing B cells of rMOG EAE mice (97.37±31.44pg/ml IL-6) was increased compared to co-cultured B cells of control treated mice of rMOG EAE (6.06±3.64pg/ml IL-6). The co-culture of reappearing B cells of MOG p35-55 EAE (41.88±8.43pg/ml IFN y) mice showed a significantly lower amount of released IFN y compared to the co-culture with B cells of control treated mice (70.04±5.12pg/ml IFN y). In general, a significantly lower release of IFN y was measured in reappearing B cells of MOG p35-55 EAE than in the co-culture with B cells from the rMOG EAE mice. The IL-6 release in B cells of MOG p35-55 EAE mice was also lower compared to the co-culture with B cells from the rMOG EAE mice. However, the co-cultured reappearing B cells of MOG p35-55 EAE mice (51.83±16.38pg/ml IL-6) showed a higher release of IL-6 compared to the co-culture of control B cells (27.31±3.03pg/ml IL-6).

At week 12 after the last aCD20 treatment (figure 13 b), B cells were fully repleted and the co-culture of reappearing B cells in rMOG EAE caused a higher MOG specific T cell proliferation (24.58±7.52% CD4+ proliferation) compared to T cell proliferation rate caused by B cells of control treated mice (18.05±2.75% CD4 proliferation). Simultaneously IL-2 release of co-culture of reappearing B cell (536.9±32.67pg/ml IL-2) and B cells of control treated mice (590.6±174.6pg/ml IL-2) was similar. The released IFN y level of reappearing B cell co-culture (424.7±120.3pg/ml IFN y) showed a higher amount of released IFN y compared to co-culture of B cells of control treated mice (248.7±115.4pg/ml IFN y). Furthermore, 8 weeks after the last aCD20 treatment, the release of IL-17 and IL-6 was also increased compared to the cytokine-release–profile of rMOG EAE mice.

The results of reappearing B cells of MOG p35-55 EAE mice 12 weeks after the last treatment were similar to the results gained 8 weeks after the last aCD20 treatment. Proliferation of reappearing B cells (61.3±1.25% CD4+proliferation) was higher in B cells 12 weeks after the last treatment compared to the B cells of control treated mice (40.55±11.45% CD4+ proliferation) in MOG p35-55 EAE mice but not significantly altered in rMOG EAE mice. The measured IL-2 production was similar in co-culture of reappearing B cells (536.9±32.67pg/ml) compared to B

cells of control treated mice (590.4±174.6pg/ml) in rMOG EAE. IFN γ, IL-17 and IL-6 release was still higher in reappearing B cells in rMOG EAE compared to co-culture of B cells of control treated mice. In contrast, proliferation rate and IL-2, IFN γ, as well as IL-17 release of reappearing B cells was lower compared to the co-culture of control treated mice in MOG p35-55 EAE mice IL-6 released by reappearing B cells was comparable to B cells of control treated mice.

To summarize, reappearing B cells of rMOG EAE in co-culture with T cells produced more pro-inflammatory T cell cytokines compared to the B cells of control treated mice, while the cytokine profile in MOG p35-55 EAE showed a less inflammatory cytokine profile.

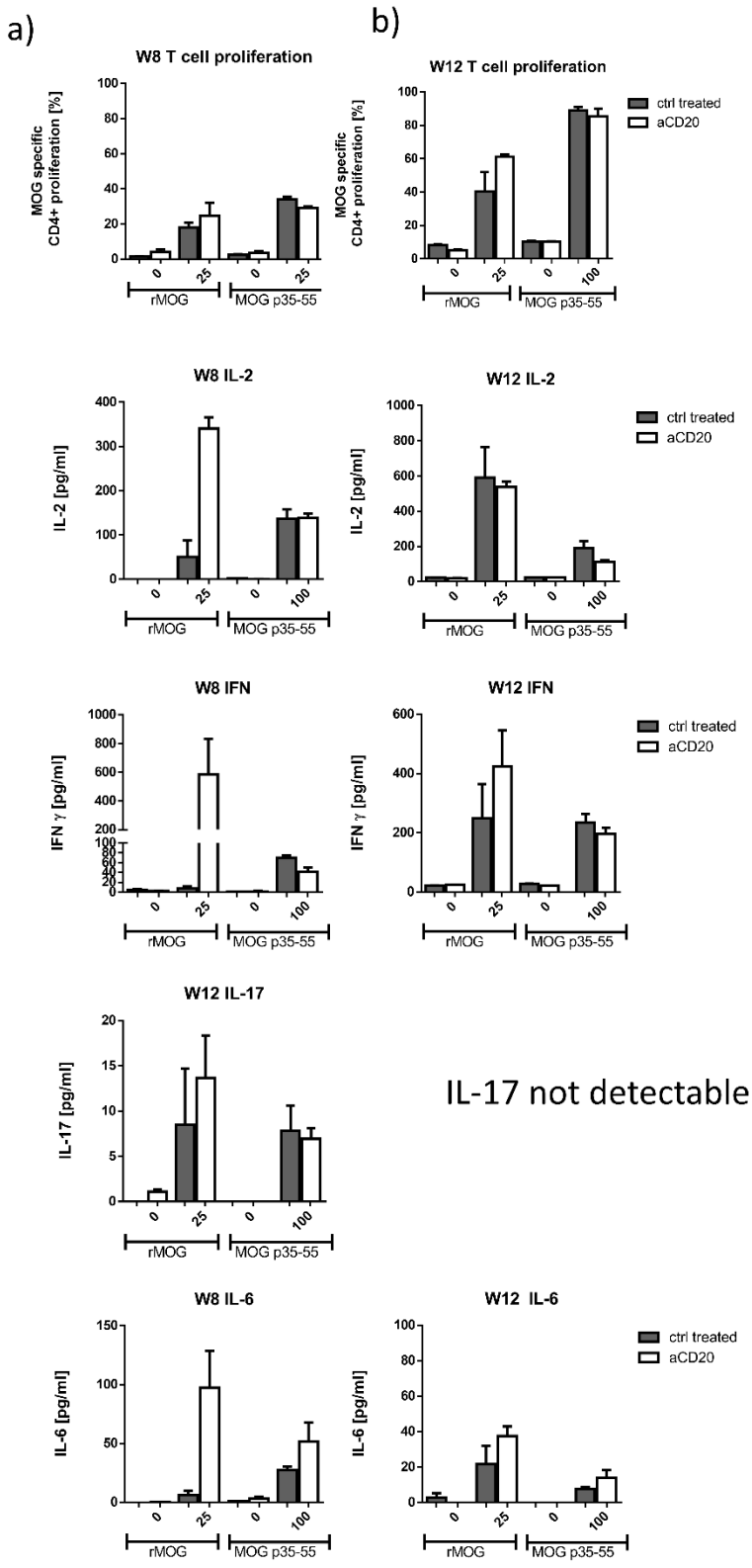

Figure 13: Cytokine release and proliferation rate of co-cultured MOG specific T cells and reappearing B cells in rMOG and MOG p35-55 EAE.

The release of IL-17, IFN y, IL-6 and IL-2 from the co-culture of MOG specific T cells and reappearing B cells or control treated B cells of rMOG or MOG p35-55 EAE at week 8 (a) or week12 (b) after last treatment is shown. Means of one representative experiment are shown n=2 per group and point in time.

3.1.7. *In vivo* proliferation of B cells after aCD20 treatment

3.1.7.1 Increased in vivo proliferation after aCD20 depletion in the EAE model

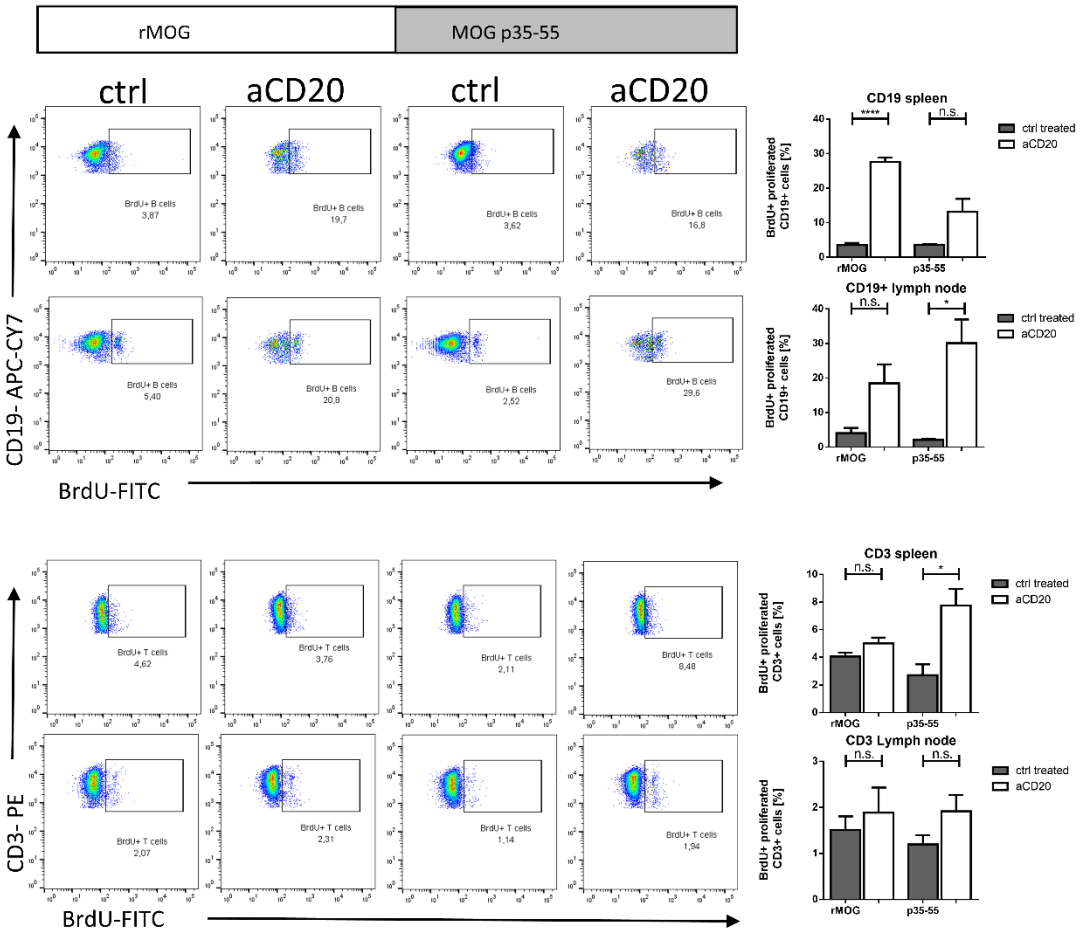

Figure 14: Increased in vivo proliferation of remaining B cells 8 weeks after aCD20 Ab treatment.
a) B cell and b) T cell proliferation after aCD20 or control treatment was investigated after BrdU injection and afterwards stained intracellular for BrdU+ cells and analysed by FACS. Representative FACS plots are shown and bar graphs show mean of one representative experiment out of three (n=3 per group).

To research the effect of aCD20 treatment on B cells *in vivo*, mice were immunized with rMOG or MOG p35-55 after aCD20 or control treatment followed by a BrdU-injection ten days after immunization, which allows the investigation of cell-proliferation after injections. Two days after BrdU-injection, spleen and lymph nodes were investigated for cell proliferation.

In the spleen, remaining B cells in rMOG, as well as in MOG p35-55 EAE showed a significantly higher proliferation rate than their controls (figure 14). B cells of control treated mice in rMOG

EAE exhibited a proliferation rate of 3.56±0.98%, which was significantly lower compared to the remaining B cells (27.6±2.26%, $p<0.001$). Indeed, the remaining B cells in MOG p35-55 EAE mice showed a proliferation rate of 13.14±6.5%, while the B cells of control treated mice had lower proliferation rate (3.6±0.43%, $p>0.05$). In the lymph node, the remaining B cells showed a higher proliferation compared to the B cells of control treated mice in rMOG (reappearing B cells 18.48±5.49% vs. ctrl treated B cells 4.05±1.50%, $p>0.05$) as well as B cells of mice in MOG p35-55 (remaining B cells 30.12±6.84% vs. ctrl treated B cells 2.09±0.26%, $p<0.05$).

Analysation of the T cell proliferation revealed no significantly altered proliferation rates of aCD20 and control treated animals in rMOG EAE in spleen (aCD20 treated 5.01±0.41% vs. ctrl treated 4.06±0.27%, $p>0.05$). In contrast, T cells of MOG p35-55 EAE mice treated with aCD20 Ab showed a significantly higher proliferation rate compared to control treated mice (aCD20 treated 7.75±1.19% vs. ctrl treated 2.7±0.78%, $p<0.05$).In the lymph node, T cells of aCD20 Ab treated mice exhibited a significantly higher proliferation rate compared to control treated mice, as well as T cells of mice with rMOG EAE (aCD20 treated 1.18±0.54% vs. ctrl treated 1.53±0.29%, $p>0.05$) and T cells of mice with MOG peptide EAE (aCD20 treated 1.91±0.35% vs. ctrl treated 1.19±0.19%, $p>0.05$).

This experiment showed that remaining B cells had a higher proliferation rate independent of immunization. Moreover, the findings suggest that B cell depletion also influenced the T cell proliferation, leading to a higher T cell proliferation rate.

3.1.7.2. *In vivo* proliferation of B and T cells 8 weeks after aCD20 Ab treatment

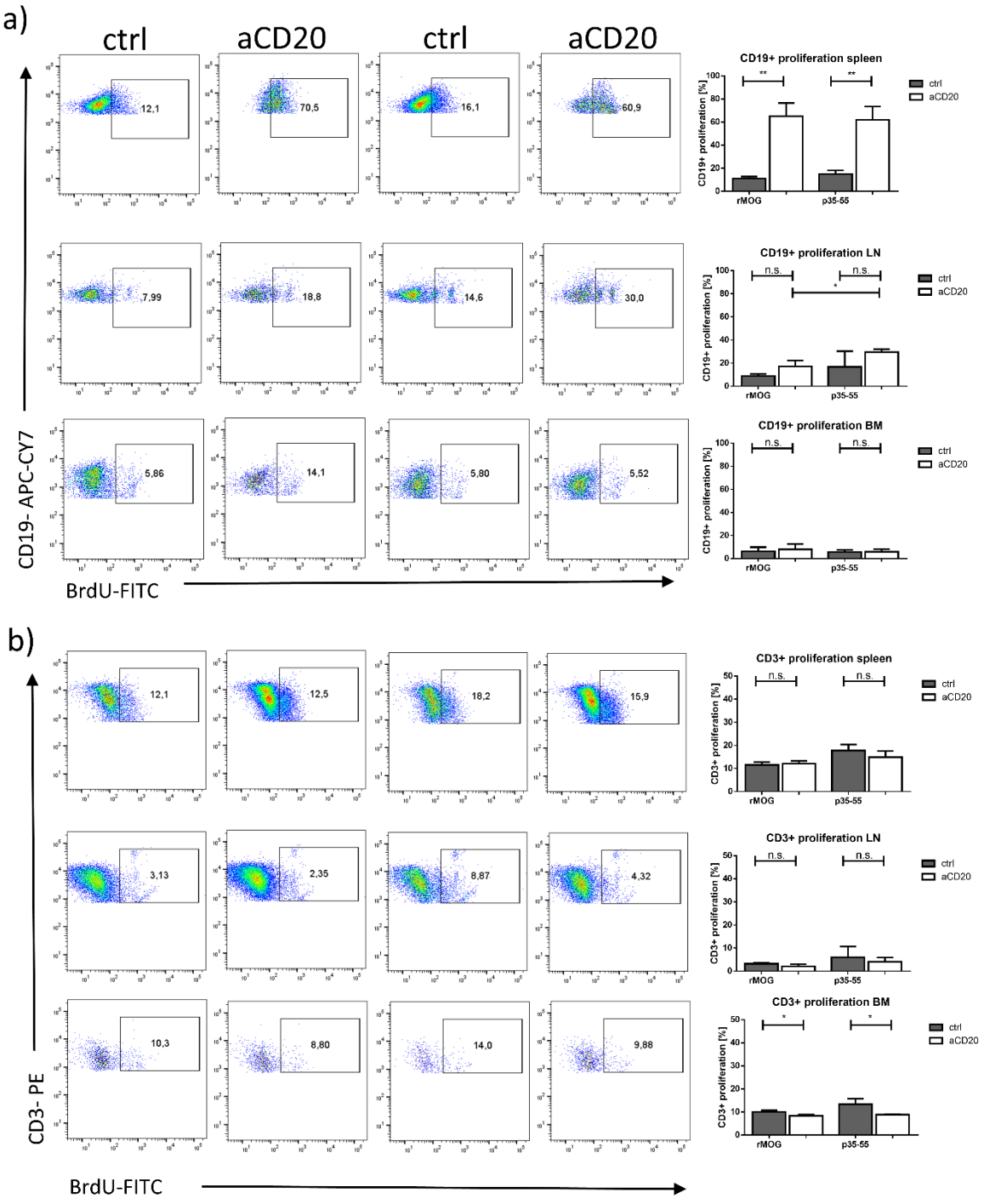

Figure 15: Increased in vivo proliferation of reappearing B cells 8 weeks after aCD20 Ab treatment.
a) B cell and b) T cell proliferation in the spleen, 8 weeks after aCD20 Ab or control Ab treatment, was investigated after BrdU injection and followed by intracellular staining for BrdU+ cells and analysis via FACS. Representative FACS plots are shown and the bar graphs represent the mean of n=4 per group.

In the previous experiments, the remaining B cells in the spleen as well as in lymph nodes showed a higher proliferation rate after aCD20 Ab treatment compared to their control. To

address the question whether these highly proliferating remaining B cells are the ones which reappear after 8 weeks, the same experiment was performed again 8 weeks after the last treatment and BrdU was injected at the end of week 7 to investigate the proliferation rate.

When B cells started to reappear around week 7, the B cell proliferation in the spleen was significantly increased compared to the control treated mice with rMOG EAE (reappearing B cells 65.01% vs 11.15% ctrl treated B cells BrdU+, $p<0.01$) as well as in MOG p35-55 EAE mice (reappearing B cells 62.01% vs 15.08% ctrl treated B cells BrdU+, $p<0.01$) (figure 15). In the lymph node, the B cell proliferation rate of reappearing B cells was increased, but not significant in both EAE rMOG (reappearing B cells 8.80% vs 17.13% ctrl treated B cells BrdU+, $p>0.05$) and MOG p35-55 (reappearing B cells 29.28% vs 16.18% ctrl treated B cells BrdU+, $p>0.05$). However, the proliferation rate of B cells in the bone marrow was low (3.48-10.48% proliferation) and not significantly increased in the reappearing B cells ($p>0.05$).

To investigate the effect of B cell depletion on T cells, the T cell proliferation was measured at the time of B cell reappearance. In spleen, the T cells of the restored mice did not show an increased proliferation rate in rMOG EAE mice (reappearing B cells 11.56% vs 12.13% ctrl treated B cells BrdU+, $p>0.05$) or MOG p35-55 (reappearing B cells 17.75% vs 14.85% ctrl treated B cells BrdU+, $p>0.05$).The same trend was seen in lymph nodes. However, the T cell proliferation in the bone marrow was significantly reduced in aCD20 treated mice compared to control treated mice (rMOG: reappearing B cells 10.09% vs 8.35% ctrl treated B cells BrdU+, $p<0.05$;MOG p35-55: reappearing B cells 13.41% vs. 8.89% ctrl treated B cells BrdU+, $p<0.05$).

In summary, the remaining B cells started to proliferate in the spleen, where repletion of B cells started. Furthermore, the performed experiments showed that the reappearance of B cells did not influence T cell proliferation in both EAE models.

3.2. Direct and indirect effects on T cells after aCD20 treatment

3.2.1. Dynamics of the T cell population during B cell repletion

We investigated the T cell population in C57Bl6/j mice after a threefold aCD20 or control treatment. To analyse the influence of aCD20 treatment on the T cell population, we investigated the CD3+ T cell frequency during B cell repletion.

The first finding was a relative increase in the frequency of T cells in all investigated compartments due to the missing B cell population. The CD3+ T cell frequency was normalized to the time according control in figure 16. Until the B cells started to reappear at week 8 after the last aCD20 treatment, the T cell frequency was at least 180% of the frequency in control treated mice and nearly returned to normal in all investigated compartments at week 12, when B cells were fully repleted.

This shift of the CD3+ T cell frequency was caused by the missing B cell population and rebalanced after the reappearance of B cells.

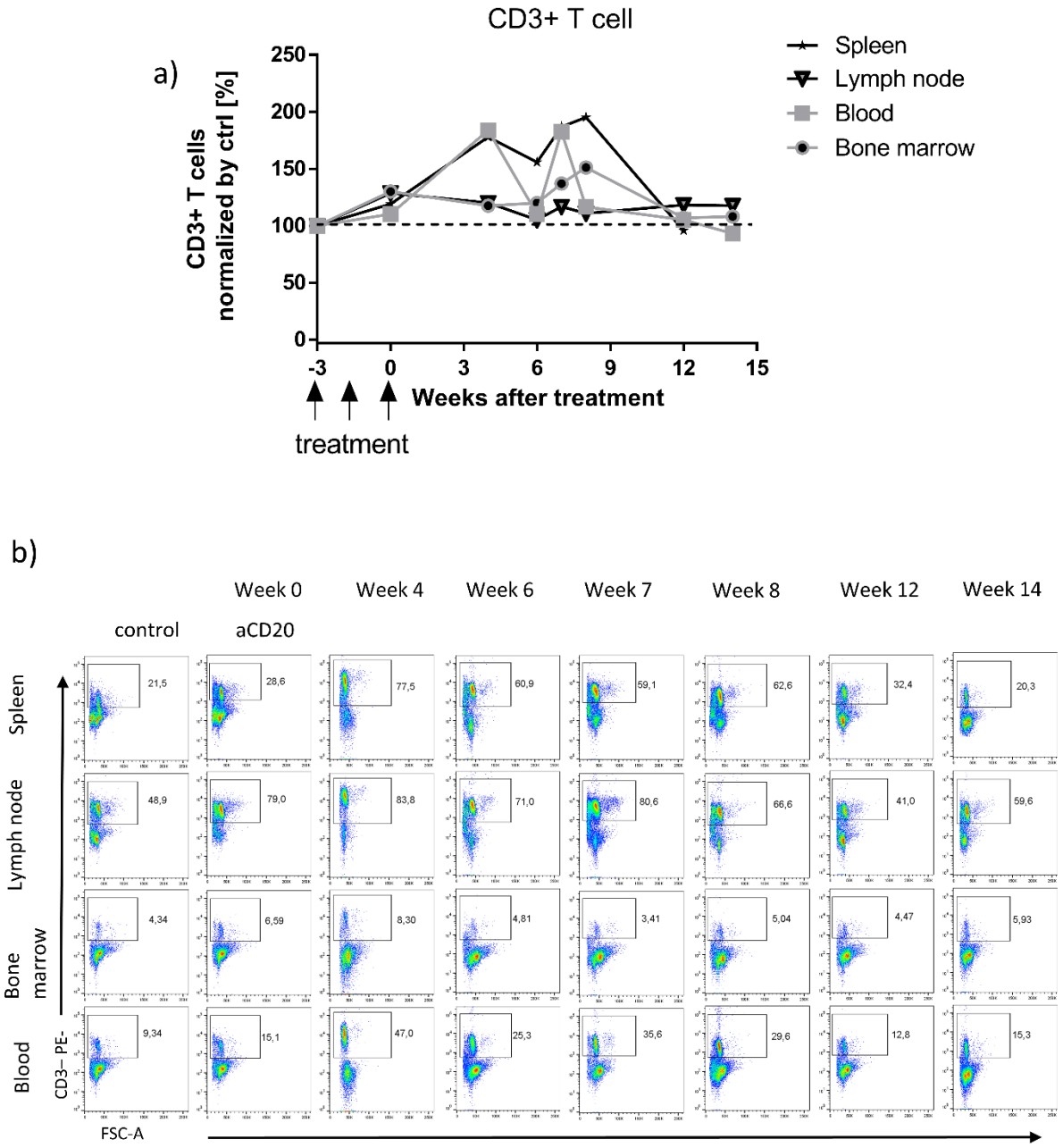

Figure 16: CD3+ T cell frequency during B cell repletion after aCD20 treatment.
a) CD3+ T cell frequency in spleen, lymph node, bone marrow and blood after aCD20 treatment was normalized to control. b) shows representative FACS plots of all investigated compartments for the analysed time points. Repletion kinetic shows mean of n=2 per group and time point.

3.2.2. Characterization of the T cell population after aCD20 treatment

The missing B cell population led to an increased frequency of CD3+ T cells in all investigated compartments (figure 17). Following the relative extension of B cell depletion, the highest increase was observed in the spleen, blood and lymph nodes, while the bone marrow showed the smallest frequency shift. In contrast, the absolute numbers of T cells, as well as in CD4+ and CD8+ T cells, was decreased in the spleen. A significant increase of CD8+ T cells in contrast to the control treated group could only be observed in the bone marrow.

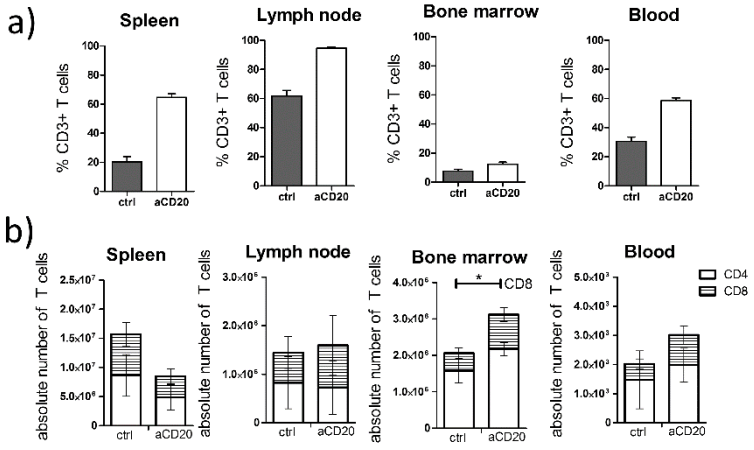

Figure 17: Increased T cell frequency and decreased absolute number of T cells after aCD20 treatment.
a) shows CD3+ T cell frequency after a threefold treatment with aCD20 Ab or control Ab treatment. b) exhibits the absolute number of the T cell frequency divided into CD4+ and CD8+ T cells. The mean of n= 3 per group is displayed.

We investigate whether the decreased number of T cells is due to a direct effect of aCD20 Ab depletion or an indirect effect of missing B cell interaction with T cells. T cells were stained for CD20 expression.

We found a CD4+CD20+ T cell population in the spleen, which was significantly reduced after a threefold aCD20 treatment compared to the control (aCD20 treated group 2.84±0.60% vs. 7.34±1.11% ctrl treated group, $p<0.05$). In the lymph node (aCD20 treated group 3.2±0.57% vs. 7.45±1.41% ctrl treated group, $p<0.05$) and blood (aCD20 treated group 0.54±0.13%vs 12.4±1.35% ctrl treated group, $p<0.05$), the CD4+CD20+T cell population was significantly reduced compared to the control treated group (figure 18). The CD4+CD20+ T cell frequency was significantly reduced in the bone marrow after aCD20 treatment from 13.28±1.49% in control treated mice to 6.54±0.69% after aCD20 treatment ($p<0.05$).

In addition, we found a CD8+CD20+ T cell population in all investigated compartments. In the control group, the CD8+CD20+ T cell population was 11.44±2.57% and thus significantly higher than 2.93±0.60% in the aCD20 treated group in the spleen ($p<0.05$). The strongest reduction was observed in the blood. Here, nearly no CD8+CD20+ T cells could be measured after CD20 treatment (aCD20 treated group 0.38±0.02%vs. 5.58±1.97% ctrl treated group, $p<0.05$). A significant reduction was observed in the lymph node (aCD20 treated group 2.28±0.32% vs. 1.12±0.14% ctrl treated group, $p<0.05$), but not in the bone marrow (aCD20 treated group 0.91± 0.10% vs. 4.69±2.15% ctrl treated group, $p>0.05$).

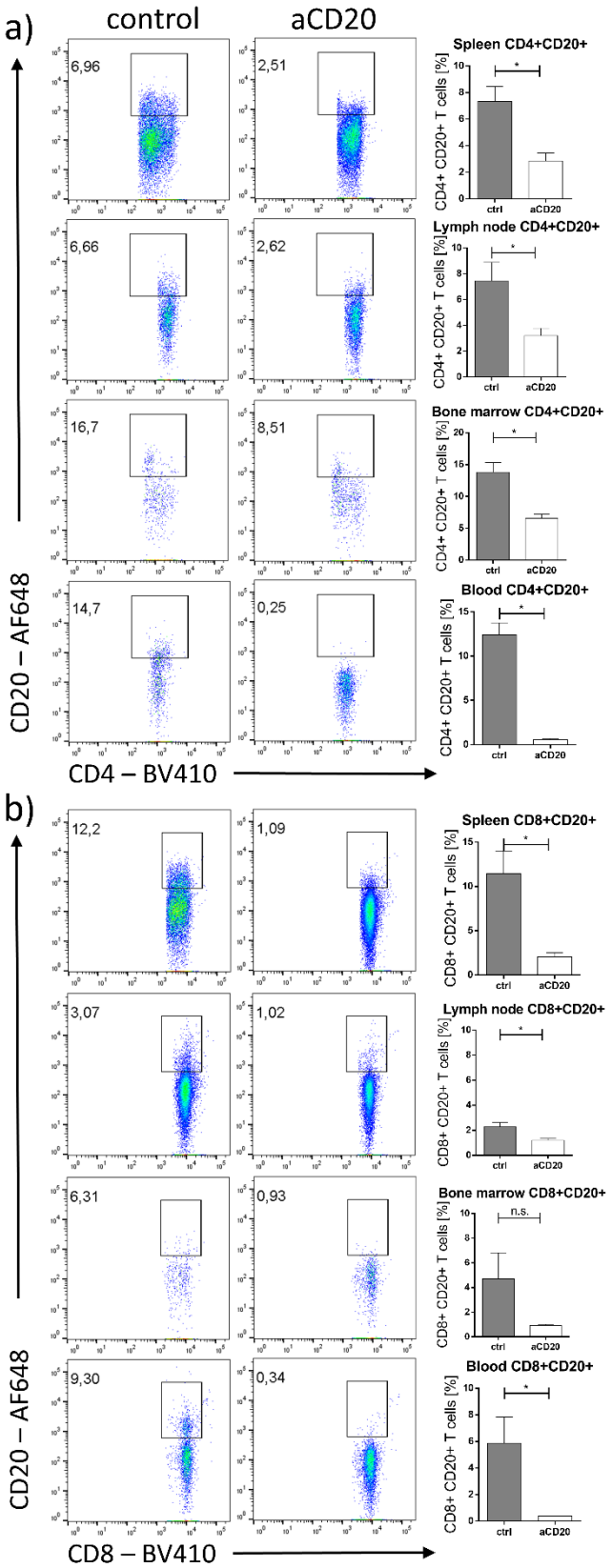

Figure 18: Characterization of T cells after CD20 treatment.
Representative FACS plots show (a) the CD4+CD20+ T cells and (b) the CD8+CD20+ T cell frequency and the according mean of the spleen, lymph node, bone marrow and blood. The mean of n=3 per group is displayed.

3.2.3. CD20+ T cell repletion

To assess whether the depleted CD20+ T cell population is able to reappear after treatment termination, observations at different points in time were analysed.

The CD20+ T cell population was depleted after three times of the aCD20 treatment in all investigated compartments, shown in figure 19. Similar to the B cell repletion kinetic after week 4 to 7, no CD20+ T cells reappeared in any investigated compartment. At week 8 after the last aCD20 treatment the CD3+CD20+ T cell population reappeared in all investigated compartments. In contrast, in naïve mice, B cells reappeared only in the spleen and lymph node. The CD3+CD20+ T cell repletion was completed in all investigated compartments at week 12 after the last aCD20 treatment.

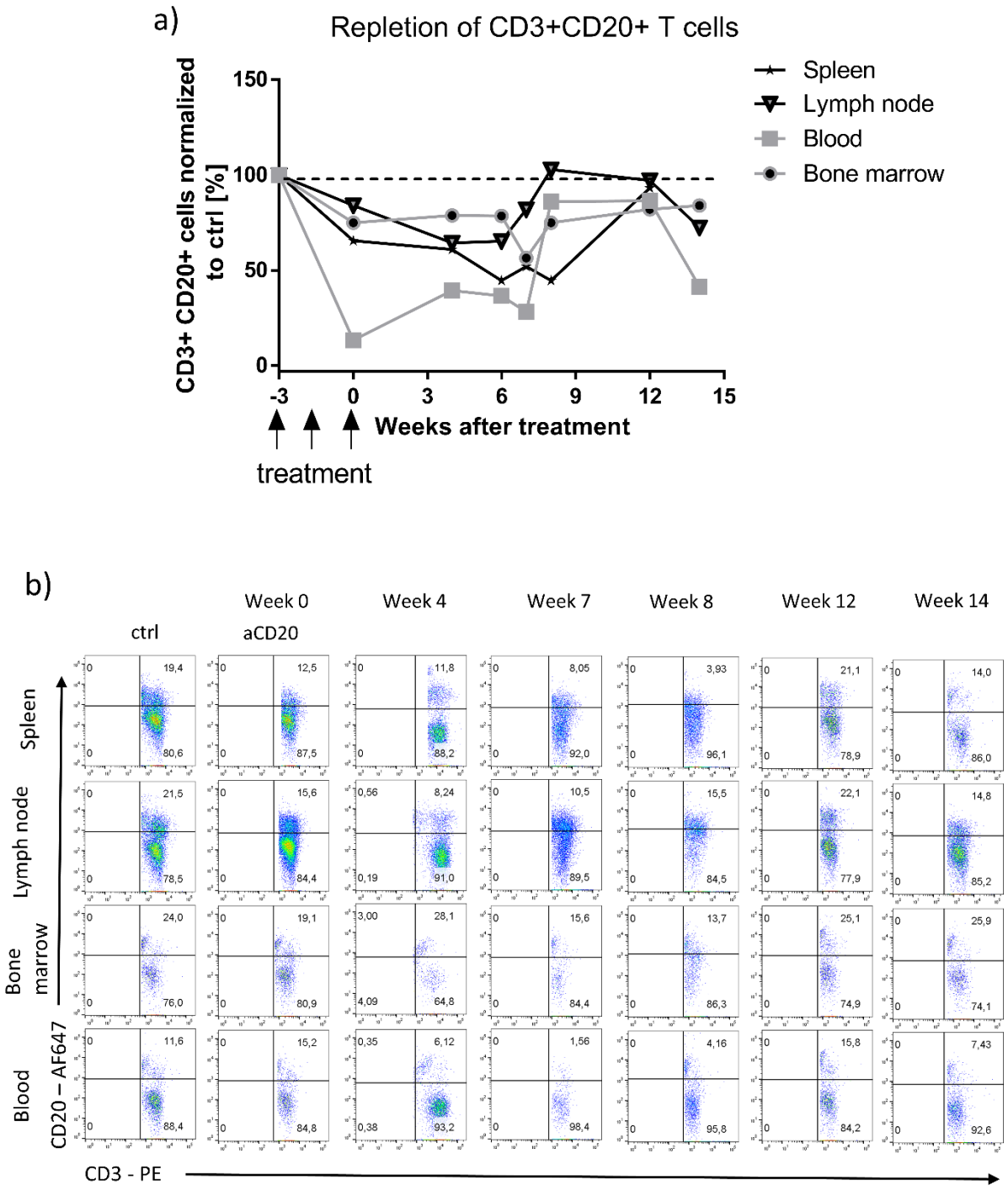

Figure 19: Repletion kinetic of CD20+CD3+ T cells after aCD20 treatment.
a) the frequencies of CD20+ CD3+ T cells are shown after three times of aCD20 treatment. T cell frequencies of spleen, lymph node, bone marrow and blood are normalized to control for each observation time. b) shows frequencies of CD20+CD3+ T cells after three times of aCD20 or control treatment and 12 weeks after the last aCD20 treatment. c) Representative FACS plots of CD20+CD3+ frequencies of all investigated compartments are shown during B cell repletion. Mean of n=2 per group and point in time.

3.2.4. CD20+ T cell repletion in EAE

The analysis of the CD20+ T cell population after aCD20 treatment in MOG p35-55 EAE showed a repletion kinetic of CD20+ T cells comparable to that in naïve mice after aCD20 treatment (figure 19). The repletion of CD20+ T cells started in the spleen, lymph node and bone marrow at week 8 after the last aCD20 treatment. In the blood, CD20+ T cells were detected for the first time at week 10 after the last treatment. A full repletion of CD20+ T cells was measured at week 12, while the spleen, lymph node and blood showed an exceeding CD20+ T cell frequency at this time (spleen 203.88%, lymph node 187.8%, blood 119.42%, bone marrow 93.55%).

Comparing the repletion kinetic of CD20+ T cells in MOG p35-55 and rMOG EAE mice (figure 20), the reappearance of the CD20+ T cells started slightly earlier in mice with rMOG EAE (week 7 spleen: 94.72% CD20+T cells of control treated) than in MOG p35-55 (week 7 spleen: 42.42% CD20+T cells of control treated). CD20+ T cells in the blood of rMOG EAE mice remain on the same level from week 4 (week 4: 55.00% CD20+T cells of control treated) up to week 12 (week 12: 60.23% CD20+T cells of control treated). The exceeding CD20+ T cell frequency was also measured in the bone marrow of rMOG EAE mice at week 8 (190.68% CD20+T cells of ctrl treated) and in their spleen at week 10 (176.36%CD20+T cells of ctrl treated) after last aCD20 treatment.

The CD20+ T cell repletion started in mice with rMOG EAE slightly earlier than in mice with MOG p35-55 EAE. Furthermore, both repletion kinetics showed an excess of CD20+ T cells in the spleen, occurring at different points of time. Here, the excess of CD20+ T cells was measured earlier in rMOG EAE than in MOG p35-55 EAE.

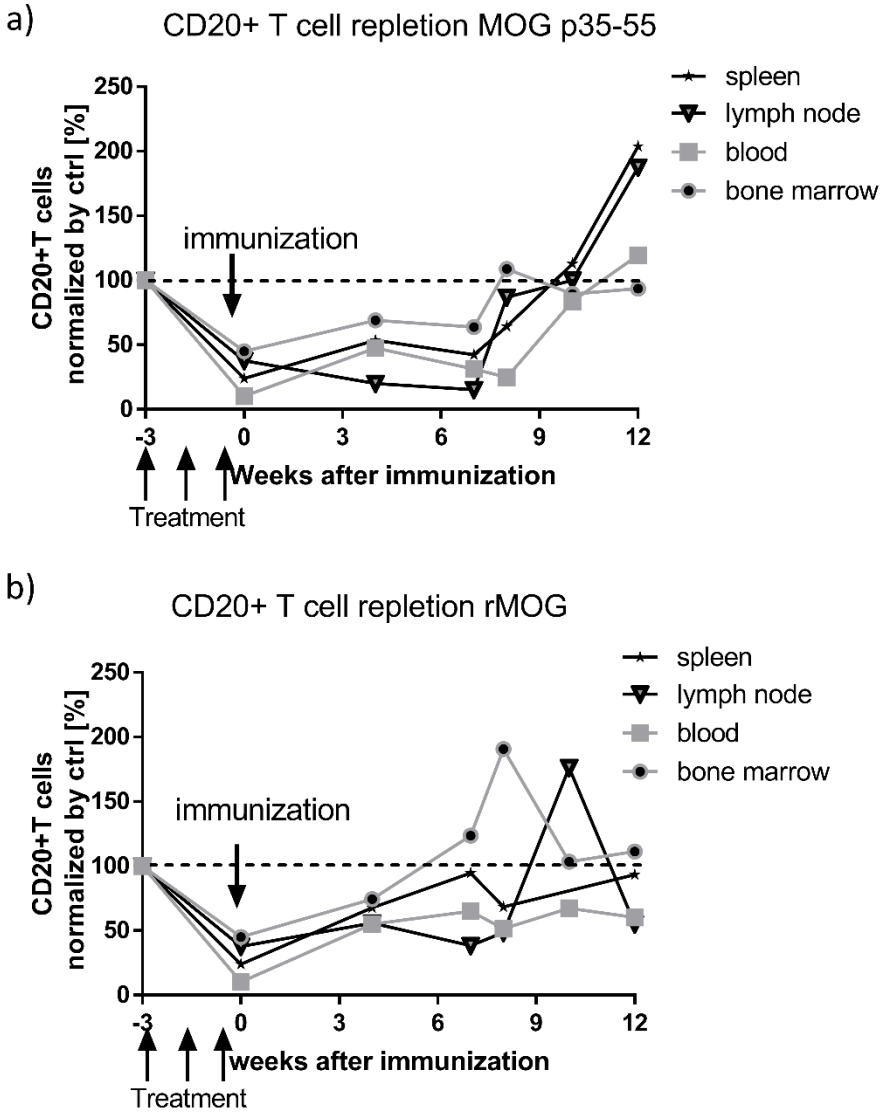

Figure 20: CD20+ T cell repletion in different EAE-models.
The frequency of CD20+ CD3+ T cells after aCD20 treatment was normalized to the time according to control for different observation times in the spleen, lymph node, bone marrow and blood in a) MOG p35-55 and b) rMOG EAE mice. The mean of n=2 per group and time point was normalized to time according to control.

3.2.5. Direct stimulation of T cells of naïve mice after aCD20 treatment *ex vivo*

The previous experiments showed that aCD20 treatment has a direct effect on the T cell population by depletion of CD20+ T cells. To address the question whether the missing interaction with the depleted B cells has an influence on the functional behaviour of T cells, isolated CFSE stained T cells were stimulated with aCD3/aCD28 antibodies and their proliferation was measured.

8 weeks after aCD20 treatment (figure 21 a), T cells showed a significantly lower proliferation rate after stimulation with aCD3/aCD28 Ab compared to the T cells of the control-treated

group (aCD20 treated group 45.58±1.02% vs. 56.05±% ctrl treated group, $p<0.01$). Similarly, a not significant ($p>0.05$) tendency in T cell proliferation could also be observed 12 weeks after aCD20 Ab treatment, where B cells were completely repleted.

Furthermore, IL-17 release was significantly inhibited after aCD20 treatment in T cells after 8 weeks (aCD20 treated group 38.19±8.23pg/ml vs. 76.64±9.92pg/ml ctrl treated group, $p<0.05$). After 12 weeks (figure 21 b), the difference in IL-17 release between aCD20 treated T cells and control treated T cells were no longer significant (aCD20 treated group 300.6±28.41pg/ml vs. 382.2±79.88% ctrl treated group, $p>0.05$). Meanwhile, the release of IFN γ and IL-6 was not significantly affected by aCD20 treatment ($p>0.05$). GM-CSF release did not differ between aCD20 treatment and T cells of control treated mice 8 weeks after the last treatment ($p>0.05$). In contrast, GM-CSF release was significantly reduced after aCD3/aCD28 stimulation (aCD20 treated group 4042.0±109.5pg/ml vs 4517.0±2.6%ctrl treated group, $p<0.01$), but not under unstimulated conditions ($p>0.05$).

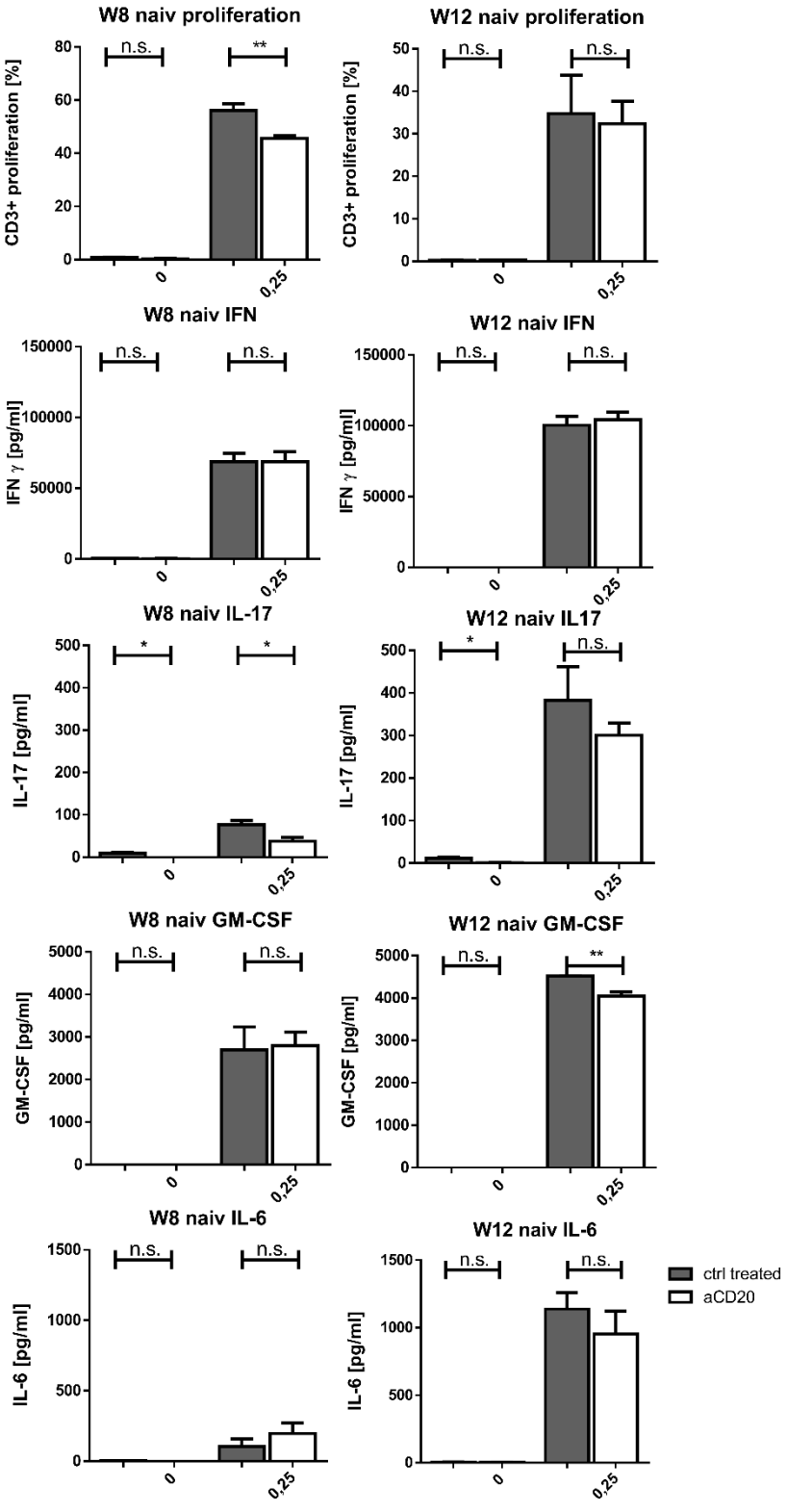

Figure 21: Reduced proliferation and cytokine release of aCD20 treated T cells after aCD3/aCD28 stimulation in naïve mice after aCd20 treatment.

The proliferation rate of CD3+T cells after aCD3/aCD28 Ab stimulation (0µg/ml aCD3 and 10µg/ml aCD28; 0.25µg/ml aCD3 and 10µg/ml aCD28) is reduced in the absence of B cell. The cytokine release of IFN y, IL-17, GM-CSF and IL-6 were measured in the supernatant by ELISA. The mean is shown of n=3 per group and point in time.

3.2.6. Direct *ex vivo* stimulation of T cells in EAE after aCD20 treatment

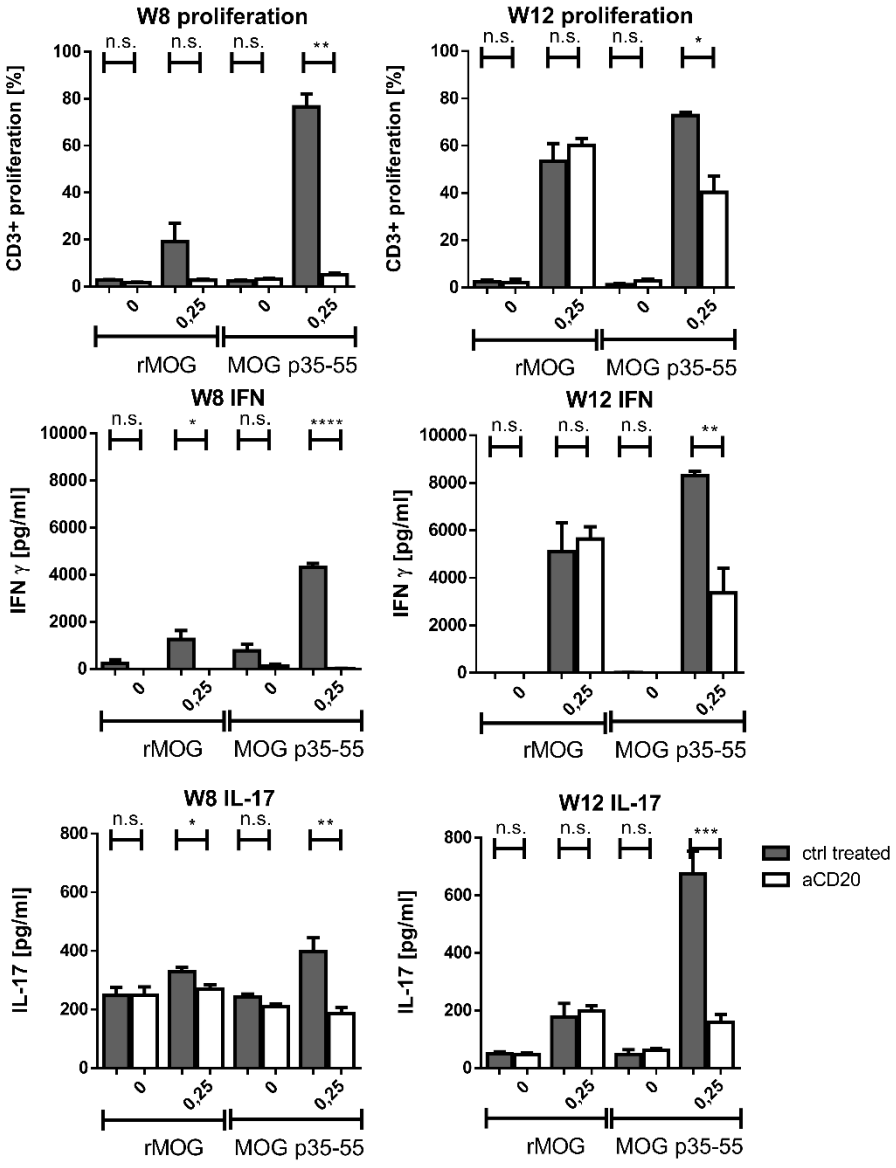

Figure 22: Reduced proliferation and cytokine release of aCD20 treated T cells after aCD3/aCD28 stimulation in rMOG and MOG p35-55 EAE after aCD20 treatment.
The proliferation rate of CD3+T cells after aCD3/aCD28 Ab stimulation (unstimulated condition: 0µg/ml aCD3 and stimulated condition 10µg/ml aCD28; 0.25µg/ml aCD3 and 10µg/ml aCD28) in rMOG and MOG p35-55 EAE is shown. The cytokine release of IFN y and IL-17 were measured in the supernatant by ELISA. The mean of n=3 per group and time point is displayed.

To answer the question what impact aCD20 treatment would have on the T cell side of EAE, T cells of rMOG EAE and MOG p35-55 EAE mice were isolated and directly stimulated with aCD3/aCD28 antibodies. Afterwards, the proliferation and cytokine release were measured.

CD3+ cell proliferation was not significantly lower after aCD3/aCD28 stimulation, which was performed 8 weeks after aCD20 treatment in rMOG EAE mice (aCD20 treated group 2.65±0.48pg/ml vs. 19.31±7.92pg/ml ctrl treated group, $p>0.05$). Following aCD3/aCD28 stimulation of T cells of mice with MOG p35-55 EAE (figure 22), the T cell proliferation was not significantly reduced in T cells isolated from mice, treated with aCD20 Ab, compared to T cell proliferation of control treated mice (aCD20 treated group 4.90±0.8%vs. 76.52±5.42% ctrl treated group, $p<0.01$). 12 weeks after aCD20 treatment, B cells fully reappeared and the tendency of a lower proliferation rate after aCD20 treatment was no longer measurable. In MOG p35-55, the proliferation of aCD20 treated T cells was still significantly lower following aCD3/aCD28 stimulation compared to the T cells of control treated mice ($p<0.05$).

T cells of aCD20 treated mice 8 weeks after the last treatment showed a significantly reduced IFN γ release in rMOG EAE (aCD20 treated group 0±0pg/ml vs. 1252±380.5pg/ml ctrl treated group, $p<0.05$) and MOG p35-55 EAE (aCD20 treated group 14.25±11.45pg/ml vs. 3606±147.9pg/ml ctrl treated group, $p<0.01$) compared to their controls. Fitting to the proliferation rate, 12 weeks after the last aCD20 treatment, the release of IFN γ was not significantly reduced in aCD20 treated T cells compared to T cells of control treated mice in rMOG EAE (aCD20 treated group 5640±513pg/ml vs. 5103±1209pg/ml ctrl treated group, $p>0.05$). However, IFN γ was still significantly reduced in aCD20 treated T cells in MOG p35-55 EAE compared to their control treated mice (aCD20 treated group 3363±1051pg/ml vs. 8295±191.4pg/ml ctrl treated group, $p<0.01$). The same release profile was observed for the IL-17 release. IL-17 release was significantly reduced in T cells after aCD20 treatment from 330.±14.2pg/ml to 269.8±18.82pg/ml in rMOG EAE mice after aCD3/aCD28 stimulation ($p<0.05$). In MOG p35-55 EAE mice, the IL-17 release of T cells was significantly reduced after aCD20 treatment from 398.6±46.04pg/ml to 185.6±21.98pg/ml ($p<0.01$).

3.3. CNS infiltration of B cells, T cells and myeloid cells in the dynamics of B cell repletion in EAE

In previous experiments of this study, reappearing B cells of rMOG EAE mice showed a more activated phenotype and *ex vivo* a superior APC function than their control. To investigate if these more activated reappearing B cells also exhibit a higher infiltration of immune cells in the CNS compared to control treated mice in rMOG and MOG p35-55 EAE, the histology of CNS 14 weeks after the last aCD20 treatment was analysed.

In the CNS of aCD20 treated rMOG EAE mice (figure 23), the B cell number was decreased (0.88±0.46 B cells/mm^2 white matter) compared to the control treated mice (5.85±2.04 B cells/mm^2 white matter, $p>0.05$). The same trend was observed for the B cell infiltration in the white matter of MOG p35-55 EAE. Here, the B cell number in the CNS of aCD20 Ab treated mice (0.69±0.31 B cells/mm^2 white matter) was lower compared to the control treated mice (4.21±1.73 B cells/mm^2 white matter, $p>0.05$).

The T cell side is also affected by the repletion of B cells. T cell infiltration was investigated in the CNS after B cell repletion. Similar to the B cell infiltration in the white matter, the amount of T cells was significantly decreased in aCD20 treated mice compared to the control treated mice in rMOG EAE (aCD20 treated 6.87±1.57 T cells/mm^2 white matter; ctrl treated 14.32±2.59 T cells/mm^2 white matter, $p<0.05$). In contrast, no significant difference was observed in mice of MOG p35-55 EAE (aCD20 treated 8.14±2.08 T cells/ mm^2 white matter, ctrl treated Ab 22.73±8.88 T cells/ mm^2 white matter, $p>0.05$).

A different observation could be made for MAC-3+ cells, which were significantly increased in the CNS of aCD20 treated mice in MOG p35-55 ($p<0.05$). The same trend could be observed in rMOG EAE mice, where the depletion of B cells caused an infiltration of MAC-3 positive cells in the white matter (31.97±15.69 MAC-3+ cells/mm^2 white matter) compared to the control treated mice (7.01±3.86 MAC-3+ cells/mm^2 white matter, $p>0.05$).

Since the meninges are the intersection between the peripheral immune cells and the CNS, we also investigated them to analyse the differences in this section. The number of meningeal B cells was similar in formerly depleted mice and control treated mice as well as in rMOG EAE ($p>0.05$) and in MOG p35-55 EAE ($p>0.05$) (figure 23). In contrast, the T cell number was decreased in the meninges in rMOG EAE compared to control treated mice (aCD20 treated 2.17±1.22 meningeal T cells/spinal cord cross section, ctrl treated Ab 12.31±0.99 meningeal T cells/ spinal cord cross section, $p>0.05$)), as well as in MOG p35-55 EAE mice (aCD20 treated 8.33±1.79 meningeal T cells/ spinal cord cross section, ctrl treated 3.75±1.09 meningeal T cells/ spinal cord cross section, $p<0.01$).

Overall, the B cell repletion is not completed in the white matter but in the meninges. The meninges of aCD20 treated mice showed the same amount of B cells compared with the control treated mice. This could be observed in rMOG EAE as well as in MOG p35-55 EAE. While the T cells in both EAE models were neither repleted in the white matter nor in the meninges, the most significant result was the massive infiltration of MAC-3+ cells in the white matter.

Next Page

Figure 23: Dynamic of B cells, T cells and myeloid cells during B cell repletion.
a) Representative figures of spinal cord sections stained for B220, CD3 and MAC-3, 14 weeks after last aCD20 or ctrl Ab treatment in rMOG or MOG p35-55 EAE. b) shows the according quantitative analysis of B220+ CD3+ and MAC+ cells per mm^2 white matter (n=5 in rMOG EAE and n=4 in MOG p35-55 EAE). In b) and c) the mean of B220+ B and CD3+ T cells in the meninges per spinal cord section is shown. d) shows the demyelinated area in percent of white matter, n=4 per group.

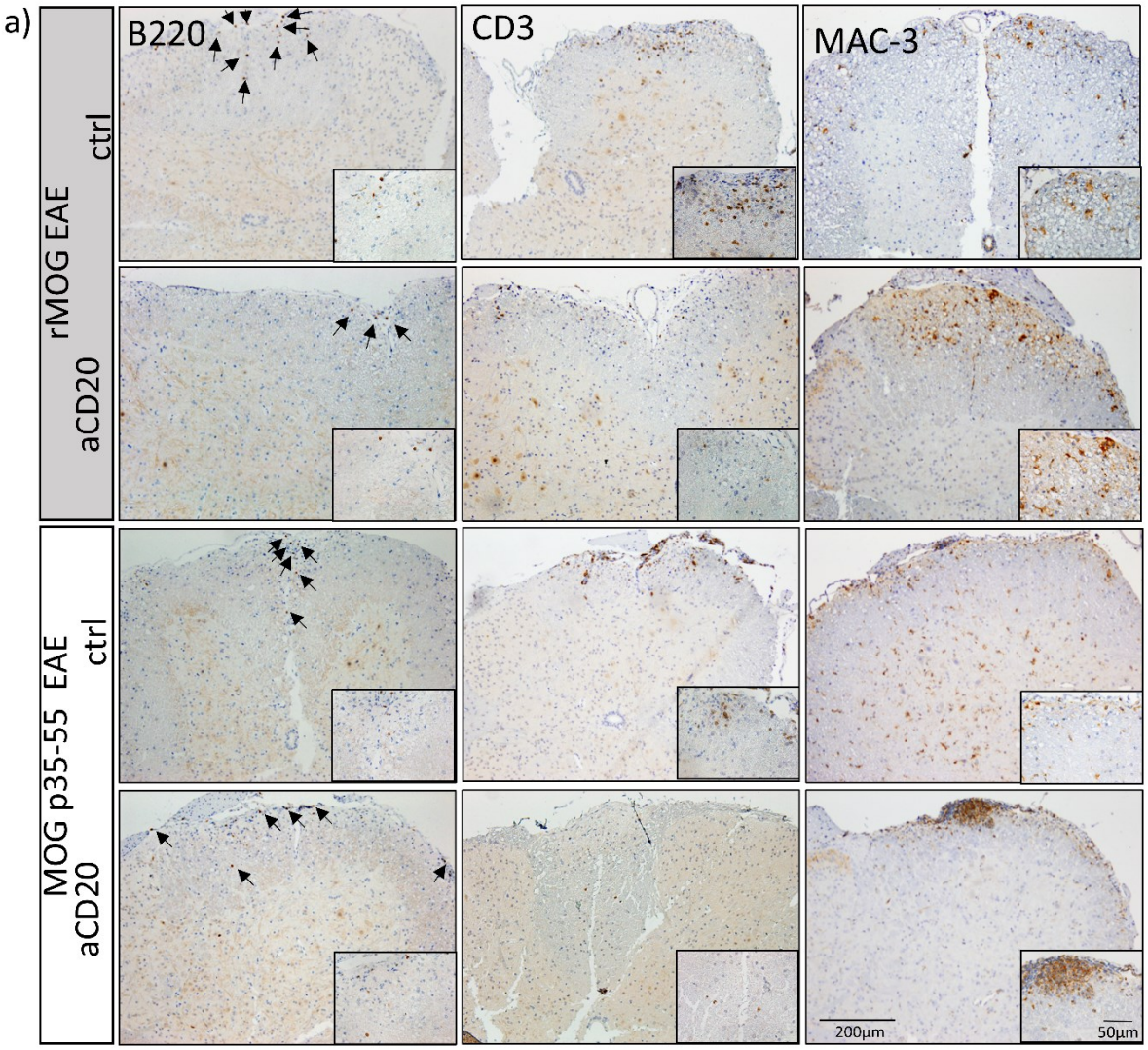
a)
B220
CD3
MAC-3
rMOG EAE
ctrl
aCD20
MOG p35-55 EAE
ctrl
aCD20
200µm
50µm

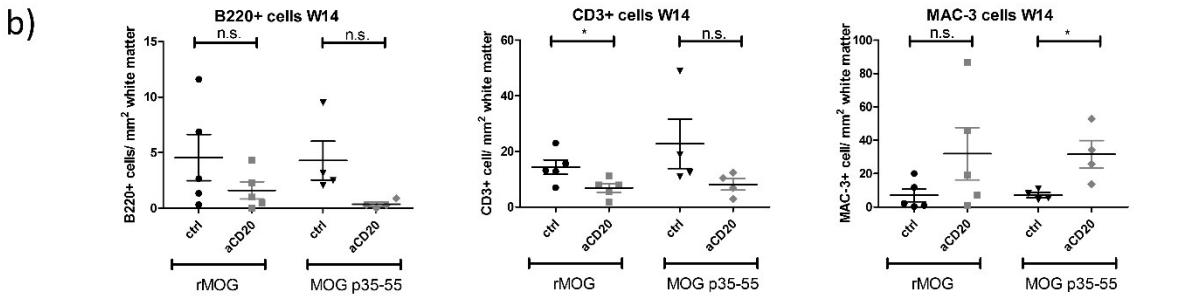
b)
B220+ cells W14
B220+ cells/ mm² white matter
CD3+ cells W14
CD3+ cell/ mm² white matter
MAC-3 cells W14
MAC-3+ cell/ mm² white matter
n.s.
*
ctrl
aCD20
rMOG
MOG p35-55

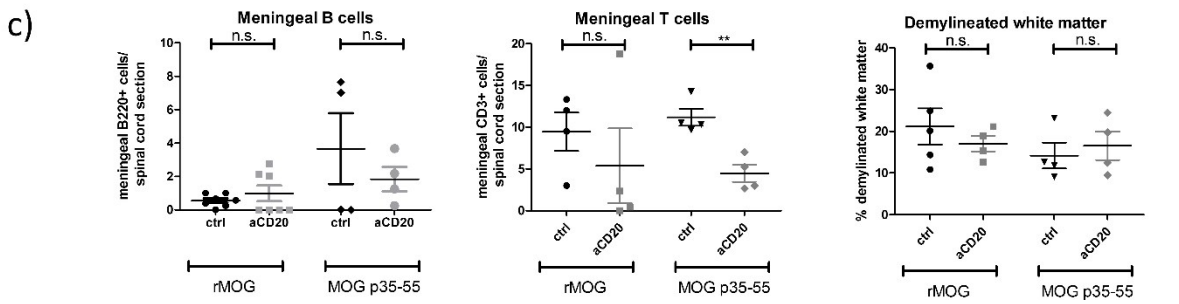
c)
Meningeal B cells
meningeal B220+ cells/ spinal cord section
Meningeal T cells
meningeal CD3+ cells/ spinal cord section
Demylineated white matter
% demylinated white matter
n.s.
**
ctrl
aCD20
rMOG
MOG p35-55

4. Discussion

The rapid clinical benefit of aCD20 therapy in most MS patients provides a new focus on the role of B cells in this disease. Nevertheless, until now a characterization of remaining and reappearing B cells is still missing. This study tries to close this gap and reveals new insights which may improve the strategy of MS therapy.

4.1. Enrichment of CD27+ activated B cells after aCD20 treatment

In MS patients, the blood is the only available compartment to observe and investigate B cell populations after aCD20 treatment, whereas diagnostic abilities in secondary lymphoid organs such as lymph node and spleen are limited. Therefore, animal models are needed to characterize remaining and reappearing B cells in these immune relevant organs.

In the present study we analysed the frequency and functional properties of remaining and reappearing B cells after aCD20 treatment. Nearly no B cells are found in the blood after aCD20 treatment whereas B cells in spleen, lymph node and especially in the bone marrow are not fully depleted by aCD20 (figure 5). The characterization of these remaining B cells in lymph node and spleen showed that they express CD20 and are theoretically depletable by aCD20 antibodies. In contrast, the remaining B cells in the bone marrow do not express CD20 and could therefore not be depleted by aCD20 treatment. These remaining B cells in the bone marrow are most probably precursor B cells which, after migration into the periphery. These precursor B cells could also be observed in rituximab-treated patients with rheumatoid arthritis[115,116].

The remaining B cells in spleen and lymph node led to the question why some of these B cells in spleen and lymph node are not affected by aCD20 treatment. Histological findings in this study showed that most of the remaining B cells are located around germinal centre structures in the spleen. This result led to the hypothesis that these B cells in germinal centres might be sterically protected against aCD20 antibodies or that other mechanisms led to the protection of these remaining B cells. Resistance to aCD20 treatment was also described in other animal models[117,118]. The binding of rituximab to the CD20 molecule leads to its translocation to lipid rafts. Alterations in lipid raft composition have been associated with reduced efficacy of rituximab[119]. Furthermore, a study in cynomologous monkeys demonstrated that germinal centres in lymph node and spleen show a lower sensitivity to aCD20 antibodies[117]. Our results revealed that the remaining B cells in spleen and lymph node are an enrichment of CD27+ B cells and are located in germinal centres (figure 5.). This finding is in line with the previous studies described above[117,120]. CD27 is a marker for B cell activation which is involved in B cell expansion and furthermore required for germinal centre formation[120]. Therefore, one hypothesis is that

reappearing B cells do not originate from a naïve population residing inside the bone marrow but rather originate from a remaining population of activated B cells. In MS patients, the recurring reappearance and depletion of B cells could lead to the enrichment of an activated B cell phenotype which may contribute to the worsening of the disease course. Additionally, an increased resistance to B cell depletion could also be a consequence. Maurer et al.[121] provided evidence for this hypothesis by demonstrating that after a single course of rituximab treatment, increased frequency of IgG+ CD27+ memory B cells were found in MS patients. This argument is even more important considering the results of the B cell repletion kinetic in our study. Until now it was unclear whether B cells reappear first in the blood or simultaneously in blood and other immune relevant compartments. In this study, B cell reappearance in naïve mice started first in spleen and bone marrow while the B cell repletion of lymph node and blood lacked behind. Conclusively, the blood is not suitable monitoring compartment for B cell reappearance. Today, MS patients which are treated with aCD20 are only monitored for reappearance of B cells in the blood. When reappearing B cells are detected in the blood, a new treatment course of aCD20 treatment is started. Considering the results of our study, a constant treatment schedule may be a better treatment strategy to avoid an enrichment of activated B cells.

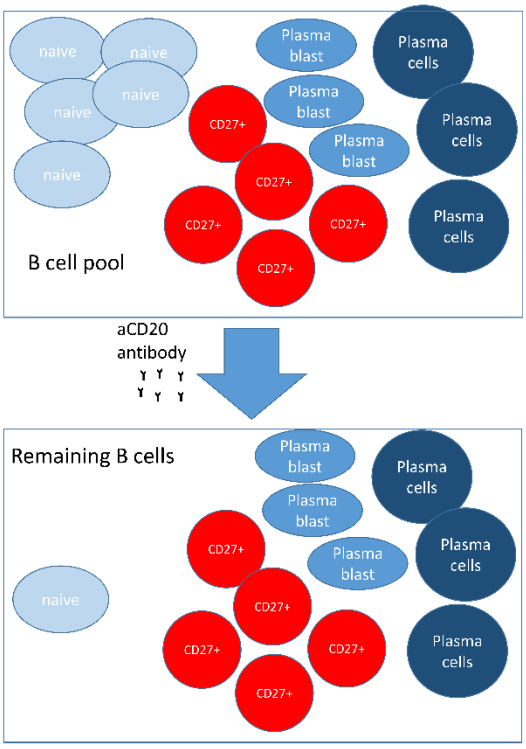

Figure 24:Schematic overview of the B cell pool before and after B cell depletion.
B cell depletion enriches the relative amount of CD27+ activated B cells of remaining B cells in spleen.

4.2. Reappearance of activated B cells causes clinical worsening of rMOG EAE and a different distribution of reappearing B cells during repletion in the immune relevant compartments

In 2010, Weber et al.[95] described an EAE model induced by immunization with rMOG in which B cells are actively involved and depletion of these B cells results in a clinical benefit. In contrast, in the T cell mediated model, induced by immunization with MOG p35-55, animals show a clinical worsening after B cell depletion[95]. In addition to the repletion kinetic after aCD20 treatment, we further analysed how these reappearing B cells influence the clinical course of rMOG and MOG p35-55 immunized mice. In rMOG EAE, a clinical worsening after reappearance of B cells is observed in aCD20 treated mice compared to control treated mice. In contrast, mice immunized with MOG p35-55 showed a clinical benefit after reappearance of B cells compared to the control-treated group. These clinical differences after the reappearance of B cells could be explained by the dichotomy of B cells. On one hand, B cells can have regulatory functions which are associated with release of IL-10. It was reported that IL-10 deficient mice do to not recover from severe EAE but after the transfer of WT IL-10 producing B cells, an improvement of the disease course could be observed[122]. In MS patients, the release of IL-10 plays a crucial role in the recovery from relapses[123]. On the other hand, B cells have pro-inflammatory features, for example the production of IL-6, which leads to the activation of T cells[39,124]. IL-6 deficient mice are reported to be resistant to EAE[125]. All in all, it could be suggested that B cells of mice with rMOG EAE reappear in a B cell-activating milieu and show a more pro-inflammatory phenotype which causes the clinical worsening. In contrast, in MOG p35-55 EAE the B cells reappeared in a milieu which may induces a more regulatory phenotype leading to an improved clinical course of EAE. These findings provide evidence for a different function of these reappearing B cells which seems to be dependent on the milieu in which B cells reappear. The study of Constant et al.[109,126] compared MOG protein EAE to MOG p35-55 EAE and found that B cells which were previously activated by an antigen show an increased capacity to act as APCs which can successfully prime CD4+ T cells. A further study could confirm these results and reported two different mechanisms which can induce EAE. The mechanism depends on the nature of the immunogen: on the one hand, MOG p35-55 EAE is mediated by an encephalitogenic T cell response, while on the other hand human MOG protein EAE showed an encephalitogenic B cell response[127]. These studies supported our findings that the B cell function is influenced by the initial immunogenic stimulus and could explain why reappearing B cells of mice in rMOG EAE cause a clinical worsening.

Further evidence that the B cell function of reappearing B cells depends on the initial stimulus is supported by our repletion kinetic data. We could observe differences in the onset of B cell

repletion and B cell distribution in the different compartments in the two used EAE models. Mice immunized with MOG p35-55 showed a similar repletion kinetic as naïve mice. Together with the clinical benefit after reappearance of B cells in these mice, it seems that B cells of mice in MOG p35-55 EAE reappeared less activated due to the missing initial B cell-activating stimulus. In contrast, in mice with rMOG EAE the repletion started earlier and B cells were more distributed in different immune relevant compartments (figure 7). The different repletion kinetics and clinical outcome are further evidence for a different phenotype of reappearing B cells which depends on the milieu and/or the initial stimulus of B cells during repletion.

4.3. Reappearing B cells show a more activated phenotype in B cell-mediated EAE

In the T cell-mediated model induced by MOG p35-55, reappearing B cells initially showed a high expression of CD27 which could not be observed at a later time point after B cell repletion was complete. In contrast, in the B cell-mediated rMOG induced model, CD27 expression of reappearing B cells remained profoundly increased even after complete reappearance of B cells. To analyse the effect of these enriched CD27+ B cells, an *in vivo* proliferation experiment was performed. Data evaluation revealed that the remaining B cells in lymph node and spleen showed a higher proliferation rate o observed in mice with rMOG as well as in MOG p35-55 EAE. This led to the hypothesis that the reappearing B cells which are detectable around week 7 in spleen and lymph node do not originate from the bone marrow but rather expand from these remaining B cells.

This experiment was repeated in both EAE models to verify the hypothesis that reappearing B cells expand from the spleen and lymph and do not migrate from the bone marrow. In the spleen of aCD20 treated mice immunized with rMOG, a significantly higher proliferation of B cells was observed during the phase of B cell repletion compared to control-treated mice. This effect could also be observed in MOG p35-55 EAE, albeit at a lower level when compared to rMOG EAE. The same trend could be seen in the lymph node but this effect was not statistically significant. In the bone marrow, a lower proliferation was observed in all investigated groups. These finding support the hypothesis that the remaining CD27+ activated B cells expand from the spleen and do not originate from naïve B cells inside the bone marrow.

In MS patients, remaining IgG+ CD27+ memory B cells were found after a single course of rituximab[121]. Similar to our findings in EAE, Maurer et al.[128] also showed in MS a clonal expansion of IgM+ memory B cell after rituximab treatment. The analysis of these remaining and expanding memory B cells in humans revealed two different pathways for the development of human memory B cells. One pathway depends on germinal centres while the other one is independent

of germinal centres. Memory B cells derived from primary germinal centre reactions are characterized as $CD27^{-}IgG^{+}$ and $CD27^{+}IgM^{+}$ whereas B cells from consecutive germinal centre responses are $CD27^{+}IgA^{+}$ and $CD27^{+}IgG^{+}$[129]. Several studies reported an expansion of $CD27^{+}IgM^{+}IgD^{-}$ and $CD27^{-}IgG^{+}$ memory B cells in autoimmune diseases[130–132]. These findings support the hypothesis of an expanding CD27+ B cell population during repletion which could be observed in the EAE models in our study.

For a further analysis of these different B cell phenotypes, isolated B cells were re-stimulated with rMOG or MOG p35-55 according to their immunization stimuli and co-cultured with MOG-specific T cells. The reappearing B cells of aCD20-treated mice immunized with rMOG caused a higher proliferation rate of MOG specific T cells compared to control-treated B cells. In contrast, the co-culture of MOG-specific T cells and reappearing B cells of MOG p35-55 immunized animals showed the opposite results (figure 12). Re-stimulation with rMOG activates the reappearing B cells and causes a superior APC function[108]. Antigen presentation of B cells is necessary for the induction of a B cell-dependent EAE, induced by human MOG protein, and contributes to the severity of the disease course[80,102]. In 2013, Molnarfi et al.[111] reported that B-cell $^{MHC\ II-/-}$mice were resistant to EAE induced by recombinant human MOG protein since antigen presentation in the context of MHC-II is necessary for EAE induction. APC function is necessary for the differentiation of CD4+ T cells into pathogenic Th1 and Th17 cells which play an important role in the pathogenesis of EAE. It could be suggested that these reappearing B cells with superior antigen-presenting function could have caused a clinical worsening in rMOG immunized mice through the activation and differentiation of Th1 and Th17 cells.

Furthermore, a higher amount of the pro-inflammatory cytokines IFN y, IL-17 and IL-6 was measured in the co-culture of MOG-specific T cells and reappearing B cells isolated from rMOG immunized animals. IL-6 is described as a pro-inflammatory cytokine which induces the differentiation of pathogenic Th1 and Th17 cells[39,124,125]. The cytokines IFN y and IL-17 released by of these induced T cells are essential for the pathogenesis of EAE [133,134]. In the co-culture of reappearing B cells isolated from MOG p35-55 immunized mice, lower concentrations of IFN y and IL-17 and higher concentration of IL-6 were observed when compared to their control. Nevertheless, the amount of IL-6 produced by reappearing B cells of MOG p35-55 immunized animals was still at a lower level when compared to the co-culture with reappearing B cells of rMOG immunized mice. These results are in line with the previous findings and could explain the clinical benefit after the reappearance of B cells in MOG p35-55 EAE. Regarding these *ex vivo* results, we assumed that the continuous presence of rMOG during EAE stimulated and induced a more activated phenotype of B cells with superior antigen presenting function. This more

phenotype may leads to an increased priming of pathogenic Th1 and Th17 cells which contribute to the clinical worsening. Similar results were demonstrated in a study by Weber et al. where they also observed a higher release of IFN γ and IL-17 in a co-culture with B cells of rMOG immunized mice and naïve T cells[95].

Further evidence that the stimulation of reappearing B cells is dependent on the antigen is provided by *ex vivo* stimulation with LPS and CpG. For this, B cells were stimulated in an antigen-independent matter by LPS and CpG, which activate TLR signalling. The earliest reappearing cells 8 weeks after repletion showed no response to either stimulus independent of whether they were isolated from mice immunized with rMOG or with MOG p35-55. B cells which were isolated from MOG p35-55 immunized animals after full repletion responded to LPS in the same way as to CpG but in a weaker manner than B cells of control-treated mice. In contrast, after full B cell repletion, reappearing B cells of rMOG immunized animals showed a similar or higher release of IL-10 and IL-6. This decreased cytokine release after *ex vivo* stimulation with TLR agonists may be caused by the missing BCR signalling or the TLR response might be inhibited at this stage of B cell expansion. Both, BCR and TRL signalling are reported to enhance the immune response[135]. Therefore, the lower cytokine amount released by recently reappearing B cells might be due to the missing BCR signalling.

Drawing a complete picture, the initial stimulus during the reappearance of B cells appears to influence the arising B cell phenotype. Reappearing B cells most likely originate from an enriched population of CD27+activated B cells which are mostly located in germinal centres in the spleen after aCD20 treatment. This location seems to protect these activated B cells from depletion by the aCD20 Ab. These remaining CD27+ B cells expand in the spleen and proliferate in mice with rMOG EAE to a more activated phenotype which shows superior APC function and induces of Th1 and TH17 cells *ex vivo*. Furthermore, these B cells are more frequent in the immune relevant compartments and repletion starts earlier. These reappearing and activated B cells in rMOG EAE could be responsible for the worsening clinical course (figure 8).

In the T cell-mediated EAE this effect is vice versa. The reappearing B cells lead to a clinical benefit and show a repletion kinetic similar to the kinetic observed in naïve mice. The composition of these reappearing B cell also shows an enrichment of CD27+ activated B cells but show a weaker APC function and a reduced induction of Th1 and Th17 cells *ex vivo*. This effect is gone after full repletion of B cells which may be due to the missing stimulus of B cell activation in the periphery.

In RRMS patients, the cytokine profile is distinct from healthy individuals. MS patients show enhanced levels of pro-inflammatory cytokines released by B cells like IL-6, Lymphotoxin (LT) and TNF-α, while anti-inflammatory cytokines like IL-10 are decreased[136]. This pro-inflammatory milieu leads in to an increased Th1 and Th17 response which is diminished after B cell-depleting therapy[40]. The presence of these activated pro-inflammatory B cells led to the hypothesis that there is a peripheral stimulus in MS patients which activates these B cells. Since clonal expansion of remaining B cells is reported in MS patients after rituximab treatment, it is important to create an anti-inflammatory milieu during B cell reappearance to avoid relapses. Maurer et al.[128] reported a patient with NMO, a MS related disease, which had a relapse during their study. As an explanation for this relapse they suggested a fast clonal expansion of the remaining IgG memory B cells induced by an increased BAFF level[128].This hypothesis of Maurer et al. fits to the findings of our study in rMOG EAE where the reappearance of B cells under B cell activating conditions led to a clinical worsening.

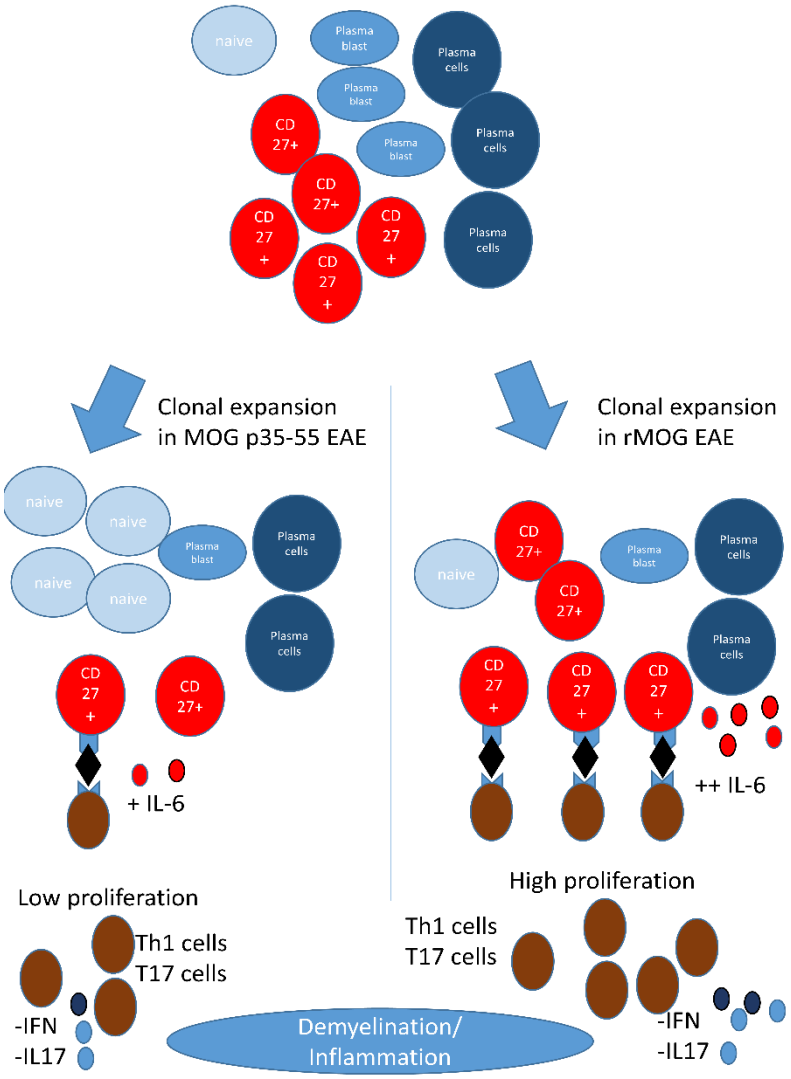

Figure 25: Overview of possible immune mechanisms during reappearance of B cell in rMOG and MOG p35-55 EAE, including T cell interaction.

4.4. Dynamic of T cells during B cell depletion and repletion after aCD20 treatment

In recent studies, the presence and the role of CD20+ T cells were discussed[137,138]. The existence of CD20+ T cell was described by Wilk et al.[137] in 2009 in patients with rheumatoid arthritis[137]. Current studies support the hypothesis that these CD20+ T cells are increased in MS patients[42]. Thus, we also investigated the direct and indirect effects of aCD20 treatment on T cells.

In this study, an increased frequency of T cells was observed in all investigated compartments after aCD20, which can be explained by a frequency shift compensating the missing B cell population. This increased frequency was reduced when B cells started to reappear and was comparable to the frequency in control-treated mice after B cell repletion was completed. This observation supports the hypothesis of a frequency shift. In contrast to the T cell frequencies, the absolute number of T cells was decreased in the spleen after aCD20 treatment. This finding provides initial evidence for a direct aCD20 effect on T cells. This effect of aCD20 treatment on T cells has been previously described. Cross et al.[139] reported a decreased T cell number in CSF of MS patients treated with rituximab.

Analysing T cell subsets in spleen, lymph node, bone marrow and blood for CD20+ T cells in aCD20-and control-treated mice showed a clear CD20+T cell population in control mice which was missing in aCD20-treated mice. The analysed population in this study was not clearly distinct from CD20- T cells but showed $CD20^{dim}$ expression which is also described for the CD20+ T cell population in MS patients and patients with rheumatic athritis[137,138]. Furthermore, the absence of this population after aCD20 treatment serves as an evidence for the existence of this these population. A previous study in MS showed a distribution of CD20+ T cells in the CD4+ and CD8+ T cell populations which is comparable to our results. Additionally, these CD20+ T cells were also reduced upon aCD20 treatment[138]. In 2014, Holley et al.[42] reported that CD20+ and CD20- T cell produce IFN and IL-4 after ex vivo stimulation in the blood of MS patients and that CD20+ T cell which were positive for IFN[41] were found in the brain. Further studies suggest that these CD20+ T cell populations mediate inflammation in other autoimmune diseases[140,141]. These CD20+ T cells undergo a shift from Th1 to Th17 cells in rheumatic atritis[142]. Th17 cells are also found in MS lesions[26]. The fact that aCD20 treatment in this study also reduces this CD20+ T cell population and causes a clinical benefit may provide evidence that CD20+ T cells play a role in MS pathogenesis and accordingly for the treatment effect of aCD20. However, our study also includes findings which may provide evidence against this hypothesis. Repletion of the CD20+ T cell population and clinical benefit in rMOG EAE take place at the same point in time and suggest that the CD20+ T cell population is somehow involved in the clinical outcome of the disease and

that the depletion could cause a clinical benefit. Evidence against this hypothesis is the comparable reappearance of CD20+ B cells of mice with rMOG and MOG p35-55 EAE and in contrast to mice with rMOG EAE, no worsening of the clinical score was visible after reappearance of CD20+ T cells in mice with MOG p35-55 EAE. This could have different reasons. For instance, the effect could be overwritten by an increased reappearance of naïve B cells with regulatory function or by missing activation of B cells as was observed in mice with rMOG EAE. Another reason for this finding could be the limitation of the EAE model which may could not show a further worsening in the clinical outcome. Although there is strong evidence for the role of CD20+ T cells in MS and EAE, it is not fully understood and further investigations are needed to proof these hypotheses. Possible experiments for elucidating the role of CD20+ T cells could be the sorting of these CD20+ T cells and *ex vivo* stimulation to characterize the exact function of these T cells. A further worthwhile experiment might be to transfer isolated CD20+ T cells into mice with EAE and to analyse the resulting clinical outcome. Another possibility is to exclusively deplete this CD20+ T cell population and investigate the outcome of this depletion. Holley et al.[42] showed that ScFvRit:sFasL, which has a pro-apoptotic activity, efficiently depletes CD20+ T cells.

4.5. Direct stimulation of T cells after aCD20 treatment *ex vivo*

Additionally, the repletion of CD20+ T cells was investigated and showed a reappearance of this population 8 weeks after the last treatment in naïve mice while full repletion was reached at week 12 similar to the B cell repletion kinetic. In conclusion, CD20+ T cells seem to be depletable and able to reappear after aCD20 treatment. Due to the fact that this population reappears shortly after the B cells, the absence may be due to the missing B cell and T cell interaction.

Further evidence for an indirect effect on T cells by B cell depletion was gained via the direct *ex vivo* stimulation of isolated T cells. For this, T cells were isolated from naïve mice 8 weeks after the last treatment when B cells just started to reappear. These T cells showed a decreased proliferation rate and release of IL-17. This effect is gone 12 weeks after the last treatment when B cell repletion is complete.

In order to analyse the direct influence of missing B cells on T cells, T cell isolation and stimulation was repeated during the B cell repletion in EAE models. In the B cell-mediated, rMOG induced model, as well as in MOG p35-55 EAE the proliferation rate of T cells is decreased compared to T cells of control-treated mice 8 weeks after the last aCD20 treatment. The amount of released IFN and IL-17 was also reduced after 8 weeks in both EAE models. When B cells are fully repleted at week 12 after the last treatment, the proliferation of T cells isolated from aCD20-treated mice immunized with rMOG is higher compared to control-treated mice whereas

the T cell proliferation in aCD20-treated mice immunized with MOG p35-55 is decreased compared to their control-treated animals. The same tendency is seen for the released IFN y and IL-17 in the supernatant after T cell stimulation of T cells from mice with MOG p35-55 EAE. The cytokine release of T cells of aCD20-treated mice immunized with rMOG is not significantly different compared to control-treated mice. In MOG p35-55 EAE instead released cytokines of aCD20-treated T cells are significantly decreased compared to control-treated mice. The results of this experiment support the previous findings which showed that reappearing B cells in rMOG EAE have a more activated phenotype and showed *ex vivo* a superior APC function. 8 weeks after the last aCD20 treatment an overall lower number of B cells was present and could not efficiently activate T cells whereas after 12 weeks, when B cells are fully reappeared an efficient T cell activation is possible. In MOG p35-55 EAE, the proliferation as well as IL-17 and IFN release is lower after full repletion of B cells. Due to the weaker APC function of reappearing B cells and thereby following lower rate of activated T cells in aCD20-treated mice this, result is in line with the previous results. Similar results were seen in rituximab-treated patients. It was reported that T cells showed a decreased expression of T cell activation markers, pro-inflammatory cytokine production and proliferation capacity[141]. This inhibition of T cell activation may contribute to the clinical benefit of aCD20 treatment in MS patients as well as in rMOG EAE.

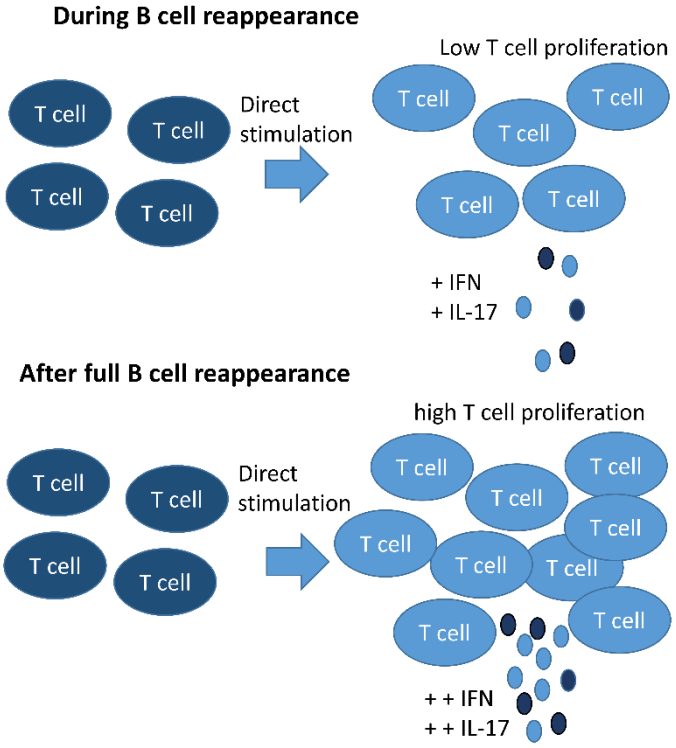

Figure 26:Overview of T cell function after aCD20 treatment.
Decreased proliferation and cytokine release during B cell proliferation which switch into high proliferation and cytokine release after full repletion of B cells

4.6. Compensation by MAC-3+ cells and meningeal B cells but not by T cells

Analysing the inflammation and demyelination after aCD20 treatment in mice with rMOG and MOG p35-55 EAE, no difference in demyelination of the spinal cord could be observed between aCD20-treated and control-treated mice in both EAE models. A reduction of B cells and T cells in the white matter of the aCD20 treated mice compared to control-treated mice was observed at the point of time when peripheral B cells are completely reappeared. In contrast, the number of myeloid MAC-3+ cells is increased in the white matter after aCD20 treatment. Additionally, the analysis of meningeal cells showed a full repletion of B cells but not T cells. Summarizing these findings, MAC-3+ cells and infiltrating meningeal B cells seem to compensate the missing B and T cell numbers in the white matter. Lehmann-Horn et al.[143] described an increased activation of peripheral myeloid cells in MOG p35-55 EAE after aCD20 treatment. The same effect was seen for human PBMCs[143]. This peripheral activation can lead to migration and infiltration of myeloid cells into the CNS, which is seen in this study. Another possible explanation of the missing differences between the groups may lead to the limited explanatory value of the EAE model. Comparing the scores in rMOG EAE, the scores of control-treated mice stay nearly at the maximum whereas the scores of aCD20-treated mice further increased after reappearance of more activated B cells. These reappearing B cells in rMOG EAE induced *ex vivo* pathogenic Th1 and Th17 cells. These T cells could cause more demyelination and adjust demyelination of aCD20-treated and control-treated mice to the same level. Furthermore, in MOG p35-55 EAE, the reappearance of B cells led to an improvement of the clinical scores of aCD20-treated mice which showed a more severe disease score compared to control-treated mice during the phase of B cell depletion. In MOG p35-55 EAE the aCD20-treated group showed after EAE onset a nearly maximal disease score. Due to this fact, no decreased demyelination could be observed in these mice even after reappearance of B cells with a more naive function. Here the value and modulation of these EAE models induced with the used immunization regime seems to be limited and could not answer the question whether the different phenotype of reappearing B cells has an influence on the CNS demyelination.

Summarizing the findings of this study, in the two used EAE models, the reappearance of B cell after aCD20 treatment has different effect on clinical course. These differences are caused by a different phenotype of the reappearing B cells with different functional capacities. After depletion, the remaining B cell population showed an enrichment of CD27+ activated B cells which expanded in the spleen and then became activated by rMOG, which seems to create a B cell activating milieu. In contrast, mice in MOG p35-55 EAE, the milieu in which B cells reappear does not seem to be B cell activating. The different activation induced two different phenotypes of B cells. The phenotype of reappearing B cells in mice of rMOG EAE is more activated and leads

to a superior APC function which induces pathogenic Th1 and Th17 cells. The phenotype of reappearing B cells in mice with MOG p35-55 EAE is more naïve and leads to weaker APC function. This finding led to the hypothesis that the phenotype of reappearing B cells depends on immunogenic stimulus during their reappearance.

In MS patients, the status of B cells and influencing the milieu should be controlled during reappearance. Further, a continuous depletion might be a better treatment schedule than monitoring reappearance of B cells in the blood. Repeating depletion and reoccurring repletion in secondary lymphoid organs could enrich remaining IgG+ memory B cells which undergo clonal expansion. Enrichment of these cells may facilitate a relapse[130–132]. Another strategy to avoid pathogenic reappearance of B cells could be to modulate the milieu during reappearance and to control the phenotype of these B cells. A promising possibility is to inhibit BCR signalling and avoid stimulation of B cells. Bruton's tyrosine kinase (BTK) is required for B-cell receptor-dependent NF-kappaB signalling pathway[144]. BTK inhibition is under investigation in EAE and MS. Combination therapy of ofatumumab, a humanised aCD20 antibody, and BTK inhibitor PCI-32765 showed good response in patients with chronic lymphocytic leukemia/small lymphocytic lymphoma (CLL/SLL) and related diseases[145].

A further possibility to prevent B and T cell interaction is the inhibition of costimulatory molecules such as CD80, CD86 or/ and CD40. Anti-inflammatory drugs may represent one possibility. IFNβ therapy decreased the levels of CD80, CD86 on human PBMC as well as the level of BAFF in MS patients. One clinical trial reported that combination therapy of rituximab and IFNβ showed no difference in clinical parameters, MRI and laboratory outcomes[146,147]. Inhibiting the APC function of these B cells could be a particularly successful strategy.

Optimising MS therapy during and after aCD20 treatment a B cell activating medication should be avoided B cell activating treatment may not should be combined with aCD20 treatment.

This study could reveal new insights in the characterization of B cells, provides a greater understanding of EAE pathogeneses after aCD20 Ab depletion and further hints towards optimising MS therapeutic strategy.

In conclusion, there is a range of evidence as to which effect of aCD220 treatment causes clinical benefit in MS patients. On the one hand the missing B cell population led to the hypothesis that depletion of B cells causes the clinical benefit. On the other hand we showed that the depletion of CD20+ T cells in rMOG as well as in MOG p35-55 EAE is possible by aCD20 treatment. These direct effects on T cells could also cause benefits of aCD20 treatment in MS patients.

Furthermore, T cells are affected by the indirect effect of aCD20 treatment, missing B cell interaction. T cells of aCD20-treated mice showed a reduced proliferation rate after direct stimulation 8 weeks after the last treatment in rMOG, MOG p35-55 EAE and naïve mice. This effect is gone in rMOG immunized mice after full repletion but not in MOG p35-55 immunized mice. Knowing the influence of aCD20 treatment on T cell gives new insight in MS pathology and new therapeutic strategies. Specific depletion of these CD20+ T cells could have beneficial effect and avoid side effect of long-term treatment. Until today, the exact cause of clinical benefit is not known and could also be a combination of direct B cell and CD20+ T cell depletion and missing B cell interaction.

5. References

1. *McAlpine's Multiple Sclerosis - 4th Edition*.
2. Murray, T. J. Robert Carswell: the first illustrator of MS. *Int. MS J.* **16,** 98–101 (2009).
3. Gomes, M. da M. & Engelhardt, E. Jean-Martin Charcot, father of modern neurology: an homage 120 years after his death. *Arq. Neuropsiquiatr.* **71,** 815–817 (2013).
4. Kurtzke, J. F. Multiple sclerosis in time and space--geographic clues to cause. *J. Neurovirol.* **6 Suppl 2,** S134-140 (2000).
5. Hein, T. & Hopfenmüller, W. [Projection of the number of multiple sclerosis patients in Germany]. *Nervenarzt* **71,** 288–294 (2000).
6. Wallin, M. T. *et al.* The Gulf War era multiple sclerosis cohort: age and incidence rates by race, sex and service. *Brain J. Neurol.* **135,** 1778–1785 (2012).
7. Muñoz-Culla, M., Irizar, H. & Otaegui, D. The genetics of multiple sclerosis: review of current and emerging candidates. *Appl. Clin. Genet.* **6,** 63–73 (2013).
8. Munger, K. L. *et al.* Vitamin D intake and incidence of multiple sclerosis. *Neurology* **62,** 60–65 (2004).
9. Munger, K. L., Levin, L. I., Hollis, B. W., Howard, N. S. & Ascherio, A. Serum 25-hydroxyvitamin D levels and risk of multiple sclerosis. *JAMA* **296,** 2832–2838 (2006).
10. Simpson, S. *et al.* Higher 25-hydroxyvitamin D is associated with lower relapse risk in multiple sclerosis. *Ann. Neurol.* **68,** 193–203 (2010).
11. Lucas, R. M. *et al.* Sun exposure and vitamin D are independent risk factors for CNS demyelination. *Neurology* **76,** 540–548 (2011).
12. Ascherio, A. & Munger, K. L. Environmental risk factors for multiple sclerosis. Part II: Noninfectious factors. *Ann. Neurol.* **61,** 504–513 (2007).
13. Hernán, M. A., Olek, M. J. & Ascherio, A. Cigarette smoking and incidence of multiple sclerosis. *Am. J. Epidemiol.* **154,** 69–74 (2001).

14. Healy, B. C. *et al.* Smoking and disease progression in multiple sclerosis. *Arch. Neurol.* **66,** 858–864 (2009).

15. Manouchehrinia, A. *et al.* Tobacco smoking and disability progression in multiple sclerosis: United Kingdom cohort study. *Brain J. Neurol.* **136,** 2298–2304 (2013).

16. Lublin, F. D. & Reingold, S. C. Defining the clinical course of multiple sclerosis: results of an international survey. National Multiple Sclerosis Society (USA) Advisory Committee on Clinical Trials of New Agents in Multiple Sclerosis. *Neurology* **46,** 907–911 (1996).

17. Lublin, F. D. *et al.* Defining the clinical course of multiple sclerosis. *Neurology* **83,** 278–286 (2014).

18. Scalfari, A. *et al.* Early Relapses, Onset of Progression, and Late Outcome in Multiple Sclerosis. *JAMA Neurol.* **70,** 214 (2013).

19. Hauser, S. L. & Oksenberg, J. R. The neurobiology of multiple sclerosis: genes, inflammation, and neurodegeneration. *Neuron* **52,** 61–76 (2006).

20. Darius Häusler. Impact of natalizumab therapy on human pathology and an animal model of multiple sclerosis (EAE) with special focus on B cell / plasma cell inflammation. (2014).

21. Hemmer, B., Kerschensteiner, M. & Korn, T. Role of the innate and adaptive immune responses in the course of multiple sclerosis. *Lancet Neurol.* **14,** 406–419 (2015).

22. Larochelle, C., Alvarez, J. I. & Prat, A. How do immune cells overcome the blood-brain barrier in multiple sclerosis? *FEBS Lett.* **585,** 3770–3780 (2011).

23. Bartholomäus, I. *et al.* Effector T cell interactions with meningeal vascular structures in nascent autoimmune CNS lesions. *Nature* **462,** 94–98 (2009).

24. Fischer, M. T. *et al.* NADPH oxidase expression in active multiple sclerosis lesions in relation to oxidative tissue damage and mitochondrial injury. *Brain J. Neurol.* **135,** 886–899 (2012).

25. Harrington, L. E. *et al.* Interleukin 17-producing CD4+ effector T cells develop via a lineage distinct from the T helper type 1 and 2 lineages. *Nat. Immunol.* **6,** 1123–1132 (2005).

26. Tzartos, J. S. *et al.* Interleukin-17 production in central nervous system-infiltrating T cells and glial cells is associated with active disease in multiple sclerosis. *Am. J. Pathol.* **172,** 146–155 (2008).

27. Weber, M. S. *et al.* Type II monocytes modulate T cell-mediated central nervous system autoimmune disease. *Nat. Med.* **13,** 935–943 (2007).

28. Viglietta, V., Baecher-Allan, C., Weiner, H. L. & Hafler, D. A. Loss of functional suppression by CD4+CD25+ regulatory T cells in patients with multiple sclerosis. *J. Exp. Med.* **199,** 971–979 (2004).

29. Haas, J. *et al.* Reduced suppressive effect of CD4+CD25high regulatory T cells on the T cell immune response against myelin oligodendrocyte glycoprotein in patients with multiple sclerosis. *Eur. J. Immunol.* **35,** 3343–3352 (2005).

30. Kabat, E. A., Moore, D. H. & Landow, H. AN ELECTROPHORETIC STUDY OF THE PROTEIN COMPONENTS IN CEREBROSPINAL FLUID AND THEIR RELATIONSHIP TO THE SERUM PROTEINS. *J. Clin. Invest.* **21,** 571–577 (1942).

31. Walsh, M. J., Tourtellotte, W. W., Roman, J. & Dreyer, W. Immunoglobulin G, A, and M--clonal restriction in multiple sclerosis cerebrospinal fluid and serum--analysis by two-dimensional electrophoresis. *Clin. Immunol. Immunopathol.* **35,** 313–327 (1985).

32. Serafini, B., Rosicarelli, B., Magliozzi, R., Stigliano, E. & Aloisi, F. Detection of ectopic B-cell follicles with germinal centers in the meninges of patients with secondary progressive multiple sclerosis. *Brain Pathol. Zurich Switz.* **14,** 164–174 (2004).

33. Magliozzi, R. *et al.* Meningeal B-cell follicles in secondary progressive multiple sclerosis associate with early onset of disease and severe cortical pathology. *Brain J. Neurol.* **130,** 1089–1104 (2007).

34. Hauser, S. L. *et al.* B-cell depletion with rituximab in relapsing–remitting multiple sclerosis. *N. Engl. J. Med.* **358,** 676–688 (2008).

35. Lucchinetti, C. *et al.* Heterogeneity of multiple sclerosis lesions: implications for the pathogenesis of demyelination. *Ann. Neurol.* **47,** 707–717 (2000).

36. Keegan, M. *et al.* Relation between humoral pathological changes in multiple sclerosis and response to therapeutic plasma exchange. *Lancet Lond. Engl.* **366,** 579–582 (2005).

37. Mathias, A. *et al.* Increased ex vivo antigen presentation profile of B cells in multiple sclerosis. *Mult. Scler. Houndmills Basingstoke Engl.* (2016). doi:10.1177/1352458516664210

38. Barr, T. A. *et al.* B cell depletion therapy ameliorates autoimmune disease through ablation of IL-6-producing B cells. *J. Exp. Med.* **209,** 1001–1010 (2012).

39. Korn, T. *et al.* IL-6 controls Th17 immunity in vivo by inhibiting the conversion of conventional T cells into Foxp3+ regulatory T cells. *Proc. Natl. Acad. Sci. U. S. A.* **105,** 18460–18465 (2008).

40. Duddy, M. *et al.* Distinct effector cytokine profiles of memory and naive human B cell subsets and implication in multiple sclerosis. *J. Immunol.* **178,** 6092–6099 (2007).

41. Palanichamy, A. *et al.* Rituximab Efficiently Depletes Increased CD20-Expressing T Cells in Multiple Sclerosis Patients. *J. Immunol.* **193,** 580–586 (2014).

42. Holley, J. E. *et al.* CD20+inflammatory T-cells are present in blood and brain of multiple sclerosis patients and can be selectively targeted for apoptotic elimination. *Mult. Scler. Relat. Disord.* **3,** 650–658 (2014).

43. Brück, W. *et al.* Monocyte/macrophage differentiation in early multiple sclerosis lesions. *Ann. Neurol.* **38,** 788–796 (1995).

44. Fox, R. J. *et al.* Placebo-controlled phase 3 study of oral BG-12 or glatiramer in multiple sclerosis. *N. Engl. J. Med.* **367,** 1087–1097 (2012).

45. McCormack, P. L. & Scott, L. J. Interferon-beta-1b: a review of its use in relapsing-remitting and secondary progressive multiple sclerosis. *CNS Drugs* **18,** 521–546 (2004).

46. Kappos, L. *et al.* Effect of early versus delayed interferon beta-1b treatment on disability after a first clinical event suggestive of multiple sclerosis: a 3-year follow-up analysis of the BENEFIT study. *Lancet Lond. Engl.* **370,** 389–397 (2007).

47. Paty, D. W. & Li, D. K. Interferon beta-1b is effective in relapsing-remitting multiple sclerosis. II. MRI analysis results of a multicenter, randomized, double-blind, placebo-controlled trial. UBC MS/MRI Study Group and the IFNB Multiple Sclerosis Study Group. *Neurology* **43,** 662–667 (1993).

48. Mikol, D. D. *et al.* Comparison of subcutaneous interferon beta-1a with glatiramer acetate in patients with relapsing multiple sclerosis (the REbif vs Glatiramer Acetate in Relapsing MS Disease [REGARD] study): a multicentre, randomised, parallel, open-label trial. *Lancet Neurol.* **7,** 903–914 (2008).

49. Claussen, M. C. & Korn, T. Immune mechanisms of new therapeutic strategies in MS: teriflunomide. *Clin. Immunol. Orlando Fla* **142,** 49–56 (2012).

50. Coles, A. J. *et al.* Alemtuzumab for patients with relapsing multiple sclerosis after disease-modifying therapy: a randomised controlled phase 3 trial. *Lancet Lond. Engl.* **380,** 1829–1839 (2012).

51. Cohen, J. A. *et al.* Oral fingolimod or intramuscular interferon for relapsing multiple sclerosis. *N. Engl. J. Med.* **362,** 402–415 (2010).

52. Polman, C. H. *et al.* Diagnostic criteria for multiple sclerosis: 2005 revisions to the 'McDonald Criteria'. *Ann. Neurol.* **58,** 840–846 (2005).

53. Langer-Gould, A., Atlas, S. W., Green, A. J., Bollen, A. W. & Pelletier, D. Progressive Multifocal Leukoencephalopathy in a Patient Treated with Natalizumab. *N. Engl. J. Med.* **353,** 375–381 (2005).

54. Freedman, M. S. Present and Emerging Therapies for Multiple Sclerosis: *Contin. Lifelong Learn. Neurol.* **19,** 968–991 (2013).

55. Kappos, L. *et al.* Ocrelizumab in relapsing-remitting multiple sclerosis: a phase 2, randomised, placebo-controlled, multicentre trial. *Lancet Lond. Engl.* **378,** 1779–1787 (2011).

56. Gold, R. *et al.* Daclizumab high-yield process in relapsing-remitting multiple sclerosis (SELECT): a randomised, double-blind, placebo-controlled trial. *Lancet Lond. Engl.* **381,** 2167–2175 (2013).

57. Vollmer, T., Stewart, T. & Baxter, N. Mitoxantrone and cytotoxic drugs' mechanisms of action. *Neurology* **74 Suppl 1,** S41-46 (2010).

58. Sellebjerg, F. *et al.* EFNS guideline on treatment of multiple sclerosis relapses: report of an EFNS task force on treatment of multiple sclerosis relapses. *Eur. J. Neurol.* **12,** 939–946 (2005).

59. Heigl, F. *et al.* Immunoadsorption in steroid-refractory multiple sclerosis: clinical experience in 60 patients. *Atheroscler. Suppl.* **14,** 167–173 (2013).

60. Trebst, C., Reising, A., Kielstein, J. T., Hafer, C. & Stangel, M. Plasma exchange therapy in steroid-unresponsive relapses in patients with multiple sclerosis. *Blood Purif.* **28,** 108–115 (2009).

61. Ontaneda, D., Thompson, A. J., Fox, R. J. & Cohen, J. A. Progressive multiple sclerosis: prospects for disease therapy, repair, and restoration of function. *Lancet Lond. Engl.* (2016). doi:10.1016/S0140-6736(16)31320-4

62. Ontaneda, D. & Fox, R. J. Progressive multiple sclerosis. *Curr. Opin. Neurol.* **28,** 237–243 (2015).

63. Stüve, O. *et al.* Mitoxantrone as a potential therapy for primary progressive multiple sclerosis. *Mult. Scler. Houndmills Basingstoke Engl.* **10 Suppl 1,** S58-61 (2004).

64. Chataway, J. *et al.* The Ms-Smart Trial in Secondary Progressive Multiple Sclerosis: A Multi-Arm, Multi-Centre Trial of Neuroprotection. *J Neurol Neurosurg Psychiatry* **86,** e4–e4 (2015).

65. Uchida, J. *et al.* Mouse CD20 expression and function. *Int. Immunol.* **16,** 119–129 (2004).

66. Smolen, J. S. *et al.* EULAR recommendations for the management of rheumatoid arthritis with synthetic and biological disease-modifying antirheumatic drugs: 2013 update. *Ann. Rheum. Dis.* **73,** 492–509 (2014).

67. Camous, L. *et al.* Complete remission of lupus nephritis with rituximab and steroids for induction and rituximab alone for maintenance therapy. *Am. J. Kidney Dis. Off. J. Natl. Kidney Found.* **52,** 346–352 (2008).

68. Dotan, E., Aggarwal, C. & Smith, M. R. Impact of Rituximab (Rituxan) on the Treatment of B-Cell Non-Hodgkin's Lymphoma. *Pharm. Ther.* **35,** 148–157 (2010).

69. Bryan, J. & Borthakur, G. Role of rituximab in first-line treatment of chronic lymphocytic leukemia. *Ther. Clin. Risk Manag.* **7,** 1–11 (2011).

70. Hawker, K. *et al.* Rituximab in patients with primary progressive multiple sclerosis: Results of a randomized double-blind placebo-controlled multicenter trial. *Ann. Neurol.* **66,** 460–471 (2009).

71. Emery, P. *et al.* Efficacy and safety of different doses and retreatment of rituximab: a randomised, placebo-controlled trial in patients who are biological naive with active rheumatoid arthritis and an inadequate response to methotrexate (Study Evaluating Rituximab's Efficacy in MTX iNadequate rEsponders (SERENE)). *Ann. Rheum. Dis.* **69,** 1629–1635 (2010).

72. Morschhauser, F. *et al.* Results of a phase I/II study of ocrelizumab, a fully humanized anti-CD20 mAb, in patients with relapsed/refractory follicular lymphoma. *Ann. Oncol. Off. J. Eur. Soc. Med. Oncol.* **21,** 1870–1876 (2010).

73. Fernandez, O. *et al.* Review of the novelties from the 31st ECTRIMS Congress, 2015, presented at the 8th Post-ECTRIMS meeting. *Rev. Neurol.* **62,** 559–569 (2016).

74. Sorensen, P. S. *et al.* Safety and efficacy of ofatumumab in relapsing-remitting multiple sclerosis: a phase 2 study. *Neurology* **82,** 573–581 (2014).

75. Zhou, X., Hu, W. & Qin, X. The Role of Complement in the Mechanism of Action of Rituximab for B-Cell Lymphoma: Implications for Therapy. *The Oncologist* **13,** 954–966 (2008).

76. Clynes, R. A., Towers, T. L., Presta, L. G. & Ravetch, J. V. Inhibitory Fc receptors modulate in vivo cytoxicity against tumor targets. *Nat. Med.* **6,** 443–446 (2000).

77. Bayry, J., Lacroix-Desmazes, S., Kazatchkine, M. D. & Kaveri, S. V. Monoclonal antibody and intravenous immunoglobulin therapy for rheumatic diseases: rationale and mechanisms of action. *Nat. Clin. Pract. Rheumatol.* **3,** 262–272 (2007).

78. Rivers, T. M., Sprunt, D. H. & Berry, G. P. OBSERVATIONS ON ATTEMPTS TO PRODUCE ACUTE DISSEMINATED ENCEPHALOMYELITIS IN MONKEYS. *J. Exp. Med.* **58,** 39–53 (1933).

79. Stromnes, I. M. & Goverman, J. M. Active induction of experimental allergic encephalomyelitis. *Nat. Protoc.* **1,** 1810–1819 (2006).

80. Bettelli, E., Baeten, D., Jäger, A., Sobel, R. A. & Kuchroo, V. K. Myelin oligodendrocyte glycoprotein–specific T and B cells cooperate to induce a Devic-like disease in mice. *J. Clin. Invest.* **116,** 2393–2402 (2006).

81. Baron, J. L., Madri, J. A., Ruddle, N. H., Hashim, G. & Janeway, C. A. Surface expression of alpha 4 integrin by CD4 T cells is required for their entry into brain parenchyma. *J. Exp. Med.* **177,** 57–68 (1993).

82. Jäger, A., Dardalhon, V., Sobel, R. A., Bettelli, E. & Kuchroo, V. K. Th1, Th17, and Th9 effector cells induce experimental autoimmune encephalomyelitis with different pathological phenotypes. *J. Immunol. Baltim. Md 1950* **183,** 7169–7177 (2009).

83. Becher, B., Durell, B. G. & Noelle, R. J. Experimental autoimmune encephalitis and inflammation in the absence of interleukin-12. *J. Clin. Invest.* **110,** 493–497 (2002).

84. Kroenke, M. A., Carlson, T. J., Andjelkovic, A. V. & Segal, B. M. IL-12- and IL-23-modulated T cells induce distinct types of EAE based on histology, CNS chemokine profile, and response to cytokine inhibition. *J. Exp. Med.* **205,** 1535–1541 (2008).

85. Kohm, A. P., Carpentier, P. A., Anger, H. A. & Miller, S. D. Cutting edge: CD4+CD25+ regulatory T cells suppress antigen-specific autoreactive immune responses and central nervous system inflammation during active experimental autoimmune encephalomyelitis. *J. Immunol. Baltim. Md 1950* **169,** 4712–4716 (2002).

86. Zhang, X. *et al.* IL-10 is involved in the suppression of experimental autoimmune encephalomyelitis by CD25+CD4+ regulatory T cells. *Int. Immunol.* **16,** 249–256 (2004).

87. Liu, Y., Teige, I., Birnir, B. & Issazadeh-Navikas, S. Neuron-mediated generation of regulatory T cells from encephalitogenic T cells suppresses EAE. *Nat. Med.* **12,** 518–525 (2006).

88. McGeachy, M. J., Stephens, L. A. & Anderton, S. M. Natural recovery and protection from autoimmune encephalomyelitis: contribution of CD4+CD25+ regulatory cells within the central nervous system. *J. Immunol. Baltim. Md 1950* **175,** 3025–3032 (2005).

89. Kurschus, F. C. T cell mediated pathogenesis in EAE: Molecular mechanisms. *Biomed. J.* **38,** 183–193 (2015).

90. Fletcher, J. M., Lalor, S. J., Sweeney, C. M., Tubridy, N. & Mills, K. H. G. T cells in multiple sclerosis and experimental autoimmune encephalomyelitis. *Clin. Exp. Immunol.* **162,** 1–11 (2010).

91. Slavin, A. J. *et al.* Requirement for endocytic antigen processing and influence of invariant chain and H-2M deficiencies in CNS autoimmunity. *J. Clin. Invest.* **108,** 1133–1139 (2001).

92. Furtado, G. C. *et al.* Swift entry of myelin-specific T lymphocytes into the central nervous system in spontaneous autoimmune encephalomyelitis. *J. Immunol. Baltim. Md 1950* **181,** 4648–4655 (2008).

93. O'Connor, R. A. *et al.* Cutting edge: Th1 cells facilitate the entry of Th17 cells to the central nervous system during experimental autoimmune encephalomyelitis. *J. Immunol. Baltim. Md 1950* **181,** 3750–3754 (2008).

94. Steinman, L. & Zamvil, S. S. Virtues and pitfalls of EAE for the development of therapies for multiple sclerosis. *Trends Immunol.* **26,** 565–571 (2005).

95. Weber, M. S. *et al.* B-cell activation influences T-cell polarization and outcome of anti-CD20 B-cell depletion in central nervous system autoimmunity: B Cells in CNS Autoimmunity. *Ann. Neurol.* **68,** 369–383 (2010).

96. Marta, C. B., Oliver, A. R., Sweet, R. A., Pfeiffer, S. E. & Ruddle, N. H. Pathogenic myelin oligodendrocyte glycoprotein antibodies recognize glycosylated epitopes and perturb oligodendrocyte physiology. *Proc. Natl. Acad. Sci. U. S. A.* **102,** 13992–13997 (2005).

97. Lyons, J. A., San, M., Happ, M. P. & Cross, A. H. B cells are critical to induction of experimental allergic encephalomyelitis by protein but not by a short encephalitogenic peptide. *Eur. J. Immunol.* **29,** 3432–3439 (1999).

98. Wolf, S. D., Dittel, B. N., Hardardottir, F. & Janeway, C. A. Experimental autoimmune encephalomyelitis induction in genetically B cell-deficient mice. *J. Exp. Med.* **184,** 2271–2278 (1996).

99. Fillatreau, S., Sweenie, C. H., McGeachy, M. J., Gray, D. & Anderton, S. M. B cells regulate autoimmunity by provision of IL-10. *Nat. Immunol.* **3,** 944–950 (2002).

100. Matsushita, T. *et al.* Inhibitory role of CD19 in the progression of experimental autoimmune encephalomyelitis by regulating cytokine response. *Am. J. Pathol.* **168,** 812–821 (2006).

101. Linington, C., Bradl, M., Lassmann, H., Brunner, C. & Vass, K. Augmentation of demyelination in rat acute allergic encephalomyelitis by circulating mouse monoclonal antibodies directed against a myelin/oligodendrocyte glycoprotein. *Am. J. Pathol.* **130,** 443–454 (1988).

102. Krishnamoorthy, G., Lassmann, H., Wekerle, H. & Holz, A. Spontaneous opticospinal encephalomyelitis in a double-transgenic mouse model of autoimmune T cell/B cell cooperation. *J. Clin. Invest.* **116,** 2385–2392 (2006).

103. Merkler, D. *et al.* Myelin oligodendrocyte glycoprotein-induced experimental autoimmune encephalomyelitis in the common marmoset reflects the immunopathology of pattern II multiple sclerosis lesions. *Mult. Scler. Houndmills Basingstoke Engl.* **12,** 369–374 (2006).

104. Lehmann-Horn, K., Kronsbein, H. C. & Weber, M. S. Targeting B cells in the treatment of multiple sclerosis: recent advances and remaining challenges. *Ther. Adv. Neurol. Disord.* **6,** 161–173 (2013).

105. Soos, J. M. *et al.* Astrocytes express elements of the class II endocytic pathway and process central nervous system autoantigen for presentation to encephalitogenic T cells. *J. Immunol. Baltim. Md 1950* **161,** 5959–5966 (1998).

106. Fontana, A., Fierz, W. & Wekerle, H. Astrocytes present myelin basic protein to encephalitogenic T-cell lines. *Nature* **307,** 273–276 (1984).

107. Greter, M. *et al.* Dendritic cells permit immune invasion of the CNS in an animal model of multiple sclerosis. *Nat. Med.* **11,** 328–334 (2005).

108. Lanzavecchia, A. Antigen-specific interaction between T and B cells. *Nature* **314,** 537–539 (1985).

109. Constant, S., Schweitzer, N., West, J., Ranney, P. & Bottomly, K. B lymphocytes can be competent antigen-presenting cells for priming CD4+ T cells to protein antigens in vivo. *J. Immunol. Baltim. Md 1950* **155,** 3734–3741 (1995).

110. Constant, S. *et al.* Peptide and protein antigens require distinct antigen-presenting cell subsets for the priming of CD4+ T cells. *J. Immunol. Baltim. Md 1950* **154,** 4915–4923 (1995).

111. Molnarfi, N. *et al.* MHC class II–dependent B cell APC function is required for induction of CNS autoimmunity independent of myelin-specific antibodies. *J. Exp. Med.* **210,** 2921–2937 (2013).

112. Samoilova, E. B., Horton, J. L., Hilliard, B., Liu, T. S. & Chen, Y. IL-6-deficient mice are resistant to experimental autoimmune encephalomyelitis: roles of IL-6 in the activation and differentiation of autoreactive T cells. *J. Immunol. Baltim. Md 1950* **161,** 6480–6486 (1998).

113. Shen, P. *et al.* IL-35-producing B cells are critical regulators of immunity during autoimmune and infectious diseases. *Nature* **507,** 366–370 (2014).

114. Bettelli, E. *et al.* Myelin oligodendrocyte glycoprotein-specific T cell receptor transgenic mice develop spontaneous autoimmune optic neuritis. *J. Exp. Med.* **197,** 1073–1081 (2003).

115. Leandro, M. J., Cooper, N., Cambridge, G., Ehrenstein, M. R. & Edwards, J. C. W. Bone marrow B-lineage cells in patients with rheumatoid arthritis following rituximab therapy. *Rheumatol. Oxf. Engl.* **46,** 29–36 (2007).

116. Rehnberg, M., Amu, S., Tarkowski, A., Bokarewa, M. I. & Brisslert, M. Short- and long-term effects of anti-CD20 treatment on B cell ontogeny in bone marrow of patients with rheumatoid arthritis. *Arthritis Res. Ther.* **11,** R123 (2009).

117. Vugmeyster, Y., Howell, K., McKeever, K., Combs, D. & Canova-Davis, E. Differential in vivo effects of rituximab on two B-cell subsets in cynomolgus monkeys. *Int. Immunopharmacol.* **3,** 1477–1481 (2003).

118. Gong, Q. *et al.* Importance of cellular microenvironment and circulatory dynamics in B cell immunotherapy. *J. Immunol. Baltim. Md 1950* **174,** 817–826 (2005).

119. Rezvani, A. R. & Maloney, D. G. Rituximab resistance. *Best Pract. Res. Clin. Haematol.* **24,** 203–216 (2011).

120. Xiao, Y., Hendriks, J., Langerak, P., Jacobs, H. & Borst, J. CD27 is acquired by primed B cells at the centroblast stage and promotes germinal center formation. *J. Immunol. Baltim. Md 1950* **172,** 7432–7441 (2004).

121. Maurer, M. A. *et al.* Rituximab induces sustained reduction of pathogenic B cells in patients with peripheral nervous system autoimmunity. *J. Clin. Invest.* **122,** 1393–1402 (2012).

122. Fillatreau, S., Sweenie, C. H., McGeachy, M. J., Gray, D. & Anderton, S. M. B cells regulate autoimmunity by provision of IL-10. *Nat. Immunol.* **3,** 944–950 (2002).

123. Cua, D. J., Hutchins, B., LaFace, D. M., Stohlman, S. A. & Coffman, R. L. Central nervous system expression of IL-10 inhibits autoimmune encephalomyelitis. *J. Immunol. Baltim. Md 1950* **166,** 602–608 (2001).

124. Neurath, M. F. & Finotto, S. IL-6 signaling in autoimmunity, chronic inflammation and inflammation-associated cancer. *Cytokine Growth Factor Rev.* **22,** 83–89 (2011).

125. Eugster, H. P., Frei, K., Kopf, M., Lassmann, H. & Fontana, A. IL-6-deficient mice resist myelin oligodendrocyte glycoprotein-induced autoimmune encephalomyelitis. *Eur. J. Immunol.* **28,** 2178–2187 (1998).

126. Constant, S. L. B lymphocytes as antigen-presenting cells for CD4+ T cell priming in vivo. *J. Immunol. Baltim. Md 1950* **162,** 5695–5703 (1999).

127. Lyons, J.-A., Ramsbottom, M. J. & Cross, A. H. Critical role of antigen-specific antibody in experimental autoimmune encephalomyelitis induced by recombinant myelin oligodendrocyte glycoprotein. *Eur. J. Immunol.* **32,** 1905–1913 (2002).

128. Maurer, M. A. *et al.* Rituximab induces clonal expansion of IgG memory B-cells in patients with inflammatory central nervous system demyelination. *J. Neuroimmunol.* **290,** 49–53 (2016).

129. Berkowska, M. A. *et al.* Human memory B cells originate from three distinct germinal center-dependent and -independent maturation pathways. *Blood* **118,** 2150–2158 (2011).

130. Weller, S. *et al.* Human blood IgM 'memory' B cells are circulating splenic marginal zone B cells harboring a prediversified immunoglobulin repertoire. *Blood* **104,** 3647–3654 (2004).

131. Fecteau, J. F., Côté, G. & Néron, S. A new memory CD27-IgG+ B cell population in peripheral blood expressing VH genes with low frequency of somatic mutation. *J. Immunol. Baltim. Md 1950* **177,** 3728–3736 (2006).

132. Wei, C. *et al.* A new population of cells lacking expression of CD27 represents a notable component of the B cell memory compartment in systemic lupus erythematosus. *J. Immunol. Baltim. Md 1950* **178,** 6624–6633 (2007).

133. Sospedra, M. & Martin, R. Immunology of multiple sclerosis. *Annu. Rev. Immunol.* **23,** 683–747 (2005).

134. Buc, M. Role of regulatory T cells in pathogenesis and biological therapy of multiple sclerosis. *Mediators Inflamm.* **2013,** 963748 (2013).

135. Alugupalli, K. R., Akira, S., Lien, E. & Leong, J. M. MyD88- and Bruton's tyrosine kinase-mediated signals are essential for T cell-independent pathogen-specific IgM responses. *J. Immunol. Baltim. Md 1950* **178,** 3740–3749 (2007).

136. Bar-Or, A. *et al.* Abnormal B-cell cytokine responses a trigger of T-cell-mediated disease in MS? *Ann. Neurol.* **67,** 452–461 (2010).

137. Wilk, E. *et al.* Depletion of functionally active CD20+ T cells by rituximab treatment. *Arthritis Rheum.* **60,** 3563–3571 (2009).

138. Palanichamy, A. *et al.* Rituximab efficiently depletes increased CD20-expressing T cells in multiple sclerosis patients. *J. Immunol. Baltim. Md 1950* **193,** 580–586 (2014).

139. Cross, A. H., Stark, J. L., Lauber, J., Ramsbottom, M. J. & Lyons, J.-A. Rituximab reduces B cells and T cells in cerebrospinal fluid of multiple sclerosis patients. *J. Neuroimmunol.* **180,** 63–70 (2006).

140. Avivi, I., Stroopinsky, D. & Katz, T. Anti-CD20 monoclonal antibodies: beyond B-cells. *Blood Rev.* **27,** 217–223 (2013).

141. Stroopinsky, D., Katz, T., Rowe, J. M., Melamed, D. & Avivi, I. Rituximab-induced direct inhibition of T-cell activation. *Cancer Immunol. Immunother. CII* **61,** 1233–1241 (2012).

142. Eggleton, P. *et al.* Frequency of Th17 CD20+ cells in the peripheral blood of rheumatoid arthritis patients is higher compared to healthy subjects. *Arthritis Res. Ther.* **13,** R208 (2011).

143. Lehmann-Horn, K. *et al.* Anti-CD20 B-cell depletion enhances monocyte reactivity in neuroimmunological disorders. *J. Neuroinflammation* **8,** 146 (2011).

144. Mohamed, A. J. *et al.* Bruton's tyrosine kinase (Btk): function, regulation, and transformation with special emphasis on the PH domain. *Immunol. Rev.* **228,** 58–73 (2009).

145. Jaglowski, S. M. *et al.* A phase Ib/II study evaluating activity and tolerability of BTK inhibitor PCI-32765 and ofatumumab in patients with chronic lymphocytic leukemia/small lymphocytic lymphoma (CLL/SLL) and related diseases. *J. Clin. Oncol.* **30,** (2012).

146. Cross, A. H., Klein, R. S. & Piccio, L. Rituximab combination therapy in relapsing multiple sclerosis. *Ther. Adv. Neurol. Disord.* **5,** 311–319 (2012).

147. Naismith, R. T. *et al.* Rituximab add-on therapy for breakthrough relapsing multiple sclerosis: a 52-week phase II trial. *Neurology* **74,** 1860–1867 (2010).